Introduction to the Fractional Distribution Families

Stephen Horng-Twu Lihn
stevelihn@gmail.com
Version: Early Draft 2025-09

ORFE, Princeton University

Dedicated to Professor John M. Mulvey for his 80th birthday.

(as of October 26, 2025)

Contents

CHAPTER 1

Introduction

In quantitative finance, we often encounter asset return data with prominent skewness and kurtosis. In the domain of portfolio optimization and the market regime model[13, 29, 23], a showcase example is the S&P 500 Index (SPX) and the CBOE Volatility Index (VIX), whose daily prices are publicly available since 1990[1]. Such data sets are easy to obtain, but it is difficult to fit them with an existing parametric distribution. Even with many probability distributions available in modern statistical software, such as **scipy.stats**, they do not work well.

In this book, a multivariate elliptical distribution system based on the Wright function[34, 35, 2] is presented. It combines and extends the α-stable distribution[12] with the multivariate skew-t distribution[1]. This super-distribution family can fit real-world data sets with pronounced fat tails more accurately.

In more detail, the daily return distribution of VIX has a high kurtosis of 16, and a skewness of 2.0. Its standardized peak density is approximately 0.55. (see Figure 12.5). Theoretically, the excess kurtosis of the t distribution[31] is $6/(k-4)$ for $k > 4$. Such kurtosis would put k very close to 4. However, the theoretical standardized peak density is only 0.53 at $k = 4$. The VIX data already push the t distribution to the limit, so to speak.

The daily return distribution of SPX is even more peculiar (see Figure 12.6). In addition to its high kurtosis of 11, its standardized peak density is approximately 0.65. It takes the t distribution of about 3 degrees of freedom ($k \approx 3$) to produce a reasonable fit. However, theoretically, finite kurtosis does not exist until $k > 4$.

These two examples demonstrate mathematical issues when fitting an existing parametric distribution. It is difficult to satisfy both the kurtosis and the peak density simultaneously.

Our new multivariate distribution is able to fit both data sets with satisfactory accuracy while matching empirical skewness, kurtosis, and peak density. Not only is the goodness-of-fit compared in terms of the density function but also how well the tails are captured by the distribution via the quadratic form. We will present these fits in Chapter 17.

The word "fractional" can be roughly understood as adding the Lévy stability index $\alpha \in [0, 2]$ to a known distribution. For example, in the Mellin transform of the PDF of a distribution, $\Gamma(s + c)$ in the classic world becomes $\Gamma(\alpha s + c)$ or $\Gamma(s/\alpha + c)$ in the fractional world. When the coefficient of s is $\frac{1}{2}$, 1, or 2, the fractional distribution subsumes the classic distribution, since the Legendre duplication formula (A.2) becomes applicable.

The change may look simple in the Mellin space. But when it is transformed back to the x space, things become quite complicated. That is what makes it interesting and powerful.

The most important chapters of the book are

- Chapter 12 on the univariate GAS-SN distribution and
- Chapter 15 on the multivariate GAS-SN elliptical distribution.

[1]SPX data: Courtesy of S&P Dow Jones Indices LLC, from https://fred.stlouisfed.org/series/SP500. VIX data: Courtesy of Chicago Board Options Exchange (CBOE), from https://fred.stlouisfed.org/series/VIXCLS). Retrieved from FRED, Federal Reserve Bank of St. Louis. Not for commercial use.

The reader can think that the entire book is aimed at developing tools in order to create these two distributions.

The univariate GAS-SN distribution is supposed to be the most flexible two-sided distribution up to date for statisticians to fit a univariate data set, such as return distributions in finance.

The multivariate GAS-SN elliptical distribution is intended to be the most flexible multivariate distribution to date that extends the multivariate skew-t and skew-normal distributions[1].

A reference implementation can be found on Github at: https://github.com/slihn/gas-impl

---

This book is divided into three parts.

Part I describes the mathematical foundation needed for the construction of fractional distributions. It contains several higher transcendental functions. Several classic special functions are extended with a fractional parameter.

Each distribution has its density function (PDF) and distribution function (CDF). Its Mellin transform. The squared variable or quadratic forms. Therefore, new mathematical tools are needed to address them.

Part II contains the univariate one-sided fractional distributions that are invented. All of them have their classic counterparts. For example, the generalized gamma distribution (GG) is upgraded. All the χ and F related distributions are also upgraded.

Part III contains the two-sided univariate fractional distributions. The Azzalini (2013) book is used as the blueprint[1]. It is integrated with the symmetric distributions developed in my 2024 work[15].

This book can be viewed as an integration between the two works, literally going chapter-by-chapter. The consistency of such integration and harmony speaks volumes.

The fourth part contains the multivariate fractional distributions. These distributions are the super families of Part III. They subsumes and all the SN/ST distributions mentioned in Azzalini's book.

The major strength of fractional distributions integrated with SN is its ability to address a very wide range of skewness, kurtosis, and peak probability density. This allows a statistician to describe the statistics of her data set properly.

In the modern computer age, large amounts of data are collected in terms of both dimensionality and the number of samples. Tail behavior becomes more obvious. In the domain of finance, it is increasingly important to adequately capture the properties of the left tail.

An adaptive version of the multivariate distribution is developed to allow each dimension to have its own set of shape parameters. This distribution is where the rubber means the road. It is used to fit one of the most difficult data sets in finance: the daily returns from the SPX and VIX indices since 1990. And it works. The methodologies are presented.

Although the two multivariate distributions present new opportunities to fit the data sets that were thought impossible formerly, the outcomes post new challenges.

On the one hand, the maximum likelihood estimate (MLE) can be implemented in a straightforward manner for the elliptical distribution. The output (Figures 17.1, 17.2, 17.3) shows a very nice fit by MLE. But its choice of (α, k) lies in an area near infinite kurtosis when the bivariate distribution is projected to its two marginal 1D distributions. This behavior is quite puzzling.

On the other hand, the adaptive distribution suffers from the curse of dimensionality. A direct MLE approach is computationally prohibitive. A modified fitting algorithm is used. The output (Figures 17.4, 17.5, 17.6) is reasonable, but with a few flaws. The SPX marginal near $\alpha = 1, k = 3$ is intrinsically challenging. It is difficult to have a theoretical correlation coefficient that matches the empirical value (about -0.7). In the absolute term, the former is always lower than the latter. The quadratic form has not yet a matching F distribution.

Hope you enjoy this new statistical and mathematical adventure.

Part 1

Mathematical Functions

CHAPTER 2

Mellin Transform

We begin the book with some mathematical foundations. The reader who wishes to dive into the statistical distributions can skip the next two chapters.

The Mellin transform is crucial in the analysis of a statistical distribution. It is named after the Finnish mathematician Hjalmar Mellin, who first proposed it in 1897[21]. It provides insight into the inner workings of a statistical distribution and makes it analytically tractable. Once the Mellin transform of the density function (PDF) is known, the moment formula of the distribution is also known. In addition, derivatives of the PDF can also be obtained.

In particular, the relations between the Wright function, the α-stable distribution, and the fractional χ distribution are best described by their Mellin transforms.

DEFINITION 2.1. This chapter provides an overview of the Mellin transform. Following the notation of [19], the Mellin transform of a function $f(x)$ properly defined for $x \geq 0$ is

$$f^*(s) := \mathcal{M}\{f(x); s\} = \int_0^\infty f(x)\, x^{s-1}\, dx, \qquad c_1 < \mathbb{R}(s) < c_2. \tag{2.1}$$

The role of c_1, c_2 will be explained in the following.

If $f^*(s)$ has analytic continuation on the complex plane, the inverse Mellin transform is

$$f(x) = \mathcal{M}^{-1}\{f^*(s); x\} = \frac{1}{2\pi i} \int_{C-i\infty}^{C+i\infty} f^*(s)\, x^{-s}\, ds, \qquad c_1 < C < c_2. \tag{2.2}$$

From (2.1), it is obvious that the Mellin transform is directly related to the moments of a distribution. When $f(x)$ is the PDF of a one-sided distribution, its n-th moment is $\mathbb{E}(X^n|f) = f^*(n+1)$.

Hence, by modifying the Mellin transform $f^*(s)$, it is equivalent to constructing a new distribution based on the original distribution.

Introducing the juxtaposition notation $\overset{\mathcal{M}}{\longleftrightarrow}$, the above expressions, (2.1) and (2.2), are consolidated to a one-liner: $f(x) \overset{\mathcal{M}}{\longleftrightarrow} f^*(s)$, with a valid range $c_1 < C < c_2$ for C. This notation is much more concise. A correct specification for C is required when performing the Mellin integral in (2.2) numerically. Otherwise, it is irrelevant to the readers most of the time.

LEMMA 2.2. The main rules of Mellin transform used in this paper are:

$$f(ax) \overset{\mathcal{M}}{\longleftrightarrow} a^{-s}\, f^*(s), \qquad a > 0 \tag{2.3}$$

$$x^k f(x) \overset{\mathcal{M}}{\longleftrightarrow} f^*(s+k), \tag{2.4}$$

$$f(x^p) \overset{\mathcal{M}}{\longleftrightarrow} \frac{1}{p}\, f^*(s/p), \qquad p \neq 0 \tag{2.5}$$

and the following ones involving an integral,

$$h(x) = \int_0^\infty f(xs)g(s)\,sds \overset{\mathcal{M}}{\longleftrightarrow} h^*(s) = f^*(s)g^*(2-s), \qquad \text{(ratio distribution)} \tag{2.6}$$

$$\gamma_f(x) = \int_0^x f(x)\,dx \overset{\mathcal{M}}{\longleftrightarrow} -s^{-1}f^*(s+1), \qquad \text{(lower incomplete function)} \tag{2.7}$$

$$\Gamma_f(x) = \int_x^\infty f(x)\,dx \overset{\mathcal{M}}{\longleftrightarrow} s^{-1}f^*(s+1). \qquad \text{(upper incomplete function)} \tag{2.8}$$

The ratio distribution rule (2.6) is widely used in our fractional distribution system. Notice that the argument of $g^*(s)$ is transformed via $s \to 2-s$.

For (2.7) and (2.8), the valid range of C is decremented by one: $c_1 - 1 < C < c_2 - 1$.

△

Example 2.3. A simple exercise is the Mellin transform of the standard normal distribution. It starts with

$$e^{-x} \overset{\mathcal{M}}{\longleftrightarrow} \Gamma(s)$$

via the definition of the gamma function itself.

By applying (2.5) then (2.3), we get

$$\mathcal{N}(x) \overset{\mathcal{M}}{\longleftrightarrow} \mathcal{N}^*(s) = \frac{2^{(s-3)/2}}{\sqrt{\pi}}\,\Gamma\left(\frac{s}{2}\right) \tag{2.9}$$

where $\mathcal{N}(x) = \frac{1}{\sqrt{2\pi}}e^{-x^2/2}$ is our notation for the PDF of a standard normal distribution.

Example 2.4. A slightly more complicated exercise is the Mellin transform of the PDF of the fractional gamma distribution (FG) in Chapter 6. But we only work out its skeleton here.

Assume we have a function $F_\alpha(x)$ whose Mellin transform is

$$F_\alpha(x) \overset{\mathcal{M}}{\longleftrightarrow} \frac{\Gamma(s)}{\Gamma(\alpha s)}.$$

It undergoes the following transforms:

$$F_\alpha(x^p) \overset{\mathcal{M}}{\longleftrightarrow} \frac{1}{|p|}\frac{\Gamma(s/p)}{\Gamma(\alpha s/p)},$$
$$x^{d-1}\,F_\alpha(x^p) \overset{\mathcal{M}}{\longleftrightarrow} \frac{1}{|p|}\frac{\Gamma((s+d-1)/p)}{\Gamma(\alpha(s+d-1)/p)},$$

which is the prototype of FG before further normalization.

2.1. Distribution Function and Moments

If $f(x)$ is a density function of a distribution, the two rules of incomplete functions provide a clear path to obtain its distribution function (CDF). On the one hand, if the distribution is one-sided, then $\gamma_f(x)$ is its CDF obviously.

2.1.1. Mellin Transform of a Two-sided CDF. On the other hand, assume the distribution is two-sided and the density function satisfies the *reflection rule* based on a skew parameter:

$$f(-x;\beta) := f(x;-\beta) \quad \text{for } x > 0.$$

In addition, assume that

$$\int_0^\infty f(x;\beta)\,dx = c_\beta < 1.$$

which leads to $c_{-\beta} + c_\beta = 1$. Then we have

LEMMA 2.5. The Mellin transform of the CDF $\Phi(x)$ of a two-sided distribution has two parts. Both can be derived from its density function transform, $f(x;\beta) \overset{\mathcal{M}}{\longleftrightarrow} f^*(s;\beta)$, in the positive domain.

From (2.7), let $\gamma_f(x;\beta) \overset{\mathcal{M}}{\longleftrightarrow} \Phi^*(s;\beta) := -s^{-1}f^*(s+1;\beta)$. Then for $x > 0$, the Mellin transform of the CDF can be expressed as

$$\Phi(x) - \Phi(0) \overset{\mathcal{M}}{\longleftrightarrow} \Phi^*(s;\beta),$$
$$1 - \Phi(0) - \Phi(-x) \overset{\mathcal{M}}{\longleftrightarrow} \Phi^*(s;-\beta).$$

△

PROOF. Note that $\Phi(0) = c_{-\beta} = 1 - c_\beta$. When $x \geq 0$, its CDF is

$$\Phi(x) = \int_{-\infty}^{x} f(x;\beta)\,dx \;= c_{-\beta} + \int_0^x f(x;\beta)\,dx \;= \Phi(0) + \gamma_f(x;\beta).$$

In the negative domain, its CDF is

$$\begin{aligned}\Phi(-x) = \int_{-\infty}^{-x} f(x;\beta)\,dx \;&= \int_x^{\infty} f(x;-\beta)\,dx \\ &= 1 - \Phi(0) - \int_0^x f(x;-\beta)\,dx \;= 1 - \Phi(0) - \gamma_f(x;-\beta).\end{aligned}$$

□

The point is that, once the Mellin transform of either the PDF or CDF is known, the other one can be derived by simple algebraic rules.

2.1.2. From Mellin Transform to Moments. By assigning $s = n+1$, it is easy to show that its n-th moment is

$$\mathbb{E}(X^n|f) = f^*(n+1;\beta) + (-1)^n f^*(n+1;-\beta) \tag{2.10}$$
$$= -n\big[\Phi^*(n;\beta) + (-1)^n\Phi^*(n;-\beta)\big] \tag{2.11}$$

The moment formula is tightly linked to $\Phi^*(n;\beta)$.

The total density can be regarded as the zeroth moment. Hence,

$$c_\beta = \int_0^\infty f(x;\beta)dx = f^*(1;\beta). \tag{2.12}$$

Its application is in (10.9).

2.2. Ramanujan's Master Theorem

In order to keep things simple, we anchor all the distributions via the Mellin transform of their PDFs. Due to Ramanujan's master theorem[3], not only can the moments be obtained from the Mellin transform but also all the derivatives of the PDF at $x = 0$. We get its series representation "for free", so to speak.

LEMMA 2.6 (Ramanujan's master theorem). If $f(x)$ has an expansion of the form

$$f(x) = \sum_{n=0}^{\infty} \frac{\varphi(n)}{n!}(-x)^n \tag{2.13}$$

then its Mellin transform is given by

$$f(x) \overset{\mathcal{M}}{\longleftrightarrow} f^*(s) = \Gamma(s)\,\varphi(-s) \tag{2.14}$$

△

Assume that $g^*(s) := f^*(s)/\Gamma(s)$ exists on the complex plane, $s \in \mathbb{C}$. Its connection to the derivatives of the PDF at $x = 0$ is as follow.

LEMMA 2.7. The Taylor series of $f(x)$ is

$$f(x) = \sum_{n=0}^{\infty} \frac{f^{(n)}(0)}{n!} x^n$$

where $f^{(n)}(0)$ is the n-th derivative of $f(x)$ at $x = 0$.

Then $f^{(n)}(0)$ can be obtained from $g^*(s)$ by

$$f^{(n)}(0) = (-1)^n g^*(-n) \tag{2.15}$$

At $x = 0$, we have $f(0) = g^*(0)$.

△

The power of the master theorem is that, once the Mellin transform is known, the Taylor series is also known immediately. We provide a contrived example from next chapter as a showcase.

EXAMPLE 2.8. The Mellin transform of the Wright function from (3.5) is $f(-x) \overset{\mathcal{M}}{\longleftrightarrow} f^*(s) = \Gamma(s)/\Gamma(\delta - \lambda s)$. Then its $g^*(s) = 1/\Gamma(\delta - \lambda s)$.

According to Lemma 2.7, its Taylor series should be

$$f(-x) := \sum_{n=0}^{\infty} \frac{(-1)^n g^*(-n)}{n!} x^n = \sum_{n=0}^{\infty} \frac{g^*(-n)}{n!} (-x)^n$$

Replace $-x$ with z, and plug in $g^*(-n)$, we have

$$f(z) := \sum_{n=0}^{\infty} \frac{z^n}{n!\,\Gamma(\lambda n + \delta)}$$

This is the series representation (3.1) where we essentially "derived" it from the master theorem.

The major application in this book is in Chapter 11. In the experimental construction of the generalized α-stable distribution, the theorem is used to remedy the discontinuity of the PDF in $x = 0$.

2.2.1. Distribution Function. The form of the Mellin transform in (2.14) has an important implication when $f(x)$ is a density function.

LEMMA 2.9. Assume $x > 0$, its complimentary distribution function $\Gamma_f(x) := \int_x^{\infty} f(x)\,dx$ has the series representation of

$$\Gamma_f(x) = \sum_{n=0}^{\infty} \frac{\varphi(n-1)}{n!} (-x)^n \tag{2.16}$$

△

PROOF. From (2.8), the Mellin transform of $\Gamma_f(x)$ is

$$\Gamma_f(x) = \int_x^{\infty} f(x)\,dx \overset{\mathcal{M}}{\longleftrightarrow} s^{-1} f^*(s+1)$$

which can be simplified to

$$\begin{aligned} s^{-1} f^*(s+1) &= s^{-1}\Gamma(s+1)\,\varphi(-s-1) \\ &= \Gamma(s)\,\varphi(-s-1). \end{aligned}$$

This is still in the form of (2.14), with a transformation rule of $s \to s+1$ in the function $\varphi(-s)$.

Applying the master theorem of (2.13), we get (2.16).

□

We use the CDF of the M-Wright function from (3.16) as an example.

LEMMA 2.10. The goal is to show

$$\int_x^\infty M_\alpha(t)dt = W_{-\alpha,1}(-x). \tag{2.17}$$

△

PROOF. We start with the Mellin transform of $M_\alpha(x)$ from (3.13),

$$M_\alpha(x) \overset{\mathcal{M}}{\longleftrightarrow} M_\alpha^*(s) = \frac{\Gamma(s)}{\Gamma((1-\alpha)+\alpha s)}$$

which yields $\varphi(-s) = 1/\Gamma((1-\alpha)+\alpha s)$.

Therefore, its $\Gamma_f(x)$ should be

$$\Gamma_f(x) = \sum_{n=0}^\infty \frac{1}{n!\,\Gamma((1-\alpha)-\alpha(n-1))}(-x)^n = \sum_{n=0}^\infty \frac{1}{n!\,\Gamma(-\alpha n+1)}(-x)^n$$

which is $W_{-\alpha,1}(-x)$ according to (3.1).

□

CHAPTER 3

The Wright Function

3.1. Definition

The Wright function is the most basic building block in our fractional distribution system. It was proposed by E. M. Wright in the 1930s[34, 35]. Bateman recorded this function together with the Mittag-Leffler function in the 1930s[2].

Its importance was gradually noticed since the late 1980's, especially through the works of F. Mainardi, who proposed the M-Wright function $M_\alpha(x)$. $M_\alpha(x)$ is considered the fractional extension of the exponential function e^{-x}. Such logic appears in many places of this book. This chapter provides an overview.

DEFINITION 3.1. The series representation of the Wright function is

$$W_{\lambda,\delta}(z) := \sum_{n=0}^{\infty} \frac{z^n}{n!\,\Gamma(\lambda n + \delta)} \qquad (\lambda \geq -1, z \in \mathbb{C}) \tag{3.1}$$

Its shape parameters are pairs (λ, δ). The apparent limit is $W_{0,1}(z) = e^z$.

The author used four variants extensively. The first group of two are

- $M_\alpha(z) := W_{-\alpha,1-\alpha}(-z)$
- $F_\alpha(z) := W_{-\alpha,0}(-z)$

where $\alpha \in [0, 1]$. They are related to each other by $M_\alpha(z) = F_\alpha(z)/(\alpha z)$.

In particular, $M_\alpha(z)$ is called *the M-Wright function* or simply *the Mainardi function*[16, 20, 17]. See Section 3.3 for further details. Conceptually, *fractional extension* of a classic exponential-based function is based on two important properties: $M_0(z) = \exp(-z)$ and $M_{\frac{1}{2}}(z) = \frac{1}{\sqrt{\pi}} \exp(-z^2/4)$.

The second group of the two are

- $W_{-\alpha,-1}(-z)$
- $-W_{-\alpha,1-2\alpha}(-z)$

The author discovers their usefulness. They are associated with the derivatives of $F_\alpha(z)$ and $M_\alpha(z)$, for the generation of random variables, such as in (3.18) and Section 11 of [15]. In some cases, they lead to beautiful polynomial solutions.

3.2. Classic Results

The recurrence relations of the Wright function are (Chapter 18, Vol 3 of [2])

$$\lambda z\, W_{\lambda,\lambda+\mu}(z) = W_{\lambda,\mu-1}(z) + (1-\mu) W_{\lambda,\mu}(z) \tag{3.2}$$

$$\frac{d}{dz} W_{\lambda,\mu}(z) = W_{\lambda,\lambda+\mu}(z) \tag{3.3}$$

The moments of the Wright function are (See (1.4.28) of [20])

$$\mathbb{E}(X^{d-1}) = \int_0^\infty x^{d-1} W_{-\lambda,\delta}(-x) dx = \frac{\Gamma(d)}{\Gamma(d\lambda + \delta)} \tag{3.4}$$

The way it is written is in fact its Mellin transform:

$$W_{\lambda,\delta}(-x) \overset{\mathcal{M}}{\longleftrightarrow} W^*_{\lambda,\delta}(s) = \frac{\Gamma(s)}{\Gamma(\delta - \lambda s)} \tag{3.5}$$

$W_{\lambda,\delta}(z)$ has the following Hankel integral representation:

$$W_{\lambda,\delta}(z) = \frac{1}{2\pi i} \int_H dt\, \frac{\exp\left(t + z\, t^{-\lambda}\right)}{t^\delta} \tag{3.6}$$

Prodanov[27] derived an integral form of the Wright function. We focus on the branch of $\lambda < 0$ and $\delta \leq 1$ from Theorem 1 there, such that

$$W_{\lambda,\delta}(z) = \frac{1}{\pi} \int_0^\infty \frac{dr}{r^\delta}\, \sin(\sin(\lambda\pi)w + \delta\pi)\, e^{\cos(\lambda\pi)w - r}, \quad \text{where } w = z\, r^{-\lambda}. \tag{3.7}$$

This integral can be calculated by the tanh-sinh quadrature with a reasonable speed.

The four-parameter Wright function is defined as

$$W\begin{bmatrix} a, & b \\ \lambda, & \mu \end{bmatrix}(z) := \sum_{n=0}^{\infty} \frac{z^n}{\Gamma(n+1)} \frac{\Gamma(an+b)}{\Gamma(\lambda n + \mu)} \tag{3.8}$$

This function is a higher-order Wright function. It was used seriously for the first time by the author[15].

3.3. The M-Wright Functions

Mainardi has introduced two auxiliary functions of Wright type (see F.2 of [16]). Assume $\alpha \in [0, 1]$,

$$F_\alpha(z) := W_{-\alpha,0}(-z) \qquad (z > 0) \tag{3.9}$$

$$M_\alpha(z) := W_{-\alpha,1-\alpha}(-z) = \frac{1}{\alpha z} F_\alpha(z) \qquad (z > 0) \tag{3.10}$$

The relation between $M_\alpha(z)$ and $F_\alpha(z)$ in (3.10) is an application of (3.2) by setting $\lambda = -\alpha, \mu = 1$.

$F_\alpha(z)$ has the following Hankel integral representation:

$$F_\alpha(z) = \frac{1}{2\pi i} \int_H dt\, \exp\left(t - z t^\alpha\right) \tag{3.11}$$

Both functions have simple Mellin transforms from (3.5):

$$F_\alpha(x) \overset{\mathcal{M}}{\longleftrightarrow} F^*_\alpha(s) = \frac{\Gamma(s)}{\Gamma(\alpha s)} \tag{3.12}$$

$$M_\alpha(x) \overset{\mathcal{M}}{\longleftrightarrow} M^*_\alpha(s) = \frac{\Gamma(s)}{\Gamma((1-\alpha) + \alpha s)} \tag{3.13}$$

$F_\alpha(z)$ is used to define fractional one-sided distributions. But its series representation isn't very useful computationally. It requires many more terms to converge to a prescribed precision.

On the other hand, $M_\alpha(z)$ has a more computationally friendly series representation, especially for small α's:

$$M_\alpha(z) = \sum_{n=0}^{\infty} \frac{(-z)^n}{n!\,\Gamma(-\alpha n + (1-\alpha))} = \frac{1}{\pi} \sum_{n=1}^{\infty} \frac{(-z)^{n-1}}{(n-1)!} \Gamma(\alpha n) \sin(\alpha n \pi) \qquad (0 < \alpha < 1) \tag{3.14}$$

$M_\alpha(z)$ also has very nice analytic properties at $\alpha = 0, 1/2$, where $M_0(z) = \exp(-z)$ and $M_{\frac{1}{2}}(z) = \frac{1}{\sqrt{\pi}} \exp(-z^2/4)$. $M_\alpha(0) = 1/\Gamma(1-\alpha)$ is monotonically decreasing from 1 to 0 as α increases from 0 to 1.

$M_\alpha(z)$ can be computed to high accuracy when properly implemented with arbitrary-precision floating point library, such as the `mpmath` package[22]. In this regard, it is much more "useful" than $F_\alpha(z)$.

This is particularly important in working with large degrees of freedom and extreme values of α, mainly close to 0 and 1. The typical 64-bit floating-point algorithm suffers from overflow and/or underflow. See Section 3.7 for more details.

$M_\alpha(z)$ has the asymptotic representation in the *generalized gamma* (GG) style: (see F.20 of [16])

$$M_\alpha\left(\frac{x}{\alpha}\right) = A\, x^{d-1}\, e^{-B\, x^p} \tag{3.15}$$
$$\text{where } p = 1/(1-\alpha), d = p/2,\ A = \sqrt{p/(2\pi)},\ B = 1/(\alpha p).$$

Additional correction terms in the asymptotic expansion have been derived up to the order $x^{-6/(1-\alpha)}$[26]. This formula is important in guiding (3.14) to high precision for large x, where the series representation often fails to converge.

$M_\alpha(x)$ can be used as the density function of a one-sided distribution[17], because $\int_0^\infty M_\alpha(x)dx = 1$ and $M_\alpha(x)$ for $x \geq 0$. Its CDF is another Wright function:

$$\int_0^x M_\alpha(t)dt = 1 - W_{-\alpha,1}(-x). \tag{3.16}$$

This is proved in Lemma 2.10.

The absolute moments of $M_\alpha(x)$ in $\mathbb{R}^+$ are

$$\int_0^\infty t^n\, M_\alpha(t)dt = \frac{\Gamma(n+1)}{\Gamma(n\alpha+1)}, \quad n > -1. \tag{3.17}$$

Hence, its mean is located at $1/\Gamma(\alpha+1)$, which is equal to 1 when $\alpha = 0, 1$. Its variance is $2/\Gamma(2\alpha+1) - 1/\Gamma(\alpha+1)^2$. The variance becomes zero when $\alpha = 1$, consistent with $M_1(x) = \delta(x-1)$.

Differentiating $M_\alpha(z)$, and from (3.14), we get

$$\frac{d}{dz}M_\alpha(z) = -W_{-\alpha,1-2\alpha}(-z) = \frac{-1}{\pi}\sum_{n=2}^{\infty}\frac{(-z)^{n-2}}{(n-2)!}\Gamma(\alpha n)\sin(\alpha n\pi) \tag{3.18}$$

Note that $\frac{d}{dz}M_\alpha(0) = -\frac{1}{\pi}\Gamma(2\alpha)\sin(2\alpha\pi)$. This also indicates that

$$\frac{d}{dz}F_\alpha(z) = \alpha\left(1 + z\frac{d}{dz}\right)M_\alpha(z) \tag{3.19}$$

which can be implemented from $M_\alpha(z)$ through (3.14) and (3.18). These differential forms lead to the concept of elasticity in Section 3.5 and below.

3.4. The Fractional Gamma-Star Function

The so-called γ^* function is documented in 8.2.6 and 8.2.7 of DLMF[6]. It is defined as follows:

$$\gamma^*(s,x) := \frac{1}{\Gamma(s)}\int_0^1 t^{s-1}\, e^{-xt}\, dt = \frac{x^{-s}}{\Gamma(s)}\gamma(s,x)$$

The finite integral in $t \in [0,1]$ is transformed from the incomplete gamma function, which takes the form of $\gamma(s,x) = \int_0^x t^{s-1}\, e^{-t}\, dt$.

$\gamma^*(s,x)$ can be extended fractionally in a straightforward manner. It is used to calculate the CDF of the FG in Chapter 6. See (6.7) for details.

Definition 3.2 (The fractional γ^* function). It is defined by replacing e^{-xt} with $M_\alpha(xt)$ such that

$$\gamma^*_\alpha(s,x) := \frac{\Gamma((1-\alpha)+\alpha s)}{\Gamma(s)}\int_0^1 dt\, t^{s-1}\, M_\alpha(xt) \tag{3.20}$$

The $\alpha \to 0$ limit of $\gamma^*_\alpha(s,x)$ subsumes the classic γ^* function, that is, $\gamma^*_0(s,x) = \gamma^*(s,x)$. This is reflected in the simple fact that $M_0(xt) = \exp(-xt)$.

The γ^* function is a subset of the fractional confluent hypergeometric function in Lemma 5.4.

3.5. The Elasticity Operator

In (3.18) and (3.19), we encountered an important mathematical structure called "elasticity" which will be used in Chapter 13. It provides an elegant view of the inner structure of the FG density functions.

DEFINITION 3.3 (The elasticity operator). Assume $f(x)$ is differentiable for $x \in \mathbb{R}$. The elasticity of $f(x)$ is defined as

$$\mathcal{L}\, f(x) := \frac{x}{f(x)} \frac{d}{dx} f(x) \tag{3.21}$$

$$= \frac{d \log f(x)}{d \log x}, \quad \text{when } x > 0 \text{ and } f(x) > 0. \tag{3.22}$$

The second line can be interpreted as the percentage change of $f(x)$ over a percentage change of x. This is often used in statistics and economics. (It is an extension of the Euler dilation operator, $x \frac{d}{dx}$.)

To illustrate its property, if $f(x) \sim x^k$ locally, then $\mathcal{L}\, f(x) \approx k$. It informs *local degree of homogeneity* in the scaling analysis.

More generally, some algebraic rules of $\mathcal{L}$ are

- $\mathcal{L}\,[f(x)\, g(x)] = \mathcal{L}\, f(x) + \mathcal{L}\, g(x)$; multiplication becomes addition.
- $\mathcal{L}\,[f(g(x))] = \mathcal{L}\, g(x) \times [\mathcal{L}\, f](g(x))$; composition becomes multiplication.
- $\mathcal{L}\,(x^k) = k$; the trivial case is $\mathcal{L}\,(x) = 1$.
- $\mathcal{L}\,(e^{-x}) = -x$;
- $\mathcal{L}\,(\text{constant})$ is zero;

As an application, it is a good exercise to derive $\mathcal{L}\,[f((x/\sigma)^p)] = p\,[\mathcal{L}\, f]((x/\sigma)^p)$.

The recurrence relations of the Wright function, (3.2) and (3.3), can be rewritten using the $\mathcal{L}$ operator. They become two expressions of the elasticity of the Wright function.

Define the ratio of two Wright functions as

$$Q_{\lambda,\mu,\delta}(z) = \frac{W_{\lambda,\mu+\delta}(z)}{W_{\lambda,\mu}(z)}. \tag{3.23}$$

It follows immediately that (3.2) becomes

$$\lambda z\, Q_{\lambda,\mu,\lambda}(z) = Q_{\lambda,\mu,-1}(z) + 1 - \mu. \tag{3.24}$$

LEMMA 3.4. The elasticity of the Wright function is expressed by the following ratios:

$$\mathcal{L}\, W_{\lambda,\mu}(z) = \frac{1}{\lambda} Q_{\lambda,\mu,-1}(z) + \frac{1-\mu}{\lambda}, \tag{3.25}$$

$$\mathcal{L}\, W_{\lambda,\mu}(z) = z\, Q_{\lambda,\mu,\lambda}(z). \tag{3.26}$$

△

PROOF. The second line is straightforward from (3.3). The first line is derived from the second line by replacing the $z\, Q_{\lambda,\mu,\lambda}(z)$ term on the RHS with (3.24).

□

3.6. The Elasticity of the M-Wright Functions

What we are most interested in is the elasticity of $M_\alpha(x)$:

$$\mathcal{L}\, M_\alpha(x) = [\mathcal{L}\, W_{-\alpha,1-\alpha}](-x) \tag{3.27}$$

which is from (3.10). Note that $\mathcal{L}\, F_\alpha(x)$ is trivial if $\mathcal{L}\, M_\alpha(x)$ is known. This is due to (3.19), we have

$$\mathcal{L}\, F_\alpha(x) = \mathcal{L}\, M_\alpha(x) + 1. \tag{3.28}$$

However, $\mathcal{L}\, F_\alpha(x)$ has a representation that is more friendly to FCM. From (3.25),

$$\mathcal{L}\, F_\alpha(x) = [\mathcal{L}\, W_{-\alpha,0}](-x) = \frac{1}{\alpha} Q_\alpha(x) - \frac{1}{\alpha}, \tag{3.29}$$

$$\text{where} \quad Q_\alpha(x) := -Q_{-\alpha,0,-1}(-x) = -\frac{W_{-\alpha,-1}(-x)}{W_{-\alpha,0}(-x)}. \tag{3.30}$$

It follows that $Q_\alpha(x) = \alpha\, \mathcal{L}\, M_\alpha(x) + (1+\alpha)$.

The following lemma converts the elasticity of the FG PDF to either $\mathcal{L}\, M_\alpha(x)$ or $Q_\alpha(x)$.

LEMMA 3.5. Let $\mathfrak{N}(x)$ represent the functional form of FG PDF (6.1) where $\mathfrak{N}(x) = x^{d-1} F_\alpha\left(\left(\frac{x}{\sigma}\right)^p\right)$ (apart from a constant multiplier). The elasticity of $\mathfrak{N}(x)$ is

$$\mathcal{L}\, \mathfrak{N}(x) = p\, [\mathcal{L}\, M_\alpha]\big((x/\sigma)^p\big) + (d + p - 1). \tag{3.31}$$

Alternatively, a useful ratio form for the FCM where p/α is a constant is

$$\mathcal{L}\, \mathfrak{N}(x) = \frac{p}{\alpha}\, Q_\alpha\left(\left(\frac{x}{\sigma}\right)^p\right) - \frac{p}{\alpha} + (d-1). \tag{3.32}$$

We observe that the role of the degrees of freedom d is very simple in $\mathcal{L}\, \mathfrak{N}(x)$. It shifts the constant level, but it does not affect the shape of $\mathcal{L}\, \mathfrak{N}(x)$.

△

$\mathcal{L}\, M_\alpha(x)$ has simple behaviors in a few cases. For example,

$$\mathcal{L}\, M_0(x) = -x;$$
$$\mathcal{L}\, M_{1/2}(x) = -x^2/2.$$

When $x \to 0$,

$$\mathcal{L}\, M_\alpha(x) \sim -b_1 x, \qquad \text{where } b_1 := \frac{\Gamma(1-\alpha)}{\Gamma(1-2\alpha)}. \tag{3.33}$$

When $\alpha \in [0, 1/2]$, $\mathcal{L}\, M_\alpha(x) < 0$ for all $x > 0$. It is a monotonically decreasing function for $x \in [0, \infty)$.

When $x \to \infty$, the GG-style asymptotic form in (3.15) leads to

$$\mathcal{L}\, M_\alpha(x) \sim -\alpha^{\alpha/(1-\alpha)}\, x^{1/(1-\alpha)} + \frac{\alpha - 1/2}{1-\alpha}, \tag{3.34}$$

in which the first term is dominant. It leads to the asymptotic limit of second-order elasticity:

$$\lim_{x\to\infty} \mathcal{L}[-\mathcal{L}\, M_\alpha](x) \to \frac{1}{1-\alpha}. \tag{3.35}$$

It follows immediately from (3.26) that (with $z \to -x$)

$$\mathcal{L}\, M_\alpha(x) = -x\, \frac{W_{-\alpha,1-2\alpha}(-x)}{W_{-\alpha,1-\alpha}(-x)} = -x\, Q_{-\alpha,1-\alpha,-\alpha}(-x) \tag{3.36}$$

where the series form of the numerator is in (3.18). We can compute the numerator and denominator individually, then take the ratio. Or we can derive its series representation as follows.

LEMMA 3.6. The series representation of $\mathcal{L}\,M_\alpha(x) = -x\,Q_{-\alpha,1-\alpha,-\alpha}(-x)$ is

$$\mathcal{L}\,M_\alpha(x) = \sum_{k=1}^{\infty} c_k x^k$$

where

$$c_k = \frac{(-1)^k}{(k-1)!}\,b_k + \sum_{j=1}^{k-1} \frac{(-1)^{(j+1)}}{j!}\,b_j\,c_{k-j}, \qquad k \geq 1; \tag{3.37}$$

$$b_n = \frac{\Gamma\big(1-\alpha\big)}{\Gamma\big(1-\alpha(n+1)\big)}, \qquad n \geq 1. \tag{3.38}$$

△

PROOF. From (3.14), we have

$$M_\alpha(x) = \sum_{n=0}^{\infty} a_n x^n, \qquad a_n = \frac{(-1)^n}{n!\,\Gamma\big(1-\alpha(n+1)\big)}.$$

Then (3.18) can be written as

$$\frac{d}{dx} M_\alpha(x) = -W_{-\alpha,1-2\alpha}(-x) = \sum_{n=1}^{\infty} n\,a_n x^{n-1}.$$

And

$$x\frac{M'_\alpha(x)}{M_\alpha(x)} = \frac{\displaystyle\sum_{n\geq 1} n\,a_n\,x^n}{\displaystyle\sum_{n\geq 0} a_n\,x^n}.$$

The coefficients satisfy the standard recurrence of series divisions, which becomes

$$c_k = \frac{1}{a_0}\left(k\,a_k - \sum_{j=1}^{k-1} a_j\,c_{k-j}\right), \qquad k \geq 1.$$

With $a_0 = \dfrac{1}{\Gamma(1-\alpha)}$, and $\dfrac{a_n}{a_0} = \dfrac{(-1)^n}{n!} b_n$, it leads to (3.37) and (3.38).

□

REMARK 3.7. The first three coefficients are explicitly derived as follows.

$$c_1 = -b_1 = -\frac{\Gamma(1-\alpha)}{\Gamma(1-2\alpha)},$$

$$c_2 = b_2 - b_1^2 = \frac{\Gamma(1-\alpha)}{\Gamma(1-3\alpha)} - \left(\frac{\Gamma(1-\alpha)}{\Gamma(1-2\alpha)}\right)^2,$$

$$c_3 = -\frac{1}{2}b_3 + \frac{3}{2}b_2 b_1 - b_1^3 = -\frac{\Gamma(1-\alpha)}{2\,\Gamma(1-4\alpha)} + \frac{3}{2}\,\frac{\Gamma(1-\alpha)^2}{\Gamma(1-2\alpha)\,\Gamma(1-3\alpha)} - \left(\frac{\Gamma(1-\alpha)}{\Gamma(1-2\alpha)}\right)^3.$$

The small-x expansion up to the x^3 term is

$$\mathcal{L}\,M_\alpha(x) = \left[-\frac{\Gamma(1-\alpha)}{\Gamma(1-2\alpha)}\right] x + \ c_2 x^2 + \ c_3 x^3 + O(x^4).$$

3.7. Numerical Methods of the M-Wright Functions

To properly compute the subsequent special functions and distributions in this book, we need a very robust numerical implementation of $F_\alpha(x)$ and $M_\alpha(x)$ for *the entire range* of $\alpha \in [0,1]$ and $x \geq 0$. Since $F_\alpha(x) = \alpha x\, M_\alpha(x)$, we can easily compute one from the other in most cases. It is a matter of which approach is faster, more convenient, and precise.

3.7.1. Handling alpha for zero and one. When $\alpha = 0$, we should use $M_0(x) = e^{-x}$. $\lim_{\alpha\to 0} F_\alpha(x)$ should be handled carefully in the fractional gamma distribution.

When $\alpha = 1$, we could use a normal distribution to simulate the delta function: $M_1(x) = \mathcal{N}(x; 1, \sigma^2)$ where $\sigma = 0.001$. This is to ensure that $\int_0^\infty M_1(x)\,dx = 1$.

3.7.2. Using scipy.stats.levy-stable. Both functions can be derived from the one-sided α-stable distribution $L_\alpha(x)$ of Section 4.2, which is implemented in `scipy.stats.levy_stable` package[**33**].

For example, $M_\alpha(x)$ can be computed using $L_\alpha(x) = \alpha x^{-\alpha-1} M_\alpha(x^{-\alpha})$ where $x > 0$. On the other hand, for $\beta > 1/2$, we can also use $M_\beta(x) = \alpha L_\alpha^{\alpha-2}(x)$ where $\beta = 1/\alpha$.

These two numerical methods are good for the bulk of α and x. However, they begin to lose precision for small $\alpha < 0.08$ and large $\alpha > 0.99$. They are also not good enough for small $x < 0.01$.

3.7.3. Using the series sum in numpy. Based on (3.14), we define the sum of the series of finite terms as

$$M_\alpha^{(m)}(x) = \frac{1}{\pi} \sum_{n=1}^{m} \frac{(-x)^{n-1}}{(n-1)!} \Gamma(\alpha n) \sin(\alpha n \pi). \qquad (0 < \alpha < 1) \tag{3.39}$$

This method implemented in `numpy` and `scipy` is good for several scenarios. First, to cover the small x area ($x < 0.01$), use $M_\alpha^{(7)}(x)$ if $\alpha < 0.9$.

Otherwise, we could use $M_\alpha^{(80)}(x)$ for $\alpha \leq 0.998$ and $x < 0.85$. The sum of 80 terms takes more time to compute. But it is a necessary path when `scipy.stats.levy_stable` approach loses precision.

3.7.4. Using the series sum in mpmath. $M_\alpha^{(m)}(x)$ implemented in `mpmath` is our de facto implementation to calibrate the precision of other approaches. In order to make it a good baseline implementation, we must carefully choose `mp.prec` and m to use.

After rigorous testing, it was found that `mp.prec` >= 64 provides sufficient precision. Therefore, `mp.prec` = 128 is more than abundant up to three decimal points in α. `mpmath` is smart about handling summing many small terms, especially with large amount of cancellation due to the $\sin(\alpha n\pi)$ factor in (3.39).

The more crucial choice is m, where $m = 40,000$ is enough for $\alpha < 0.9$. Much larger m ($m = 80,000$) is needed for α very close to 1 ($\alpha = 0.998$). Obviously, a very large m makes the series sum more compute-intensive. This can be used during the calibration phase, but not for the actual numpy-style implementation.

This will be elaborated on in the next section.

3.7.5. Using the asymptotic approximation. Paris et al. [**26**] derived a more refined asymptotic formula, where (3.15) is simply its first term. Theorem 2.2 of that paper is recaptured in the following.

Lemma 3.8.

$$M_\alpha(x) \sim \frac{A(\alpha)}{2\pi} X^{\alpha-1/2} e^{-X} \sum_{n=0}^{\infty} c_j(\alpha)(-X)^{-j}. \qquad (0 < \alpha < 1) \tag{3.40}$$

where $c_j(\alpha)$ is in its (2.4) up to $j = 6$. Other parameters are $A(\alpha) = \sqrt{\frac{2\pi}{\alpha}} \left(\frac{\alpha}{\kappa}\right)^\alpha$ and $X = \kappa(hx)^{1/\kappa}$ with $\kappa = 1 - \alpha$ and $h = \alpha^\alpha$.

△

When $M_\alpha(x)$ is small, (3.40) could be very precise with an error as small as 10^{-5}. Our strategy is to use other implementations to get $M_\alpha(x)$ to a small number, e.g. 10^{-6} in most cases, and at least 10^{-3} in some difficult cases. Then use (3.40) for larger x up to infinity (the maximum 64-bit float).

This right-tail strategy works for the bulk of α from 0.1 to 0.9. The transition interval (defined as $M_\alpha(x) \in [10^{-5}, 10^{-6}]$) could be precomputed by the faster (3.15).

For α from 0.9 to 0.99, the `mpmath` version of $M_\alpha^{(m)}(x)$ is more precise to determine the transition interval.

For α from 0.001 to 0.1, the asymptotic form is adjusted to

$$M_\alpha(x) \sim A'(\alpha)\, e^{-B'(\alpha)X'}, \quad \text{where } X' = x^{1/\kappa}. \tag{3.41}$$

$A'(\alpha)$ and $B'(\alpha)$ are obtained from a linear regression in the transition interval: $\log M_\alpha(x) \sim \log A'(\alpha) - B'(\alpha)X'$.

3.7.6. Using the integral form. For α from 0.99 to 0.998, the `scipy` version of $M_\alpha(x)$ loses precision very quickly in the right tail. We use (3.7) to supplement this deficiency for this range of α as long as $M_\alpha(x) > 10^{-3}$.

The numerical difficulty arises in the integral when the target $M_\alpha(x)$ is very small. The integrand in (3.7) becomes fast oscillating and is non-zero only in a very small range of r^δ. It is hard for existing integration algorithms to detect this small range, capture these oscillations, and perform the cancellation properly. A more sophisticated quadrature integration algorithm is needed. It is left for future research.

For $M_\alpha(x) < 10^{-3}$ at large x, we still use (3.40) asymptotically. This equation is fine for large α, as long as the numeric overflow is handled properly.

CHAPTER 4

The Alpha-Stable Distribution - Review

The two-sided distributions in this book are based on the α-stable distribution, which was published in the seminal 1925 book of Paul Lévy[12]. These distributions have a major parameter, among others, called *the stability index* $\alpha \in (0, 2]$. We call it the *fractional* parameter.

In this chapter, we provide a review of the α-stable distribution based on the Mellin transform framework. This framework lays the foundation for further generalization in subsequent chapters.

The ratio distribution approach for its density function in Section 4.3 is invented by the author.

4.1. Classic Result

The α-stable distribution has two shape parameters. There are many parametrizations that have been studied (see p.5 of [24]). We are primarily concerned with Feller's (α, θ) parametrization[8, 9], where α is called the stability index with a range of $0 < \alpha \leq 2$, and θ is an angle that injects skewness to the distribution when it is not zero.

An innovative approach is to study its Mellin transform. This presentation is used because it is *simpler* and provides great insight into its structure.

LEMMA 4.1. The Mellin transform of its PDF is

$$L_\alpha^\theta(x) \overset{\mathcal{M}}{\longleftrightarrow} \epsilon \frac{\Gamma(s)\Gamma(\epsilon(1-s))}{\Gamma(\gamma(1-s))\Gamma(1-\gamma+\gamma s)} \tag{4.1}$$

$$\text{where } \epsilon = \frac{1}{\alpha}, \gamma = \frac{\alpha - \theta}{2\alpha}.$$

where $0 < C < 1$ implicitly. This is defined for $x \geq 0$. The reflection rule is used for $x < 0$ such that $L_\alpha^\theta(x) := L_\alpha^{-\theta}(-x)$.

△

This result was first derived in 1986 by Schneider[28], then rediscovered in 2001 by Mainardi et al.[18], and summarized by Mainardi and Pagnini in (2.8) of [19], from which we quote.

In (4.1), instead of using (α, θ) directly, it uses a different representation, which we call the (ϵ, γ) representation. In the Mellin transform space, such representation is often more elegant.

The constraint on θ in the Feller parameterization: $|\theta| \leq \min\{\alpha, 2 - \alpha\}$, is called the "Feller-Takayasu diamond". In the (ϵ, γ) parametrization, the constraint becomes (a) $0 \leq \gamma \leq 1$ when $\epsilon > 1$; and (b) $1 - \epsilon \leq \gamma \leq \epsilon$ when $\epsilon \leq 1$.[1]

4.1.1. The Reflection Rule. Note that the reflection of $\theta \to -\theta$ in the (α, θ) parametrization is equivalent to the reflection of $\gamma \to 1 - \gamma$ in the (ϵ, γ) parametrization.

Since we often mingle the two parameterizations, this alternative view can be very helpful in certain scenarios. For example, the total density in the positive domain is $\int_0^\infty L_\alpha^\theta(x) = \gamma$. By the reflection rule, $\int_0^\infty L_\alpha^{-\theta}(x) = 1 - \gamma$. Hence, the total density $\int_{-\infty}^\infty L_\alpha^\theta(x) = \gamma + (1 - \gamma) = 1$.

[1] Conversely, if γ is fixed, (b) puts a constraint on the largest α allowed: $\alpha \leq \min\{1/\gamma, 1/(1-\gamma)\}$.

4.2. Extremal Distributions

There are two types of the so-called "extremal distributions", where θ is pushed to the limit, so to speak. They are especially intriguing because the M-Wright functions, $F_\alpha(x), M_\alpha(x)$ in Section 3.3, can be derived from them.

They can be understood from (4.1). The first kind of extremal distribution lies in $\gamma = 0$ or $\gamma = 1$ when $\theta = \pm\alpha \leq 1$. Due to the reflection rule, we only need to study the case of $\theta = -\alpha$, that is, $\gamma = 1$.

This defines the one-sided α-stable distribution:

$$L_\alpha(x) := L_\alpha^{-\alpha}(x) \overset{\mathcal{M}}{\longleftrightarrow} \epsilon \frac{\Gamma(\epsilon(1-s))}{\Gamma(1-s)}$$

Apply three manipulations of Mellin transform on $F_\alpha(x)$: First, $x \to x^\alpha$; second, multiply x; third, $x \to x^{-1}$. We obtain the classic result of

$$L_\alpha(x) = x^{-1} F_\alpha(x^{-\alpha}) \quad (x \geq 0 \text{ and } 0 < \alpha \leq 1) \tag{4.2}$$

and $L_1(x) = \delta(x-1)$ is the upper bound of this relation.

$L_\alpha(x)$ can be computed via `scipy.stats.levy_stable`[33] using 1-Parameterization with `beta`=1, `scale`= $\cos(\alpha\pi/2)^{1/\alpha}$ for $0 < \alpha < 1$.[2] It might seem somewhat peculiar that we can use the existing implementation of $L_\alpha(x)$ to develop all the new fractional distributions for proof of concept.

The second kind of extremal distribution (but not necessarily one-sided) occurs when $\theta = \alpha - 2$, which leads to $\epsilon = \gamma = 1/\alpha$ and

$$L_\alpha^{\alpha-2}(x) \overset{\mathcal{M}}{\longleftrightarrow} \epsilon \frac{\Gamma(s)}{\Gamma(1-\epsilon+\epsilon s)}$$

Compare it to (3.13), we get the classic result of (e.g. see (F.49) of [16])

$$L_\alpha^{\alpha-2}(x) = \frac{1}{\alpha} M_{1/\alpha}(x) \quad (x \in \mathbb{R} \text{ and } 1 < \alpha \leq 2) \tag{4.3}$$

Notice that it extends the M-Wright function to $x < 0$ because $L_\alpha^{\alpha-2}(x)$ is two-sided.

4.3. Ratio Distribution Approach

Important insight can be obtained by interpreting (4.1) as a ratio distribution (2.6). We split (4.1) into two components:

$$L_\alpha^\theta(x) \overset{\mathcal{M}}{\longleftrightarrow} \epsilon \left[\frac{\Gamma(s)}{\Gamma(1-\gamma+\gamma s)}\right] \left[\frac{\Gamma(\epsilon(1-s))}{\Gamma(\gamma(1-s))}\right] \tag{4.4}$$

The first bracket is the Mellin transform of the M-Wright function (3.13).

The second bracket comes from the Mellin transform of the PDF of the fractional χ-mean distribution (FCM) at $k = 1$:

$$\begin{aligned} \overline{\chi}_{\alpha,1}^\theta(x) &\overset{\mathcal{M}}{\longleftrightarrow} \overline{\chi}_{\alpha,1}^{\theta\ *}(s) \\ &= \epsilon\gamma^{\gamma(s-1)-1} \frac{\Gamma(\epsilon(s-1))}{\Gamma(\gamma(s-1))} \end{aligned} \tag{4.5}$$

According to the Mellin transform rule of a ratio distribution, s should be replaced by $2-s$ in $\overline{\chi}_{\alpha,1}^{\theta\ *}(s)$. Therefore, $s-1$ in the second line of (4.5) becomes $1-s$ in the second bracket of (4.4).

[2] See Chapter 1 of [24] for more detail on different parameterizations. We would not go into the issue of stable parameterizations.

4.3.1. Rescaled M-Wright Function. Additionally, a small nuance here is to deal with scaling factors. Define the rescaled M-Wright function

$$\tilde{M}_\gamma(x) := \gamma^{1-\gamma} M_\gamma(x/\gamma^\gamma) \tag{4.6}$$

such that it matches the standard normal distribution: $\tilde{M}_{1/2}(x) = \frac{1}{\sqrt{2\pi}} e^{-x^2/2}$ of $\mathcal{N}(0,1)$. And $\int_0^\infty \tilde{M}_\gamma(x)\,dx = \gamma$ since $\int_0^\infty M_\gamma(x) = 1$.

Notice that, according to the reflection rule, $\int_0^\infty \tilde{M}_\gamma(-x)\,dx = \int_0^\infty \tilde{M}_{1-\gamma}(x)\,dx = 1-\gamma$. We get $\int_{-\infty}^\infty \tilde{M}_\gamma(x)\,dx = 1$. Hence, $\tilde{M}_\gamma(x)$ is a valid two-sided density function.

According to (2.3), the rescaling of PDF modifies the Mellin transform from (3.13) to

$$\begin{aligned} \tilde{M}_\gamma(x) &\overset{\mathcal{M}}{\longleftrightarrow} \tilde{M}^*_\gamma(s) \\ &= \gamma^{1-\gamma+\gamma s} \frac{\Gamma(s)}{\Gamma(1-\gamma+\gamma s)} \end{aligned} \tag{4.7}$$

from which the $\gamma^{1-\gamma+\gamma s}$ term cancels out its counterpart in ${\overline{\chi}^\theta_{\alpha,1}}^*(2-s)$ nicely.

Therefore, we find a new method to construct the α-stable distribution using the following integral.

LEMMA 4.2 (The ratio-distribution representation of the α-stable distribution). The Mellin transform of the PDF (4.1) becomes

$$L^\theta_\alpha(x) \overset{\mathcal{M}}{\longleftrightarrow} \tilde{M}^*_\gamma(s)\,{\overline{\chi}^\theta_{\alpha,1}}^*(2-s) \tag{4.8}$$

from which the PDF can be written in a ratio distribution form of

$$L^\theta_\alpha(x) := \int_0^\infty \tilde{M}_\gamma(xs)\,\overline{\chi}^\theta_{\alpha,1}(s)\,s\,ds \quad (x \geq 0) \tag{4.9}$$

Since the Mellin integral is only valid for $x > 0$, it is supplemented with *the reflection rule*:

$$L^\theta_\alpha(-x) := L^{-\theta}_\alpha(x) \tag{4.10}$$

△

This construction places $\overline{\chi}^\theta_{\alpha,1}$ in the central role. We define it at one degree of freedom $k = 1$. In Chapter 7, we will add *degrees of freedom* k to it and make it $\overline{\chi}^\theta_{\alpha,k}$, which is the fractional extension of the classic χ distribution.

Subsequently, in Chapter 11, we will add *degrees of freedom* k to the α-stable distribution and merge it with Student's t distribution.

4.4. SaS

Note that $\theta = 0$ is equivalent to $\gamma = 1/2$. The distribution is symmetric, with the nickname of "SaS", which stands for "Symmetric α-Stable".

Its Mellin transform is simplified to

$$\begin{aligned} L^0_\alpha(x) &\overset{\mathcal{M}}{\longleftrightarrow} \epsilon \left[\frac{\Gamma(s)}{\Gamma((1+s)/2)}\right] \left[\frac{\Gamma(\epsilon(1-s))}{\Gamma((1-s)/2)}\right] \\ &= \epsilon \left[\frac{2^{s-1}}{\sqrt{\pi}}\Gamma\left(\frac{s}{2}\right)\right] \left[\frac{\Gamma(\epsilon(1-s))}{\Gamma((1-s)/2)}\right]. \end{aligned} \tag{4.11}$$

The first bracket is the Mellin transform of a normal distribution (2.9) with a scale. The second bracket is ${\overline{\chi}^0_{\alpha,1}}^*(2-s)$ from above.

Hence, the PDF of SaS is

$$L^0_\alpha(x) = \int_0^\infty \mathcal{N}(xs)\, \overline{\chi}^0_{\alpha,1}(s)\, s\, ds. \tag{4.12}$$

This is one of the foundations of GAS-SN in (12.1).

4.4.1. Method of Normal Mixture. SaS in (4.12) will be generalized to GSaS in (12.3) in Chapter 12. Both integrals are in the normal mixture structure (9.1) that enjoys several nice properties described in Chapter 9.

The classic exponential power distribution (Section 3.11.1 of [**24**]) is the characteristic function transform in Lemma 9.2.

CHAPTER 5

Fractional Hypergeometric Functions

In this chapter, we extend both the confluent hypergeometric function ${}_1F_1(a,b;x)$ or $M(a,b;x)$ (Chapter 13, DLMF[6]); and the Gauss hypergeometric function ${}_2F_1(a,b,c;x)$ (Chapter 15 of DLMF).

The former occurs when dealing with the CDF of the FG and FCM distributions. The latter occurs when handling the CDF of the GSaS and F distributions.

The reader who is not interested in the hypergeometric functions can safely skip this chapter without losing direction.

To clear up the situation, we first recite the DLMF formulas and convert them to our convention according to (2.2).

From DLMF 13.2.4 and 13.4.16, the Mellin transform of the Kummer function is

$$M(a,b;-x) = \frac{\Gamma(b)}{2\pi i\,\Gamma(a)} \int_{C-i\infty}^{C+i\infty} \frac{\Gamma(a-s)\Gamma(s)}{\Gamma(b-s)}\, x^{-s}\, ds,$$

where $a \neq 0, -1, -2, ...$

From DLMF 15.1.2 and 15.6.6, the Mellin transform of the Kummer function is

$${}_2F_1(a,b,c;-x) = \frac{\Gamma(c)}{2\pi i\,\Gamma(a)\Gamma(b)} \int_{C-i\infty}^{C+i\infty} \frac{\Gamma(a-s)\Gamma(b-s)\Gamma(s)}{\Gamma(c-s)}\, x^{-s}\, ds,$$

where $a, b \neq 0, -1, -2, ...$

Use our Mellin transform notation, they become

$$M(a,b;-x) \overset{\mathcal{M}}{\longleftrightarrow} M^*(a,b;s) = \frac{\Gamma(b)}{\Gamma(a)} \frac{\Gamma(a-s)\Gamma(s)}{\Gamma(b-s)}, \tag{5.1}$$

$${}_2F_1(a,b,c;-x) \overset{\mathcal{M}}{\longleftrightarrow} {}_2F_1^*(a,b,c;s) = \frac{\Gamma(c)}{\Gamma(a)\Gamma(b)} \frac{\Gamma(a-s)\Gamma(b-s)\Gamma(s)}{\Gamma(c-s)}. \tag{5.2}$$

Now let us add the fractional components to them!

5.1. Fractional Confluent Hypergeometric Function

The fractional confluent hypergeometric function (FCHF) is the union of the Kummer function and the Wright function. It allows us to extend many classic functions to their fractional forms.

We start with its Mellin transform. And we follow with the integral and series representations.

Definition 5.1. The Mellin transform of the FCHF is

$$M_{\lambda,\delta}(a,b;-x) \overset{\mathcal{M}}{\longleftrightarrow} M^*_{\lambda,\delta}(a,b;s) = \frac{\Gamma(b)}{\Gamma(a)} \frac{\Gamma(a-s)\Gamma(s)}{\Gamma(\delta-\lambda s)\Gamma(b-s)} \tag{5.3}$$

where the $\Gamma(\delta - \lambda s)$ term is from the Wright function (3.5).

Lemma 5.2. The integral representation from DLMF 13.4.1 is extended to

$$M_{\lambda,\delta}(a,b;z) = \frac{\Gamma(b)}{\Gamma(a)\Gamma(b-a)} \int_0^1 W_{\lambda,\delta}(zt)\, t^{a-1}(1-t)^{b-a-1}\, dt \tag{5.4}$$

The obvious limit $W_{0,1}(zt) = e^{zt}$ restores it to the classic DLMF formula.

△

PROOF. Replace the Wright function in (5.4) with its Hankel integral (3.6),

$$M_{\lambda,\delta}(a,b;z) = \frac{\Gamma(b)}{2\pi i\,\Gamma(a)} \int_0^1 \int_{Ha} \left(\frac{e^{s+zt\,s^{-\lambda}}}{s^{\delta}} ds \right) t^{a-1}(1-t)^{b-a-1}\,dt$$

which can be simplified to

$$M_{\lambda,\delta}(a,b;z) = \frac{1}{2\pi i} \int_{Ha} \left(s^{-\delta}\, e^{s}\, ds \right)\; M(a,b;-z\,s^{-\lambda})$$

Substitute the Mellin integral from (5.1) to it,

$$\begin{aligned} M_{\lambda,\delta}(b,c;-z) &= \frac{1}{2\pi i} \int_{Ha} \left(s^{-\delta}\, e^{s}\, ds \right)\; \frac{\Gamma(b)}{2\pi i\Gamma(a)} \int_{C-i\infty}^{C+i\infty} \frac{\Gamma(b-t)\Gamma(t)}{\Gamma(c-t)}\,(z\,s^{-\lambda})^{-t}\,dt \\ &= \frac{\Gamma(b)}{2\pi i\Gamma(a)} \int_{C-i\infty}^{C+i\infty} \left[\frac{1}{2\pi i} \int_{Ha} s^{\lambda t-\delta}\, e^{s}\, ds \right] \frac{\Gamma(b-t)\Gamma(t)}{\Gamma(c-t)}\, z^{-t}\,dt \\ &= \frac{\Gamma(b)}{2\pi i\Gamma(a)} \int_{C-i\infty}^{C+i\infty} \left[\frac{1}{\Gamma(\delta-\lambda t)} \right] \frac{\Gamma(b-t)\Gamma(t)}{\Gamma(c-t)}\, z^{-t}\,dt \end{aligned}$$

which is the Mellin transform in (5.3).

From the second line to the third line, we use the well-known Hankel integral of the reciprocal gamma function:

$$\frac{1}{2\pi i} \int_{Ha} s^{-z}\, e^{s}\, ds = \frac{1}{\Gamma(z)}$$

□

LEMMA 5.3. The series representation is

$$M_{\lambda,\delta}(a,b;z) := \sum_{n=0}^{\infty} \left[\frac{(a)_n}{(b)_n\,\Gamma(\lambda n+\delta)} \right] \frac{z^n}{n!} \tag{5.5}$$

where $(a)_n, (b)_n$ are Pochhammer symbols.

△

PROOF. Take (5.3) and apply Ramanujan's master theorem from Section 2.2. This produces $(M^{*}_{\lambda,\delta}(a,b;s)/\Gamma(s))|_{s=-n}$, which is equal to the bracket term, since $(x)_n = \Gamma(x+n)/\Gamma(x)$. □

5.1.1. FCHF Subsumes the Kummer Function. It is obvious that $M_{0,1}(a,b;x) = M(a,b;x)$.

5.1.2. FCHF Subsumes the M-Wright Function. By using the same setting from (3.10), we get

$$M_{\alpha}(z) = M_{-\alpha,1-\alpha}(c,c;-z) \qquad (c \neq 0)$$

5.1.3. FCHF Subsumes Fractional Gamma-Star Function. An important variant of FCHF is the fractionalization of the incomplete gamma function. The reader is referred to Sections 8 and 13 of DLMF[6] and Wikipedia for background information.

We are mainly concerned with the following setup:

$$M_{-\alpha,1-\alpha}(c,c+1;-x) = c \int_0^1 M_{\alpha}(xt)\, t^{c-1}\,dt$$

This integral is found in (3.20). Hence, we obtain -

LEMMA 5.4. The fractional γ^* function (3.20) has the following FCHF representation:

$$\gamma^*_\alpha(s,x) = \frac{\Gamma(\alpha s-\alpha+1)}{\Gamma(s+1)}\, M_{-\alpha,1-\alpha}(s,s+1;-x) \tag{5.6}$$

△

The fractional γ^* function is the basis for expressing the CDF of the fractional gamma distribution in Section 6.5. In fact, this was the main motivation to enrich the classic confluent hypergeometric function.

5.2. Fractional Gauss Hypergeometric Function

The fractional Gauss hypergeometric function (FGHF) arises from the ratio distribution between an elementary function and FCM2 ($\widehat{\chi}^2_{\alpha,k}$) in Section 7.5.

When $\alpha = 1$, the Mellin transform of FCM2 is reduced from a fractional form to a classic form in (7.26). The ratio distribution is reduced to a Gauss hypergeometric function ${}_2F_1$. Hence, we consider the general form of such a ratio distribution as fractional ${}_2F_1$.

We start by modifying the Mellin transform from (5.2) (DLMF 15.6.6). Then we derive the integral and series representations from it.

DEFINITION 5.5. The Mellin transform of the fractional Gauss hypergeometric function is

$$\begin{aligned} {}_2F_1(a,b,c,\epsilon;-x) &\overset{\mathcal{M}}{\longleftrightarrow} {}_2F_1^*(a,b,c,\epsilon;s) \\ &= \Big[M^*\left(a,c;s\right)\Big]\,\left[\frac{B(k/2,1/2)}{\Gamma(1/2)}\,\widehat{\chi}^{2*}_{\alpha,k}(3/2-s)\right] \end{aligned} \tag{5.7}$$

where $\epsilon = 1/\alpha$ is the convention from (4.1), and $b = (k+1)/2$. $M^*\left(a,c;s\right)$ is from (5.1), and $\widehat{\chi}^{2*}_{\alpha,k}(s)$ is from (7.25) (we jump ahead). And $B(x,y)$ is the beta function.

This structure is a fractional form of the generalized hypergeometric function ${}_3F_2$ (DLMF 16.5.1, replace s with $-s$). To see this, expand (5.7) and we get

$${}_2F_1^*(a,b,c,\epsilon;s) = \left[\frac{\Gamma(c)}{\Gamma(a)}\frac{\Gamma(a-s)\Gamma(s)}{\Gamma(c-s)}\right]\left[2^{2s-1}\,\frac{B(k/2,1/2)}{\Gamma(1/2)}\,\frac{\Gamma((k-1)/2)}{\Gamma(\epsilon(k-1))}\frac{\Gamma(2\epsilon\,(k/2-s))}{\Gamma(k/2-s)}\right]. \tag{5.8}$$

There are five gamma functions that contain s: three in the numerator, two in the denominator. And the $\Gamma(2\epsilon\,(k/2-s))$ term is fractional.

5.2.1. FGHF Subsumes the Gauss Hypergeometric Function.

LEMMA 5.6. When $\epsilon = 1$,

$${}_2F_1^*(a,b,c,\epsilon=1;s) = {}_2F_1^*(a,b,c;s)$$

△

PROOF. Let $\epsilon = 1$, the second bracket becomes

$$\frac{B(k/2,1/2)}{\Gamma(1/2)}\frac{\Gamma(k/2+1/2-s)}{\Gamma(k/2)} = \frac{\Gamma(k/2+1/2-s)}{\Gamma(k/2+1/2)} = \frac{\Gamma(b-s)}{\Gamma(b)}. \tag{5.9}$$

Hence, (5.7) is reduced to the classic limit of ${}_2F_1^*(a,b,c;s)$ in (5.2). □

5.2.2. The Integral Form.

LEMMA 5.7. The integral form of FGHF is

$$ {}_2F_1(a,b,c,\epsilon;-x) := \frac{B(k/2,1/2)}{\Gamma(1/2)}\int_0^\infty M(a,c;-x\nu)\,\widehat{\chi}^2_{\alpha,k}(\nu)\,\sqrt{\nu}d\nu \tag{5.10}$$

where $\epsilon = 1/\alpha$ and $b = (k+1)/2$. $M(a,c;x)$ is the Kummer function (Chapter 13, DLMF). $\widehat{\chi}^2_{\alpha,k}(x)$ is from (7.17).

△

PROOF. We use the generalized convolution formula:

$$h(x) = \int_0^\infty f(xs)g(s)\,s^p\,ds \overset{\mathcal{M}}{\longleftrightarrow} h^*(s) = f^*(s)g^*(1+p-s),$$

Clearly f is M, and g is $\widehat{\chi}^2_{\alpha,k}$. Substitute $p = 1/2$ due to the $\sqrt{\nu}$ term. The Mellin transform of (5.10) is

$${}_2F_1(a,b,c,\epsilon;-x) \overset{\mathcal{M}}{\longleftrightarrow} \frac{B(k/2,1/2)}{\Gamma(1/2)}M^*(a,c;s)\,\widehat{\chi}^{2*}_{\alpha,k}(3/2-s)$$

This is exactly (5.7).

□

5.2.3. Relation between FGHF and Real-World Usage. This section addresses a broader issue. How does FGHF relate to FCM and GAS (and GAS-SN) in general? The reader can skip this section and come back later after she read the later chapters.

This topic is important. In an abstract sense, most of the univariate PDFs in their ratio distribution forms can be understood by the integral form of FGHF.

Let us make (5.10) more abstract, by ignoring some cumbersome parameters. Assume $F(-x) := {}_2F_1(a,b,c,\epsilon;-x)$ and $M(-x) := M^*(a,c;-x)\,(x \geq 0)$, then (5.10) becomes

$$F(-x) := B\int_0^\infty M(-x\nu)\,\overline{\chi}^2_{\alpha,k}(\nu;\sigma=1/4)\,\sqrt{\nu}d\nu \tag{5.11}$$

where we employ the notation $\widehat{\chi}^2_{\alpha,k}(x) = \overline{\chi}^2_{\alpha,k}(x;\sigma=\frac{1}{4})$ from (7.17), and $B := B(\frac{k}{2},\frac{1}{2})/\Gamma(\frac{1}{2})$.

LEMMA 5.8. Let $F'(-x)$ be the scaled FGHF, which is more closely related to real-world use cases. The following ratio-distribution integrals can be converted to F' such as

$$\left.\begin{array}{l}\int_0^\infty M(-xs)\,\overline{\chi}^2_{\alpha,k}(s)\,\sqrt{s}ds \\ \int_0^\infty M(-xs^2)\,\overline{\chi}_{\alpha,k}(s)\,s\,ds\end{array}\right\} = F'(-x) := \frac{2\sqrt{\pi}\,\sigma_{\alpha,k}}{B(\frac{k}{2},\frac{1}{2})}\,F\left(-4\sigma^2_{\alpha,k}\,x\right) \tag{5.12}$$

Or use the full FGHF notation explicitly:

$$\left.\begin{array}{l}\int_0^\infty M(a,c;-xs)\,\overline{\chi}^2_{\alpha,k}(s)\,\sqrt{s}ds \\ \int_0^\infty M(a,c;-xs^2)\,\overline{\chi}_{\alpha,k}(s)\,s\,ds\end{array}\right\} = F'_{\alpha,k}(a,c;-x) := \frac{2\sqrt{\pi}\,\sigma_{\alpha,k}}{B(\frac{k}{2},\frac{1}{2})}\,{}_2F_1\left(a,b,c,\epsilon;-4\sigma^2_{\alpha,k}\,x\right) \tag{5.13}$$

where $\epsilon = 1/\alpha$ and $b = (k+1)/2$ on the RHS.

△

PROOF. Let Q be the scale that we want to solve. (5.11) is rewritten to $F'(-x)$ such that

$$F'(-x) := \frac{\sqrt{Q}}{B}F\left(-Qx\right) = \sqrt{Q}\int_0^\infty M(-Qx\nu)\,\overline{\chi}^2_{\alpha,k}(\nu;\sigma=1/4)\,\sqrt{\nu}d\nu.$$

Let $s = Q\nu$,

$$F'(-x) = \int_0^\infty M(-xs)\,\overline{\chi}^2_{\alpha,k}(s/Q;\sigma = 1/4)/Q\,\sqrt{s}ds$$
$$= \int_0^\infty M(-xs)\,\overline{\chi}^2_{\alpha,k}(s;\sigma = Q/4)\,\sqrt{s}ds$$

Let $Q = 4\sigma^2_{\alpha,k}$, we obtain the integral form in terms of FCM2,

$$F'(-x) = \int_0^\infty M(-xs)\,\overline{\chi}^2_{\alpha,k}(s)\,\sqrt{s}ds$$

This is the first line of (5.12). Then apply (7.19) and (7.20) to get the second line. And on the FGHF side, we have

$$F'(-x) = \frac{\sqrt{Q}}{B}F\left(-Qx\right) = \frac{2\sqrt{\pi}\,\sigma_{\alpha,k}}{B(\frac{k}{2},\frac{1}{2})}\,F(-4\sigma^2_{\alpha,k}\,x)$$

□

5.2.4. Example 1: GSaS. In Lemma 8.3 of [15], a fractional extension was explored for the CDF of GSaS. We formalized it further here. However, we note that the $M(-x)$ function needed to describe GAS-SN is more complicated than a Kummer function. See (10.2) and (10.3).

LEMMA 5.9. Assume $\Phi[L_{\alpha,k}](x)$ is the CDF of a GSaS, which is (12.2) with $\beta = 0$. It can be expressed by the scaled FGHF via

$$\Phi[L_{\alpha,k}](x) = \frac{1}{2} + \frac{x}{\sqrt{2\pi}}\,F'_{\alpha,k}\left(\frac{1}{2},\frac{3}{2};-\frac{x^2}{2}\right). \tag{5.14}$$

△

PROOF. From Lemma 8.3 of [15],

$$\Phi[L_{\alpha,k}](x) = \frac{1}{2} + \frac{x}{\sqrt{k}}M_{\alpha,k}\left(a,c;-\frac{x^2}{k}\right),$$

where $a = \frac{1}{2}, c = \frac{3}{2}$ and

$$M_{\alpha,k}(a,c;x) := \sqrt{\frac{k}{2\pi}}\int_0^\infty s\,ds\,M\left(a,c;\frac{xks^2}{2}\right)\,\overline{\chi}_{\alpha,k}(s).$$

This pattern fits right in with the second line of (5.13). It is immediately clear that its $M_{\alpha,k}(a,c;x)$ is our $\sqrt{k/2\pi}F'_{\alpha,k}\,(a,c;kx/2)$. Therefore,

$$\Phi[L_{\alpha,k}](x) = \frac{1}{2} + \frac{x}{\sqrt{2\pi}}\,F'_{\alpha,k}\left(a,c;-\frac{x^2}{2}\right),$$

where $a = \frac{1}{2}, c = \frac{3}{2}$.

□

Notice that this formula is much cleaner, without the cluttering of k in the previous attempt in [15].

5.2.5. Example 2: Fractional F.

LEMMA 5.10. From (8.2), the standard CDF of a fractional F distribution $F_{\alpha,d,k}$ is

$$\Phi[F_{\alpha,d,k}](x) = \frac{1}{\Gamma\left(\frac{d}{2}\right)} \int_0^\infty ds\, \gamma\left(\frac{d}{2}, \frac{dxs}{2}\right) \overline{\chi}^2_{\alpha,k}(s).$$

It can be expressed by the scaled FGHF via

$$\Phi[F_{\alpha,d,k}](x) = \left[C_{\alpha,d,k}\, \frac{(dx/2)^{d/2}}{\Gamma\left(\frac{d}{2}+1\right)}\right] F'_{\alpha,k+d-1}\left(\frac{d}{2}, \frac{d}{2}+1; -\frac{dx}{2\Sigma}\right). \tag{5.15}$$

where $C_{\alpha,d,k}$ is defined in (5.16) and $\Sigma := \sigma^2_{\alpha,k+d-1}/\sigma^2_{\alpha,k}$. △

PROOF. Note that

$$\frac{1}{\Gamma\left(\frac{d}{2}\right)}\gamma\left(\frac{d}{2}, \frac{x}{2}\right) = \frac{(x/2)^{d/2}}{\Gamma\left(\frac{d}{2}+1\right)} M\left(\frac{d}{2}, \frac{d}{2}+1; -\frac{x}{2}\right).$$

Then

$$\begin{aligned}\Phi[F_{\alpha,d,k}](x) &= \int_0^\infty \left[\frac{(dxs/2)^{d/2}}{\Gamma\left(\frac{d}{2}+1\right)} M\left(\frac{d}{2}, \frac{d}{2}+1; -\frac{dxs}{2}\right)\right] \overline{\chi}^2_{\alpha,k}(s)\, ds \\ &= \frac{(dx/2)^{d/2}}{\Gamma\left(\frac{d}{2}+1\right)} \int_0^\infty M\left(\frac{d}{2}, \frac{d}{2}+1; -\frac{dxs}{2}\right) s^{(d-1)/2}\, \overline{\chi}^2_{\alpha,k}(s)\, \sqrt{s}\, ds.\end{aligned}$$

When $d = 1$, it fits right in with FGHF. When $d > 1$, it needs more work.

From (7.5), let $m = (d-1)/2$, then $k + 2m = k + d - 1$ and

$$\Phi[F_{\alpha,d,k}](x) = C_{\alpha,d,k}\, \frac{(dx/2)^{d/2}}{\Gamma\left(\frac{d}{2}+1\right)} \int_0^\infty M\left(\frac{d}{2}, \frac{d}{2}+1; -\frac{dxy}{2\Sigma}\right) \overline{\chi}^2_{\alpha,k+d-1}(y)\, \sqrt{y}\, dy,$$

where $\Sigma := \sigma^2_{\alpha,k+d-1}/\sigma^2_{\alpha,k}$ and $y = \Sigma\, s$, and

$$C_{\alpha,d,k} := \frac{\sigma^{d-1}_{\alpha,k}}{\sqrt{\Sigma}}\, \frac{C_{\alpha,k}}{C_{\alpha,k+d-1}} = \frac{\sigma^d_{\alpha,k}}{\sigma_{\alpha,k+d-1}}\, \frac{C_{\alpha,k}}{C_{\alpha,k+d-1}}. \tag{5.16}$$

The integral matches the FGHF pattern in Lemma 5.12, and we get (5.15).

□

REMARK 5.11. One final note. There is a connection between (5.14) and (5.15). When $d = 1$, $\Sigma = 1$ and $C_{\alpha,d,k} = 1$. Then

$$\Phi[F_{\alpha,1,k}](x^2) = \frac{2x}{\sqrt{2\pi}}\, F'_{\alpha,k}\left(\frac{1}{2}, \frac{3}{2}; -\frac{x^2}{2}\right) \tag{5.17}$$

which is $2\,\Phi[L_{\alpha,k}](x) - 1$ in (5.14).

This is a reflection of Lemma 8.3. If the variable X distributes as a GSaS $L_{\alpha,k}$, then X^2 distributes as a one-dimensional F, aka $F_{\alpha,1,k}$. It is particularly easy to see this relation in the FGHF form above.

Part 2

One-Sided Distributions

CHAPTER 6

FG: Fractional Gamma Distribution

FG is the backbone that allows many features in this book. In particular, FCM is a member of FG. It is a fractional version of the generalized gamma distribution, as would become clear to the reader in this chapter.

In my 2024 work[15], it was called *the generalized stable count distribution*, where the name "stable count distribution" came from my 2020 work[14]. However, after several years of study, it became clear that it is better to name it after *the gamma distribution*.

6.1. Definition

DEFINITION 6.1 (Fractional Gamma distribution (FG)). FG is a four-parameter one-sided distribution family, whose PDF is defined as

$$\mathfrak{N}_\alpha(x;\sigma,d,p) := C\left(\frac{x}{\sigma}\right)^{d-1} F_\alpha\left(\left(\frac{x}{\sigma}\right)^p\right) \qquad (x \geq 0) \tag{6.1}$$

where $F_\alpha(x) = W_{-\alpha,0}(-x)$ from (3.9) and $\alpha \in [0,1]$ controls the shape of the Wright function; σ is the scale parameter; p is also the shape parameter controlling the tail behavior ($p \neq 0, dp \geq 0$); d is the *degree of freedom* parameter. When $\alpha \to 1$, the PDF becomes a Dirac delta function: $\delta(x-\sigma)$ assuming σ is finite. When $d \geq 1$, all the moments of the FG exist and have closed forms.

6.2. Determination of C

The normalization constant C is:

$$C = \begin{cases} \frac{|p|}{\sigma}\frac{\Gamma(\alpha d/p)}{\Gamma(d/p)} & , \text{ for } \alpha \neq 0, d \neq 0. \\ \frac{|p|}{\sigma\alpha} & , \text{ for } \alpha \neq 0, d = 0. \end{cases} \tag{6.2}$$

It is important to note that d and p are allowed to be negative, as long as $dp \geq 0$.

PROOF. The normalization constant C in (6.1) is obtained from the requirement that the integral of the PDF must be 1:

$$\int_0^\infty \mathfrak{N}_\alpha(x;\sigma,d,p)\,dx = \frac{C\sigma}{|p|}\frac{\Gamma(\frac{d}{p})}{\Gamma(\frac{d}{p}\alpha)} = 1$$

where the integral is carried out by the moment formula of the Wright function.

We typically constrain $dp \geq 0$ and p is typically positive. However, it becomes negative in the inverse distribution and/or characteristic distribution types. So we need $|p|$ to ensure that C is positive.

For the case of $\alpha \neq 0$ and $d \to 0$, due to (A.3), we have

$$C = \frac{|p|}{\sigma\alpha} \qquad (\alpha \neq 0, d = 0)$$

These two cases are combined to form (6.2). □

6.3. FG Subsumes Generalized Gamma Distribution

Since the Wright function extends an exponential function to the fractional space, FG is the fractional extension of the generalized gamma (GG) distribution[30], whose PDF is defined as:

$$f_{\mathrm{GG}}(x;a,d,p) = \frac{|p|}{a\Gamma(d/p)}\left(\frac{x}{a}\right)^{d-1} e^{-(x/a)^p}. \tag{6.3}$$

The parallel use of parameters is obvious, except that a in GG is replaced by σ in FG to avoid confusion with α.

GG is subsumed to FG in two ways:

$$f_{\mathrm{GG}}(x;\sigma,d,p) := \begin{cases} \mathfrak{N}_0(x;\sigma,d=d-p,p) & , \text{ at } \alpha=0. \\ \mathfrak{N}_{\frac{1}{2}}\left(x;\sigma=\frac{\sigma}{2^{2/p}},d=d-\frac{p}{2},p=\frac{p}{2}\right) & , \text{ at } \alpha=\frac{1}{2}. \end{cases} \tag{6.4}$$

The first line is treated as the definition of FG at $\alpha = 0$. The proof is given in [15].

Although the first line is more obvious, it is the second line that leads to the fractional extension of the χ distribution.

6.4. Mellin Transform

From Example 2.4, we add σ and C. The Mellin transform of the PDF of the fractional gamma distribution is

$$\begin{aligned} \mathfrak{N}_\alpha(x;\sigma,d,p) &\overset{\mathcal{M}}{\longleftrightarrow} \frac{C\,\sigma^s}{|p|}\frac{\Gamma((s+d-1)/p)}{\Gamma(\alpha(s+d-1)/p)} \\ &= \sigma^{s-1}\frac{\Gamma(\alpha d/p)}{\Gamma(d/p)}\frac{\Gamma((s+d-1)/p)}{\Gamma(\alpha(s+d-1)/p)}, \end{aligned} \tag{6.5}$$

where C is from Section 6.2. The typical limiting case for the gamma functions shall be taken care in each scenario.

FG is often used in a ratio distribution, such as the role of $g^*(s)$ in (2.6), where $s \to 2-s$. The term $s+d-1$ becomes $d+1-s$. Furthermore, in the FCM case, since $d = k-1$, it becomes the elegant $k-s$ term.

6.5. CDF and Fractional Incomplete Gamma Function

The CDF of FG is

$$\Phi(x) := \int_0^x \mathfrak{N}_\alpha(s;\sigma,d,p)\,ds \quad (x \geq 0). \tag{6.6}$$

This integral leads to fractionalization of the incomplete gamma function in Section 3.4.

LEMMA 6.2. The CDF of FG can be represented by γ^*_α in (3.20) as

$$\Phi(x) = z^{d+p}\,\gamma^*_\alpha\left(d/p+1, z^p\right) \tag{6.7}$$

where $z = x/\sigma$ is the standardized variable.

This could be viewed as one form of fractional extension to the regularized lower incomplete function, $\gamma(s,z)/\Gamma(s)$, which is the CDF of GG mentioned above.

Due to this result, it may even be suitable to call FG the *fractional gamma distribution*.

△

772 PROOF. The CDF of FG is

$$\begin{aligned}\Phi(x) &= \int_0^x \mathfrak{N}_\alpha(s;\sigma,d,p)\,ds \\ &= C\int_0^x ds\left(\frac{s}{\sigma}\right)^{d-1} W_{-\alpha,0}\left(-\left(\frac{s}{\sigma}\right)^p\right). \\ &= C\int_0^x ds\left(\frac{s}{\sigma}\right)^{d-1} F_\alpha\left(\left(\frac{s}{\sigma}\right)^p\right).\end{aligned}$$

773 Since $F_\alpha(x) = \alpha x\, M_\alpha(x)$ from (3.9), and let $u = s/x$, then

$$\begin{aligned}\Phi(x) &= \alpha C\int_0^x ds\left(\frac{s}{\sigma}\right)^{d+p-1} M_\alpha\left(\left(\frac{s}{\sigma}\right)^p\right) \\ &= \alpha C\, x\int_0^1 du\left(\frac{xu}{\sigma}\right)^{d+p-1} M_\alpha\left(\left(\frac{xu}{\sigma}\right)^p\right)\end{aligned}$$

774 Recognize that, if $u \in [0,1]$, then $u^p \in [0,1]$. Let $t = u^p$, and $dt/t = p\,du/u$,

$$\Phi(x) = \frac{\alpha\sigma C}{p}\, z^{d+p}\int_0^1 dt\, t^{d/p}\, M_\alpha\left(z^p t\right)$$

775 Compare the last line with γ_α^* in (3.20), and we get

$$\Phi(x) = \frac{\alpha\sigma C}{p}\,\frac{\Gamma(\frac{d}{p}+1)}{\Gamma((1-\alpha)+\alpha(\frac{d}{p}+1))}\, z^{d+p}\,\gamma_\alpha^*\left(d/p+1, z^p\right)$$

776 Using the case of $\alpha \neq 0, d \neq 0$ for C, it can be shown that the constant part is just 1. Hence,

$$\Phi(x) = z^{d+p}\,\gamma_\alpha^*\left(d/p+1, z^p\right)$$

777 □

778 6.6. Inverse Expression of Several Fractional Distributions

779 Several known fractional distributions could be expressed in the FG in Table 1. This shows that
780 the FG is the super set of the one-sided fractional distribution system. Its parametrization provides
781 immense flexibility to express other formerly known one-sided distributions.

Distribution (PDF)	Wright Equiv.	FG: $\mathfrak{N}_\alpha(x;\sigma,d,p)$			
		α	σ	d	p
One-sided stable: $L_\alpha(x)$	$x^{-1}W_{-\alpha,0}(-x^{-\alpha})$	α	1	0	$-\alpha$
Stable Count: $\mathfrak{N}_\alpha(x)$		α	1	1	α
Stable Vol: $V_\alpha(x)$		$\frac{\alpha}{2}$	$\frac{1}{\sqrt{2}}$	1	α
M-Wright: $M_\alpha(x)$	$\frac{1}{\alpha x}W_{-\alpha,0}(-x)$	α	1	0	1
M-Wright II: $\Gamma(\alpha)F_\alpha(x)$	$\Gamma(\alpha)W_{-\alpha,0}(-x)$	α	1	1	1

TABLE 1. FG mapping of several known fractional distributions in the literature. $\mathfrak{N}_\alpha(x)$ and $V_\alpha(x)$ first appeared in [14], which led to this work.

6.7. Alternative Definition

DEFINITION 6.3. It is reasonable to argue that the PDF of FG can be defined via the M-Wright function directly, such that

$$\mathfrak{N}'_\alpha(x;\sigma,d',p) := C' \left(\frac{x}{\sigma}\right)^{d'-1} M_\alpha\left(\left(\frac{x}{\sigma}\right)^p\right). \qquad (x \geq 0) \tag{6.8}$$

However, since $F_\alpha(z) = \alpha z\, M_\alpha(z)$, it is easy to see that

$$\mathfrak{N}'_\alpha(x;\sigma,d',p) = \alpha\, C' \left(\frac{x}{\sigma}\right)^{d'+p-1} F_\alpha\left(\left(\frac{x}{\sigma}\right)^p\right).$$

Therefore, this is merely a reparameterization of $d = d' + p$. This definition will encounter some issues in FCM later due to the assignment of $d \to k-1$, $\alpha \to \alpha/2$ and $p \to \alpha$ (see (7.4)). We learn from Figures 12.1 and 12.2 that there is a natural linear relation between k and $\epsilon = 1/\alpha$. Mixing the role of d with α from p is not a good idea.

CHAPTER 7

Fractional Chi Distributions

7.1. Introduction to Fractional Chi Distribution

In Chapter 4, we've discussed the insight that leads to the fractional χ is to interpret the Mellin transform of the PDF of the α-stable distribution as a ratio distribution of two components:

$$L_\alpha^\theta(x) \overset{\mathcal{M}}{\longleftrightarrow} \epsilon \left[\frac{\Gamma(s)}{\Gamma(1-\gamma+\gamma s))}\right] \left[\frac{\Gamma(\epsilon(1-s))}{\Gamma(\gamma(1-s))}\right]$$
$$\text{where } \epsilon = \frac{1}{\alpha}, \gamma = \frac{\alpha-\theta}{2\alpha}.$$

The first bracket is the Mellin transform of the M-Wright function.

The second bracket is interpreted as the Mellin transform of the PDF of the fractional χ-mean distribution (FCM) at $k = 1$:

$$\overline{\chi}_{\alpha,1}^\theta(x) \overset{\mathcal{M}}{\longleftrightarrow} \overline{\chi}_{\alpha,1}^\theta{}^*(s) \propto \frac{\Gamma(\epsilon(s-1))}{\Gamma(\gamma(s-1))},$$

apart from the normalization constant and scale in the PDF.

It becomes obvious after replacing $s \to 2-s$ in $\overline{\chi}_{\alpha,1}^\theta{}^*(s)$ in order to comply with the rule of Mellin transform of a ratio distribution.

In this chapter, the "degrees of freedom" parameter k is inserted by replacing $s-1$ with $s+k-2$, such that

$$\overline{\chi}_{\alpha,k}^\theta(x) \overset{\mathcal{M}}{\longleftrightarrow} \overline{\chi}_{\alpha,k}^\theta{}^*(s) \propto \frac{\Gamma(\epsilon(s+k-2))}{\Gamma(\gamma(s+k-2))}. \tag{7.1}$$

This forms the foundation for more rigorous treatment of FCM.

7.2. FCM: Fractional Chi-Mean Distribution

There are two ways to define FCM. The first approach is to define it via Mellin transform. The second approach is to define the shape of its PDF.

Definition 7.1 (Fractional χ-mean distribution (FCM) via Mellin Transform). The Mellin transform of FCM's PDF is enriched from (7.1) to

$$\begin{aligned}\overline{\chi}_{\alpha,k}^\theta(x) &\overset{\mathcal{M}}{\longleftrightarrow} \overline{\chi}_{\alpha,k}^\theta{}^*(s) \\ &= (\sigma_{\alpha,k}^\theta)^{s-1} \frac{\Gamma(\gamma(k-1))}{\Gamma(\epsilon(k-1))} \frac{\Gamma(\epsilon(s+k-2))}{\Gamma(\gamma(s+k-2))}, \\ &\text{where } \sigma_{\alpha,k}^\theta := \gamma^\gamma k^{\gamma-\epsilon}.\end{aligned} \tag{7.2}$$

The main differences are (1) to address the normalization of the total density, and (2) to have a proper scale $\sigma_{\alpha,k}^\theta$ such that it is consistent with the classic χ distribution ans α-stable distribution.

For positive k, the PDF of an FCM is

$$\overline{\chi}^{\theta}_{\alpha,k}(x) := \mathfrak{N}_{\gamma\alpha}(x;\sigma=\sigma^{\theta}_{\alpha,k},d=k-1,p=\alpha) \qquad (x\geq 0) \tag{7.3}$$
$$= \frac{\Gamma(\gamma(k-1))}{\epsilon\Gamma(\epsilon(k-1))}\left(\sigma^{\theta}_{\alpha,k}\right)^{1-k} x^{k-2}\, F_{\gamma\alpha}\left(\left(\frac{x}{\sigma^{\theta}_{\alpha,k}}\right)^{\alpha}\right),$$

where $\mathfrak{N}_\lambda(x;\sigma,d,p)$ is FG (6.1), and $F_\lambda(x) := W_{-\lambda,0}(-x)$ is the Wright function of the second kind (3.9).

Notice the appearances of γ that replaces all the $1/2$ in Section 7.6 of [15]. That is is how θ comes into play in the upgraded FCM. This full representation is used in Chapter 11.

However, for GAS-SN in Chapter 12 and beyond, such θ upgrade is unnecessary. The skew-normal framework is based on modulation of normal distributions. It is required to have $\theta = 0$ ($\gamma = 1/2$).

Hence, we recite the original definition of FCM PDF ($k > 0$):

$$\overline{\chi}_{\alpha,k}(x) = \overline{\chi}^{0}_{\alpha,k}(x) := \mathfrak{N}_{\alpha/2}(x;\sigma=\sigma_{\alpha,k},d=k-1,p=\alpha) \qquad (x\geq 0) \tag{7.4}$$
$$= (C_{\alpha,k})\left(\sigma_{\alpha,k}\right)^{1-k} x^{k-2}\, F_{\frac{\alpha}{2}}\left(\left(\frac{x}{\sigma_{\alpha,k}}\right)^{\alpha}\right),$$

where

$$C_{\alpha,k} := \frac{\alpha\Gamma((k-1)/2)}{\Gamma((k-1)/\alpha)} \tag{7.5}$$

$$\sigma_{\alpha,k} := \frac{|k|^{1/2-1/\alpha}}{\sqrt{2}}. \tag{7.6}$$

Note that the difference between (7.3) and (7.4) is very small: Just replace $\mathfrak{N}_{\gamma\alpha}(...)$ to $\mathfrak{N}_{\alpha/2}(...)$.

7.2.1. FCM CDF. Extending directly from Lemma 6.2, we have

LEMMA 7.2. The CDF of FCM can be represented by γ^*_α in (3.20) as

$$\Phi[\overline{\chi}_{\alpha,k}](x) = z^{k-1+\alpha}\,\gamma^*_{\alpha/2}\left(\frac{k-1+\alpha}{\alpha}, z^{\alpha}\right), \qquad (k>0,\alpha\in[0,2]) \tag{7.7}$$

where $z = x/\sigma_{\alpha,k}$.

△

7.2.2. FCM for Negative k. We quote Definition 3.2 of [15] for FCM in the negative k space. It is the characteristic FCM (χ_ϕ) in Lemma 9.6, whose PDF is:

$$\overline{\chi}_{\alpha,-k}(x) := \mathfrak{N}_{\alpha/2}(x;\sigma=(\sigma_{\alpha,k})^{-1},d=-k,p=-\alpha). \qquad (x\geq 0,k>0) \tag{7.8}$$

This is used to define the fractional exponential power distribution within the GSaS (and GAS-SN) nomenclature. See Section 12.7.

7.3. FCM Moments

By letting $s = n+1$ and $\theta = 0$ in (7.2), its n-th moment is

$$\mathbb{E}(X^n|\overline{\chi}_{\alpha,k}) = (\sigma_{\alpha,k})^n\,\frac{\Gamma((k-1)/2)}{\Gamma((k-1)/\alpha)}\,\frac{\Gamma((n+k-1)/\alpha)}{\Gamma((n+k-1)/2)}, \qquad (k>0,\alpha>0) \tag{7.9}$$

which requires $k > 1$ and $n + k > 1$ to avoid singularity of the gamma functions (See Section 7.6 of [15]).

The moment formula of FCM is fundamental to all the fractional distributions built on top of it. But ironically, due to the nature of a ratio distribution, it is often evaluated as negative moments, $n < 0$. Hence, n is confined in the range of $1 - k < n < 0$.

This results in non-existing moments when k is not "large enough", which happens to be a core feature of the α-stable distribution and Student's t distribution. Our two-dimensional parameter space (α, k) adds more complexity to it.

7.3.1. FCM at Infinite Degrees of Freedom. The choice of $\sigma_{\alpha,k}$ is intentional, such that

$$\lim_{k\to\infty} \mathbb{E}(X^n|\overline{\chi}_{\alpha,k}) = \alpha^{-n/\alpha}. \qquad (k > 0, \alpha > 0) \tag{7.10}$$

Under such condition, its variance is zero. That is, FCM becomes a delta function, $\delta(x - \alpha^{-1/\alpha})$, as $k \to \infty$.

7.4. FCM Reflection Formula

When $k < 0$, the PDF of FCM is defined as

$$\overline{\chi}_{\alpha,k}(x) := \mathfrak{N}_{\alpha/2}(x; \sigma = 1/\sigma_{\alpha,k}, d = k, p = -\alpha) \qquad (k < 0). \tag{7.11}$$

But it also noted that we might not repeat the $k < 0$ scenario everywhere. It is too tedious to the readers. So we choose not to do it for conciseness. The readers interested in full detail are referred to the FCM sections in [15].

The $k < 0$ case is born out of the properties of the α-stable characteristic function in Chapter 9. It is used to build a generalized two-sided distribution (Section 9 of [15]) that subsumes the exponential power distribution (Section 3.11.1 of [24]).

Here we quote the FCM reflection formula from Section 7 of [15] to summarize the relation:

$$\mathbb{E}(X^n|\overline{\chi}_{\alpha,-k}) = \frac{\mathbb{E}(X^{-n+1}|\overline{\chi}_{\alpha,k})}{\mathbb{E}(X|\overline{\chi}_{\alpha,k})}, \ k > 0. \tag{7.12}$$

7.5. FCM2: Fractional Chi-Squared-Mean Distribution

If $Z \sim \overline{\chi}_{\alpha,k}$, then $X \sim Z^2$ is FCM2, denoted as $X \sim \overline{\chi}^2_{\alpha,k}$. This is the fractional extension of the classic χ^2_k/k, which is subsumed by it at $\alpha = 1$.

$\overline{\chi}^2_{\alpha,k}$ is used in the fractional F distribution in the area of the squared variable and the quadratic form in the multivariate elliptical distribution.

DEFINITION 7.3. The PDF of FCM2 is

$$\overline{\chi}^2_{\alpha,k}(x) = \frac{1}{2\sqrt{x}}\,\overline{\chi}_{\alpha,k}(\sqrt{x}) \qquad (x \ge 0, \alpha \in [0,2]) \tag{7.13}$$

Expressed in FG and (7.4), it is

$$\begin{aligned}\overline{\chi}^2_{\alpha,k}(x) &:= \mathfrak{N}_{\alpha/2}(x; \sigma = \sigma^2_{\alpha,k}, d = (k-1)/2, p = \alpha/2) \qquad (k > 0) \\ &= \frac{C_{\alpha,k}}{2\,\sigma^2_{\alpha,k}} \left(\frac{x}{\sigma^2_{\alpha,k}}\right)^{k/2-3/2} F_{\frac{\alpha}{2}}\left(\left(\frac{x}{\sigma^2_{\alpha,k}}\right)^{\alpha/2}\right).\end{aligned} \tag{7.14}$$

Or for $k < 0$,

$$\overline{\chi}^2_{\alpha,k}(x) := \mathfrak{N}_{\alpha/2}(x; \sigma = \sigma^{-2}_{\alpha,k}, d = k/2, p = -\alpha/2) \qquad (k < 0) \tag{7.15}$$

When dealing with the fractional Gauss hypergeometric function (FGHF) in Section 5.2, we need two more variations from FCM2. The first allows an FCM2 to take a different scale:

$$\overline{\chi}^2_{\alpha,k}(x; \sigma) := \mathfrak{N}_{\alpha/2}(x; \sigma = \sigma, d = (k-1)/2, p = \alpha/2) \qquad (k > 0) \tag{7.16}$$

from which the constant-scale variant is defined by replacing $\sigma_{\alpha,k}$ with $1/2$,

$$\widehat{\chi}^2_{\alpha,k}(x) := \overline{\chi}^2_{\alpha,k}(x; \sigma = 1/4) = \mathfrak{N}_{\alpha/2}(x; \sigma = 1/4, d = (k-1)/2, p = \alpha/2) \qquad (k > 0) \tag{7.17}$$

Notice the hat symbol replaces the bar symbol.

7.5.1. FCM2 CDF.

Extending directly from Lemma 6.2, we have:

LEMMA 7.4. The CDF of FCM2 can be represented by γ^*_α as

$$\Phi[\overline{\chi}^2_{\alpha,k}](x) = z^{(k-1+\alpha)/2}\,\gamma^*_{\alpha/2}\left(\frac{k-1+\alpha}{\alpha}, z^{\alpha/2}\right) \qquad (k > 0, \alpha \in [0,2]) \tag{7.18}$$

where $z = x/\sigma^2_{\alpha,k}$. △

7.5.2. Representing FCM by FCM2.

In (7.13), let $s = \sqrt{x}$, we get the inverse relation:

$$\overline{\chi}_{\alpha,k}(s) = 2s\,\overline{\chi}^2_{\alpha,k}(s^2) \qquad (s \ge 0) \tag{7.19}$$

Many ratio distribution integrals involving FCM can be rewritten in terms of FCM2, such that

$$\begin{aligned} f(x) &:= \int_0^\infty g(xs)\,\overline{\chi}_{\alpha,k}(s)\,s\,ds \\ &= \int_0^\infty g(x\sqrt{\nu})\,\overline{\chi}^2_{\alpha,k}(\nu)\,\sqrt{\nu}\,d\nu \end{aligned} \tag{7.20}$$

For the CDF case, the incomplete integral can be transformed as

$$\begin{aligned} F(x) := \int_0^x f(x)\,dx &= \int_0^\infty G(xs)\,\overline{\chi}_{\alpha,k}(s)\,ds \\ &= \int_0^\infty G(x\sqrt{\nu})\,\overline{\chi}^2_{\alpha,k}(\nu)\,d\nu \end{aligned} \tag{7.21}$$

where $G(x) := \int_0^x g(x)\,dx$. The lower bound of the incomplete integrals can be $-\infty$ such as $\int_{-\infty}^x dx$ too.

7.5.3. Universal Expression. Assume $x \geq 0$, let $M(x^2) := G(x)/x$ in (7.21) or $g(x)$ in (7.20), we get the universal expression of

$$F(x) = x \int_0^\infty M(x^2\nu)\, \overline{\chi}^2_{\alpha,k}(\nu)\, \sqrt{\nu}\, d\nu \tag{7.22}$$

$$f(x) = \int_0^\infty M(x^2\nu)\, \overline{\chi}^2_{\alpha,k}(\nu)\, \sqrt{\nu}\, d\nu \tag{7.23}$$

Most of the univariate PDFs and CDFs in subsequent chapters can be understood in such framework. It is just a matter of what $M(x)$ is.

When $M(x)$ can be expressed by a Kummer function (apart from a negative sign), these integrals are members of the FGHF in Section 5.2.

7.6. FCM2 Mellin Transform

From (6.5), the Mellin transform of FCM2's PDF is

$$\begin{aligned} &\overline{\chi}^2_{\alpha,k}(x) \overset{\mathcal{M}}{\longleftrightarrow} \overline{\chi}^{2*}_{\alpha,k}(s) \\ &\qquad = (\sigma_{\alpha,k})^{2s-2}\, \frac{\Gamma((k-1)/2)}{\Gamma((k-1)/\alpha)} \frac{\Gamma((s+k/2-3/2)\ \times 2/\alpha)}{\Gamma(s+k/2-3/2)}. \qquad (k>0) \end{aligned} \tag{7.24}$$

Likewise, for the constant-scale variant, it becomes

$$\begin{aligned} &\widehat{\chi}^2_{\alpha,k}(x) \overset{\mathcal{M}}{\longleftrightarrow} \widehat{\chi}^{2*}_{\alpha,k}(s) \\ &\qquad = 2^{2-2s}\, \frac{\Gamma((k-1)/2)}{\Gamma((k-1)/\alpha)} \frac{\Gamma((s+k/2-3/2)\ \times 2/\alpha)}{\Gamma(s+k/2-3/2)}, \qquad (k>0) \end{aligned} \tag{7.25}$$

whose most important special case is $\alpha = 1$,

$$\widehat{\chi}^2_{1,k}(x) \overset{\mathcal{M}}{\longleftrightarrow} \widehat{\chi}^{2*}_{1,k}(s) = \frac{\Gamma(s+k/2-1)}{\Gamma(k/2)} \tag{7.26}$$

$\Gamma(s+k/2-1)$ in $\widehat{\chi}^{2*}_{1,k}(s)$ is just an ordinary gamma function without a fractional coefficient in front of s. This property is the basis that connects the fractional Gauss hypergeometric function to its classic form in Section 5.2.

7.7. FCM2 Moments

From the Mellin transform by $s = n+1$, its n-th moment is

$$\begin{aligned} &\mathbb{E}(X^n|\overline{\chi}^2_{\alpha,k}) = \mathbb{E}(X^{2n}|\overline{\chi}_{\alpha,k}) \\ &\qquad = (\sigma_{\alpha,k})^{2n}\, \frac{\Gamma((k-1)/2)}{\Gamma((k-1)/\alpha)} \frac{\Gamma((n+k/2-1/2)\ \times 2/\alpha)}{\Gamma(n+k/2-1/2)}. \qquad (k>0) \end{aligned} \tag{7.27}$$

As mentioned in Section 7.3, due to the nature of a ratio distribution, it is often evaluated as negative moments, $n < 0$. Hence, n is confined in the range of $1/2 - k/2 < n < 0$.

This puts stricter constraint on non-existing moments than FCM when k is not "large enough". For instance, in the case of fractional F distribution in Section 8.4, $k \approx 3$ is in the neighborhood where it second moment barely exists. This makes it rather hard for the statistics of the SPX daily return data set, since its k is just slightly larger than 3 while α is slightly below 1.

7.8. FCM2 Increment of k

LEMMA 7.5. When x^m is multiplied to $\overline{\chi}^2_{\alpha,k}(x)$, it follows a scaling rule where k is incremented to $k+2m$ in the parametrization.

$$x^m\,\overline{\chi}^2_{\alpha,k}(x) = \sigma^{2m}_{\alpha,k}\,Q\,\frac{C_{\alpha,k}}{C_{\alpha,k+2m}}\,\overline{\chi}^2_{\alpha,k+2m}(y). \tag{7.28}$$

where $Q := \sigma^2_{\alpha,k+2m}/\sigma^2_{\alpha,k}$ and $y = Q\,x$. △

PROOF. From (7.14),

$$x^m\,\overline{\chi}^2_{\alpha,k}(x) = \sigma^{2m}_{\alpha,k}\,\frac{C_{\alpha,k}}{2\,\sigma^2_{\alpha,k}}\left(\frac{x}{\sigma^2_{\alpha,k}}\right)^{(k+2m)/2-3/2} F_{\frac{\alpha}{2}}\left(\left(\frac{x}{\sigma^2_{\alpha,k}}\right)^{\alpha/2}\right).$$

We see that $\overline{\chi}^2_{\alpha,k}$ should become $\overline{\chi}^2_{\alpha,k+2m}$ according to the power in the $x^{(k+2m)/2-3/2}$ term, but other parts of the formula need to be adjusted too.

Since

$$\overline{\chi}^2_{\alpha,k+2m}(y) = \frac{C_{\alpha,k+2m}}{2\,\sigma^2_{\alpha,k+2m}}\left(\frac{y}{\sigma^2_{\alpha,k+2m}}\right)^{(k+2m)/2-3/2} F_{\frac{\alpha}{2}}\left(\left(\frac{y}{\sigma^2_{\alpha,k+2m}}\right)^{\alpha/2}\right),$$

we obtain $y = x\,\sigma^2_{\alpha,k+2m}/\sigma^2_{\alpha,k}$ in order to match the two structurally.

Then take the ratio of $x^m\,\overline{\chi}^2_{\alpha,k}(x)/\overline{\chi}^2_{\alpha,k+2m}(y)$ to determine the needed constant, we arrive at (7.28).

□

7.9. Sum of Two Chi-Squares with Correlation

The sum of bivariate variables is studied here.

LEMMA 7.6. Let $Z = Z_1/s_1 + Z_2/s_2$ where Z_1, Z_2 are two independent χ^2_1 variables. The PDF of Z is

$$\begin{aligned}\chi^2_{11}(z, s_1, s_2) &= \frac{\sqrt{s_1 s_2}}{2} e^{-s_2 z/2}\,{}_1F_1\left(\frac{1}{2}, 1; \frac{(s_2 - s_1)z}{2}\right) \\ &= \frac{\sqrt{s_1 s_2}}{2} e^{-(s_1+s_2)z/4} I_0(|s_2 - s_1|z/4)\end{aligned}$$

We apply DLMF 12.6.9 to get the second line, where the symmetry of a, b is explicit since $I_0(x)$ is symmetric. For $x \gg 1$, $I_0(x) \approx e^x/\sqrt{2\pi x}$ (DLMF 10.40.5). △

When $Z_1 = U_1^2$, $Z_2 = U_2^2$, and U_1, U_2 has correlation ρ, then s_1, s_2 must be modified by the eigenvalue solution of $\bar{\Omega}^{-1}\mathrm{diag}(\boldsymbol{s})$ such that

$$\begin{aligned}\chi^2_{11}(z, s_1, s_2, \rho) &= \chi^2_{11}(z, s_1', s_2') \\ \text{where} \quad (s_1', s_2') &= \frac{(s_1 + s_2) \pm \sqrt{(s_1 - s_2)^2 - 4\rho^2 s_1 s_2}}{2(1 - \rho^2)}\end{aligned}$$

CHAPTER 8

Fractional F Distribution

The classic F distribution comes from the ratio of two χ^2 distributions. Assume $U_1 \sim \chi^2_d/d$ and $U_2 \sim \chi^2_k/k$, then $F \sim U_1/U_2$ is an F distribution, $F_{d,k}$.

Two use cases were mentioned in Azzalini (2013)[1]. In Section 4.3 there, the squared variable of a univariate skew-t with k degrees of freedom is distributed as $F_{1,k}$.

In Section 6.2 there, the quadratic from a $d \times d$ multivariate skew-t with k degrees of freedom is distributed as $F_{d,k}$.

Thus, the meaning of d and k is quite clear in such a context: d is the dimension of the multivariate skew-normal process; k is the degree of freedom in the denominator of the ratio distribution. This chapter extends it fractionally.

8.1. Definition

DEFINITION 8.1. Assume $U_1 \sim \chi^2_d/d$ and $U_2 \sim \overline{\chi}^2_{\alpha,k}$, then $F \sim U_1/U_2$ is a fractional F distribution. We use the notation $F \sim F_{\alpha,d,k}$.

The standard PDF of $F_{\alpha,d,k}$ is

$$F_{\alpha,d,k}(x) = \int_0^\infty s\, ds \left[d\, \chi^2_d(dxs)\right] \overline{\chi}^2_{\alpha,k}(s) \tag{8.1}$$

and note that the classic term in the integrand, $d\, \chi^2_d(d\, z)$, is equivalent to our $\bar{\chi}^2_{1,d}(z)$.

The reader should be aware of the subtlety that "ds" in "$s\, ds$" is the calculus notation, while d in $\left[d\, \chi^2_d(dxs)\right]$ is the constant from $F_{\alpha,d,k}$.

The standard CDF of $F_{\alpha,d,k}$ is

$$\Phi[F_{\alpha,d,k}](x) = \int_0^x F_{\alpha,d,k}(x)\, dx \tag{8.2}$$

$$= \int_0^\infty \left[\frac{1}{\Gamma\left(\frac{d}{2}\right)} \gamma\left(\frac{d}{2}, \frac{dxs}{2}\right)\right] \overline{\chi}^2_{\alpha,k}(s)\, ds \tag{8.3}$$

since the CDF of a χ^2_d is the regularized lower incomplete gamma function of $\gamma\left(\frac{d}{2}, \frac{x}{2}\right)/\Gamma\left(\frac{d}{2}\right)$.

It can also be represented by a fractional Gauss hypergeometric function. See Section 5.2.5.

8.1.1. The Origin of Fractional F. $F_{\alpha,d,k}$ is connected to the quadratic form of a d-dimensional multivariate GAS-SN distribution, $L_{\alpha,k}(0, \bar{\Omega}, \boldsymbol{\beta})$. Indeed, its three parameters, α, d, k, are designated such that the symbols convey the same meanings. However, $\bar{\Omega}$ and β doesn't affect the outcome of $F_{\alpha,d,k}$.

To elaborate from Section 15.6, assume Z is a $d \times d$ multivariate skew-normal (SN) distribution $SN(0, \bar{\Omega}, \beta)$, and $\overline{\chi}_{\alpha,k}$ is a standard FCM. Then $X = Z/\overline{\chi}_{\alpha,k}$ is an $L_{\alpha,k}(0, \bar{\Omega}, \boldsymbol{\beta})$.

The quadratic form of X is $Q = \frac{1}{d} X^\intercal \bar{\Omega}^{-1} X$. And $Q \sim F_{\alpha,d,k}$ is a fractional F distribution.

8.1.2. Fractional F Subsumes F.

LEMMA 8.2. When $\alpha = 1$, it becomes a classic F. That is, $F_{1,d,k} = F_{d,k}$. △

8.1.3. Fractional F Subsumes GSaS-Squared and GAS-SN-Squared. The following cases are for $d = 1$:

LEMMA 8.3. If $X_1 \sim L_{\alpha,k}$, then $X_1^2 \sim F_{\alpha,1,k}$. △

LEMMA 8.4. If $X_2 \sim L_{\alpha,k}(\beta)$, then $X_2^2 \sim F_{\alpha,1,k}$, independent of β. △

They will be discussed in Chapter 12.

8.2. PDF at Zero

The PDF of an F distribution is singular as $x \to 0$ when $d < 2$. We can see that from

$$\begin{aligned} F_{\alpha,d,k}(x) &\approx \frac{(d/2)^{d/2}}{\Gamma(d/2)} x^{d/2-1} \int_0^\infty s^{d/2}\, ds\, \overline{\chi}^2_{\alpha,k}(s) \\ &= \frac{(d/2)^{d/2}}{\Gamma(d/2)} \mathbb{E}(X^d|\overline{\chi}_{\alpha,k})\, x^{d/2-1} \end{aligned} \tag{8.4}$$

for very small x.

When $d = 1$, the peak is divergent as $F_{\alpha,1,k}(x) \approx \frac{1}{\sqrt{2\pi}} \mathbb{E}(X|\overline{\chi}_{\alpha,k}) \sqrt{x}^{-1}$. But its CDF $\propto \sqrt{x}$.

When $d = 2$, this peak is finite. $F_{\alpha,2,k}(0) = \mathbb{E}(X^2|\overline{\chi}_{\alpha,k})$.

When $d > 2$, $F_{\alpha,d,k}(x)$ drops to zero at $x = 0$. This strange phenomenon seems to indicate that the bivariate system is the lowest dimension to have stable quadratic statistics. And a three dimension system is likely more stable. But we only analyze the bivariate case in this book.

8.3. Mellin Transform

From (7.24), and note that $\bar{\chi}^2_d = \bar{\chi}^2_{1,d}$, the Mellin transform of Fractional F's PDF is

$$F_{\alpha,d,k}(x) \overset{\mathcal{M}}{\longleftrightarrow} (\bar{\chi}^2_{1,d})^*(s)\, (\bar{\chi}^2_{\alpha,k})^*(2-s) \qquad (d > 0, k > 0) \tag{8.5}$$

$$= \left(\sqrt{2d}\, \sigma_{\alpha,k}\right)^{2-2s} \left[\frac{\Gamma((d-1)/2)}{\Gamma(d-1)} \frac{\Gamma((k-1)/2)}{\Gamma((k-1)/\alpha)}\right] \left[\frac{\Gamma(2p(s))}{\Gamma(p(s))} \frac{\Gamma(2q(s)/\alpha)}{\Gamma(q(s))}\right], \tag{8.6}$$

$$\text{where } \; p(s) := s + d/2 - 3/2, \; q(s) := 1/2 + k/2 - s.$$

The number of gamma functions can be reduced via the Legendre duplication formula (A.2).

8.4. Moments

Its n-th moment is

$$\begin{aligned} \mathbb{E}(X^n|F_{\alpha,d,k}) &= d^{-n}\, \mathbb{E}(X^n|\chi^2_d)\, \mathbb{E}(X^{-n}|\overline{\chi}^2_{\alpha,k}) \\ &= \left(\frac{2}{d}\right)^n (d/2)_n\, \mathbb{E}(X^{-n}|\overline{\chi}^2_{\alpha,k}). \end{aligned} \tag{8.7}$$

where $(d/2)_n$ is the Pochhammer symbol, $(a)_n := \Gamma(a+n)/\Gamma(a)$.

Its first moment is $\mathbb{E}(X^{-1}|\overline{\chi}^2_{\alpha,k}) = \mathbb{E}(X^{-2}|\overline{\chi}_{\alpha,k})$, independent of d. This is due to $\mathbb{E}(X|\chi^2_d) = d$.

Note that this first moment is also the second moment of an univariate GAS-SN in (12.9), or simply the variance of the corresponding GSaS.

Its second moment is $(1 + 2/d)\, \mathbb{E}(X^{-2}|\overline{\chi}^2_{\alpha,k})$. Hence, its variance is

$$\begin{aligned} \text{var}\{F_{\alpha,d,k}\} &= (1 + 2/d)\, \mathbb{E}(X^{-2}|\overline{\chi}^2_{\alpha,k}) - \mathbb{E}(X^{-1}|\overline{\chi}^2_{\alpha,k})^2 \\ &= (1 + 2/d)\, \mathbb{E}(X^{-4}|\overline{\chi}_{\alpha,k}) - \mathbb{E}(X^{-2}|\overline{\chi}_{\alpha,k})^2. \end{aligned} \tag{8.8}$$

8.4.1. Stability Issue of the Second Moment. The moment formula appears to be straightforward. But the devil is in the detail.

The stability of moments symbolizes the challenge of stability in the α-stable distribution. Even the second moment has dramatic behaviors when k is smaller than 4.

First, we shall recognize that the first moment of F is actually the second moment of the underlying two-sided distribution, because the variable of F is squared. Having a finite and stable first moment in F is quite meaningful. But it is much harder to make sense of the variance when k is too small.

Notice that, when $d \to \infty$, the variance is independent of d,

$$\mathrm{var}\{F_{\alpha,\infty,k}\} = \mathbb{E}(X^{-2}|\overline{\chi}^2_{\alpha,k}) - \mathbb{E}(X^{-1}|\overline{\chi}^2_{\alpha,k})^2$$

This is the most relevant quantity, if exists, that other variances of finite d are relative to in an inverse d relation, such as

$$\mathrm{var}\{F_{\alpha,d,k}\} - \mathrm{var}\{F_{\alpha,\infty,k}\} = \frac{2}{d}\,\mathbb{E}(X^{-2}|\overline{\chi}^2_{\alpha,k}).$$

8.5. Sum of Two Fractional Chi-Square Mixtures with Correlation

This section addresses a complication that arises from the multivariate adaptive distribution.

TODO need to re-write this. but I may not have enough result to write it though. Alas...

Consider $X_1^2 \sim F_{\alpha_1,1,k_1}$ and $X_2^2 \sim F_{\alpha_2,1,k_2}$. Assume that there is a correlation between X_1 and X_2 as described in Section 7.9. The PDF of the quadratic form $Q = (X_1^2 + X_2^2)/2$ is a convolution that wraps around $Z \sim \chi^2_{11}(\rho)$ such that

$$\begin{aligned} f_Q(x) &= 2\int_0^{2x} F_{\alpha_1,1,k_1}(w)\cdot F_{\alpha_2,1,k_2}(2x-w)\,dw \\ &= 2\int_0^{\infty} ds_1\,\bar{\chi}^2_{\alpha_1,k_1}(s_1)\int_0^{\infty} ds_2\,\bar{\chi}^2_{\alpha_2,k_2}(s_2)\,\chi^2_{11}(2x,s_1,s_2,\rho) \end{aligned}$$

This is the PDF of the quadratic form of a standard 2-dimensional adaptive GAS-SN distribution.

TODO When ρ and β mingle together, there are additional complications.

8.6. Fractional Adaptive F Distribution

It should look like this: $\overrightarrow{F}_{\boldsymbol{\alpha},d,\boldsymbol{k}}$, but it is a bit strange, mixing vectors and numbers together...

TODO Ah, this is much harder than I thought !!!

Part 3

Two-Sided Univariate Distributions

CHAPTER 9

Framework of Continuous Gaussian Mixture

The construction of a symmetric two-sided distribution is in the form of a continuous Gaussian mixture. Both the ratio and product distribution methods are used.

In the case of the symmetric α-stable distribution (SaS)[5], the exponential power distribution comes from its characteristic function (CF)[24]. We would like to present a unified framework and familiarize the reader with the notations, which would be otherwise subtle and confusing.

Assume the PDF of a two-sided symmetric distribution is $L(x)$ where $x \in \mathbb{R}$. It has zero mean, $\mathbb{E}(X|L) = 0$. Assume the PDF of a one-sided distribution is $\chi(x)\,(x > 0)$ such that

$$L(x) := \int_0^\infty s\,ds\,\mathcal{N}(xs)\,\chi(s) \tag{9.1}$$

This is nothing new. It is the definition of a ratio distribution with a standard normal variable $\mathcal{N}$. This is the first form of the Gaussian mixture: $L \sim \mathcal{N}/\chi$. A contrive example is that L is a Student's t distribution when χ is $(\chi_k^2)^{1/2}$.

The skewness is added by replacing the normal distribution $\mathcal{N}$ with its skew-normal counterpart $\mathcal{N}(\beta)$. See next chapter for more detail.

It has the equivalent expression in terms of a product distribution by way of *the inverse distribution* $\chi^\dagger$ such that $L \sim \mathcal{N}\chi^\dagger$. This is the second form of the Gaussian mixture.

$\chi^\dagger$ is closer to our typical understanding of the marginal distribution of a volatility process. For example, when the Brownian motion process $dX_t = \sigma_t\,dW_t$ is measured in a particular time interval Δt, we have $\Delta X_t \sim L$ and $\sigma_t \sim \chi^\dagger$.

However, χ in the first form is more natural in the expression of the α-stable distribution. So we are more inclined to use the ratio distribution. The reader should keep this subtlety in mind.

LEMMA 9.1. (Inverse distribution) The inverse distribution is defined as[10]

$$\chi^\dagger(s) := s^{-2}\,\chi\left(\frac{1}{s}\right) \tag{9.2}$$

such that

$$\int_0^\infty s\,ds\,\mathcal{N}(xs)\,\chi(s) = \int_0^\infty \frac{ds}{s}\,\mathcal{N}\left(\frac{x}{s}\right)\,\chi^\dagger(s) \qquad (x \in \mathbb{R}) \tag{9.3}$$

$$\int_0^\infty s\,ds\,\mathcal{N}(xs)\,\chi^\dagger(s) = \int_0^\infty \frac{ds}{s}\,\mathcal{N}\left(\frac{x}{s}\right)\,\chi(s) \tag{9.4}$$

The proof is straightforward by a change of variable $t = 1/s$. You can move between LHS and RHS easily.

△

We use the notation $\mathrm{CF}\{g\}(t) = \mathbb{E}(e^{itX}|g)$ to represent the characteristic function transform of the PDF $g(x)$. Note that $\mathcal{N}$ has a special property that its CF is still itself: $\mathrm{CF}\{\mathcal{N}\}(t) = \sqrt{2\pi}\,\mathcal{N}(t)$.

LEMMA 9.2. (Characteristic function transform of L) Let $\phi(t)$ be the CF of L such that $\phi(t) := \mathrm{CF}\{L\}(t) = \int_{-\infty}^{\infty} dx\, \exp(itx)\, L(x)$. (9.1) is transformed to

$$\phi(t) = \sqrt{2\pi} \int_0^{\infty} ds\, \mathcal{N}\left(\frac{t}{s}\right) \chi(s) \qquad (t \in \mathbb{R}) \tag{9.5}$$

This allows us to define a new distribution pair: L_ϕ and $\chi_\phi^\dagger$, in terms of a product distribution such that

$$L_\phi(x) := \int_0^{\infty} \frac{ds}{s}\, \mathcal{N}\left(\frac{x}{s}\right) \chi_\phi^\dagger(s) \qquad (x \in \mathbb{R}) \tag{9.6}$$

$$\chi_\phi^\dagger(s) := \frac{s\,\chi(s)}{\mathbb{E}(X|\chi)} \tag{9.7}$$

where $\mathbb{E}(X|\chi)$ is the first moment of χ. Here $\chi_\phi^\dagger$ is the inverse distribution of χ_ϕ, which can be reverse-engineered according to (9.2),

$$\chi_\phi(s) := \frac{s^{-3}}{\mathbb{E}(X|\chi)}\, \chi\left(\frac{1}{s}\right) \tag{9.8}$$

△

We are in an interesting place: We start with a one-sided distribution χ, we derive two variants from it: χ_ϕ and $\chi_\phi^\dagger$. We also obtain two two-sided distributions: L and L_ϕ.

We shall call χ_ϕ *the characteristic distribution* of χ since it facilitates the following parallel relation:

$$L \sim \mathcal{N}/\chi$$
$$L_\phi \sim \mathcal{N}/\chi_\phi$$

χ symbolizes the fractional χ distribution we are about to present. The ϕ suffix will be replaced with the *negation* (sign change) of the degree of freedom.

CHAPTER 10

SN: The Skew-Normal Distribution - Review

10.1. Definition

The skew-normal distribution family is well documented in A. Azzalini's 2013 monograph[1]. We recap the results and clarify the symbology. My contribution is to incorporate the skew-normal methodology into the fractional distributions wherever suitable. The enhanced distributions are flexible and can adapt to many different shapes and tails with high skewness and kurtosis.

10.1.1. The Selective Sampling. The *selective sampling* method is used to inject skewness into the stochastic system, which is otherwise symmetric. This mechanism is fairly common in an applied context, for example, in social sciences, where a variable X_0 is observed only when a correlated variable X_1, which is usually unobserved, satisfies a certain condition (p.128 of [1]).

In quantitative finance, the condition could be market regimes. In a two-regime model, a market index such as the S&P 500 index (SPX) is classified into the growth regime or the crash regime at a given time. It is well known that the volatility of the market behaves differently in each regime. In the growth regime, volatility tends to be low, and the market is trending upward. In the crash regime, volatility tends to be high, and the market is trending downward.

A univariate random variable $Z \sim SN(0,1,\beta)$ is a standard skew-normal variable with skew parameter $\beta \in \mathbb{R}$ (Section 2.1 of [1]). The sign of β determines the sign of its skewness (10.14).

One of its stochastic representations is

$$Z = \begin{cases} X_0 & \text{if } X_1 < \beta X_0, \\ -X_0 & \text{otherwise.} \end{cases} \tag{10.1}$$

where X_0, X_1 are independent $\mathcal{N}(0,1)$ variables.

An alternative representation uses filtering, or rejection, such that $Z = (X_0 | X_1 < \beta X_0)$. That is, X_0 is accepted as Z only when the condition $X_1 < \beta X_0$ is satisfied. Otherwise, it is discarded.

10.1.2. The PDF and CDF. The standard PDF is

$$\mathcal{N}(x;\beta) := 2\,\mathcal{N}(x)\Phi_{\mathcal{N}}(\beta x), \quad (x \in \mathbb{R}) \tag{10.2}$$

where $\mathcal{N}(x)$ and $\Phi_{\mathcal{N}}(x)$ are the PDF and CDF of $\mathcal{N}(0,1)$.

Its extremal distribution occurs at $\beta \to \infty$, where $\Phi_{\mathcal{N}}(\beta x)$ becomes a step function. The PDF becomes that of a half-normal distribution.

The standard CDF is

$$\Phi_{SN}(x;\beta) := \Phi_{\mathcal{N}}(x) - 2\,T(x,\beta) \tag{10.3}$$

where $T(h,a)$ is called the Owen's T function[25]. Its numerical methods are widely implemented in modern software packages.

Several important properties are quoted from Proposition 2.1 of [1]:

- $\mathcal{N}(0;0) = 1/\sqrt{2\pi}$. Universal anchor at $x = 0, \beta = 0$.
- $\mathcal{N}(x;0) = \mathcal{N}(x)$. Continuity at $\beta = 0$.
- $\mathcal{N}(-x;\beta) = \mathcal{N}(x;-\beta)$. This is the reflection rule.

- $Z^2 \sim \chi^2_1$, irrespective of β.

Notice that Z^2 is independent of β. This is an important property, but may not be intuitive for new students. This is due to the fact that the squares of X_0 and $-X_0$ are the same in (10.1). This property is carried into the quadratic form of the multivariate elliptical distribution.

10.2. The Location-Scale Family

Its location-scale family is $Y = \xi + \omega Z \sim SN(\xi, \omega^2, \beta)$, where $\xi \in \mathbb{R}$ and $\omega > 0$. Its PDF becomes

$$\frac{1}{\omega}\mathcal{N}\left(\frac{x-\xi}{\omega};\beta\right). \tag{10.4}$$

10.3. Invariant Quantities

The following quantity plays an important role in the selective sampling concept of SN:

$$\delta = \frac{\beta}{\sqrt{1+\beta^2}}, \quad \delta \in (-1,1). \tag{10.5}$$

It can be thought of as some kind of correlation in the following. Inversely, β can be calculated from

$$\beta = \frac{\delta}{\sqrt{1-\delta^2}}. \tag{10.6}$$

These two quantities will appear in many places in the ensuing chapters. They are invariants in the context of the multivariate elliptical distribution, called the Canonical Form.

In a trigonometry representation, one can think of δ as $\sin(\theta)$ of a right triangle, where one leg is 1, the other leg is β, and θ is the angle facing β.

Three representations use δ as the correlation coefficient to generate SN. (Section 2.1.3 of [1]) First, designate the correlation matrix as

$$\bar{\Omega} = \begin{pmatrix} 1 & \delta \\ \delta & 1 \end{pmatrix}.$$

The Cholesky factor of $\bar{\Omega}$ is

$$L \;=\; \begin{pmatrix} 1 & 0 \\ \delta & \sqrt{1-\delta^2} \end{pmatrix},$$

so that $L\,L^T = \bar{\Omega}$.

Assume U_0 and U_1 are two independent $\mathcal{N}(0,1)$ variates. The first representation of $Z \sim SN(0,1,\beta)$ is

$$Z = \begin{cases} X_0 & \text{if } X_1 > 0, \\ -X_0 & \text{otherwise.} \end{cases} \tag{10.7}$$

where X_0, X_1 are marginals of a standard correlated normal bivariate with $\text{cor}\{X_0, X_1\} = \delta$ such that

$$\begin{pmatrix} X_0 \\ X_1 \end{pmatrix} \;=\; L \begin{pmatrix} U_0 \\ U_1 \end{pmatrix}.$$

The second representation is from

$$\begin{pmatrix} - \\ Z \end{pmatrix} \;=\; L \begin{pmatrix} U_0 \\ |U_1| \end{pmatrix}$$

such that $Z = \sqrt{1-\rho^2}\,U_0 + \delta\,|U_1| \sim SN(0,1,\beta)$.

The third representation is $Z = \max\{X_0, X_1\} \sim SN(0, 1, \beta)$, where X_0, X_1 are marginals of a standard correlated bivariate such that

$$\begin{pmatrix} X_0 \\ X_1 \end{pmatrix} = \begin{pmatrix} 1 & 0 \\ \rho & \sqrt{1-\rho^2} \end{pmatrix} \begin{pmatrix} U_0 \\ U_1 \end{pmatrix}.$$

and $\text{cor}\{X_0, X_1\} = \rho = 1 - 2\delta^2$.

10.4. Mellin Transform

The following result is elegant, but also peculiar. It is discovered by the author.

LEMMA 10.1. The Mellin transform of the SN PDF is

$$\mathcal{N}(x;\beta) \overset{\mathcal{M}}{\longleftrightarrow} \mathcal{N}^*(s;\beta) := 2\,\mathcal{N}^*(s)\,\Phi[t_s](\beta\sqrt{s}), \tag{10.8}$$
$$\text{where} \quad \mathcal{N}^*(s) = \frac{1}{2}\frac{2^{s/2}}{\sqrt{2\pi}}\Gamma\left(\frac{s}{2}\right)$$

is the Mellin transform of the PDF of $\mathcal{N}(0,1)$ in (2.9). And $\Phi[t_k](x)$ is the CDF of a Student's t distribution with k degrees of freedom. But it is used in a strange way, where s substitutes k and goes into x at the same time.

△

PROOF. We prove (10.8) via the CDF of GSaS with $\alpha = 1$. By definition,

$$\mathcal{N}^*(s;\beta) = \int_0^\infty x^{s-1}\ [2\mathcal{N}(x)\Phi_{\mathcal{N}}(\beta x)]\,dx.$$

We use the known result from $\bar{\chi}_{1,k}$ where

$$x^{k-1}\mathcal{N}(x) = \frac{2^{k/2-1}\Gamma(k/2)}{\sqrt{2\pi k}}\,\bar{\chi}_{1,k}(x/\sqrt{k}) = \frac{1}{\sqrt{k}}\,\mathcal{N}^*(k)\,\bar{\chi}_{1,k}(x/\sqrt{k}).$$

Then

$$\begin{aligned}\mathcal{N}^*(s;\beta) &= \frac{2\,\mathcal{N}^*(s)}{\sqrt{s}}\int_0^\infty \Phi_{\mathcal{N}}(\beta x)\,\bar{\chi}_{1,s}(x/\sqrt{s})\,dx \\ &= 2\,\mathcal{N}^*(s)\int_0^\infty \Phi_{\mathcal{N}}(\beta\sqrt{s}t)\,\bar{\chi}_{1,s}(t)\,dt \quad \text{via} \quad t = x/\sqrt{s}.\end{aligned}$$

The integral is exactly the CDF of a GSaS, $L_{1,s}$, with the argument $\beta\sqrt{s}$. That is, $\mathcal{N}^*(s;\beta) = 2\,\mathcal{N}^*(s)\,\Phi[L_{1,s}](\beta\sqrt{s})$.

When $\alpha = 1$, $L_{1,s}$ becomes t_s. Therefore, $\mathcal{N}^*(s;\beta) = 2\,\mathcal{N}^*(s)\,\Phi[t_s](\beta\sqrt{s})$.

□

The beauty of this lemma is that $\mathcal{N}^*(s;\beta)$ is the multiplication of a symmetric component and a skew component, just like its PDF counterpart.

From (2.12), we also obtain that

$$\Phi_{SN}(0;\beta) = 1 - \mathcal{N}^*(1;\beta) = \frac{1}{2} - \frac{1}{\pi}\arctan(\beta). \tag{10.9}$$

This is due to $\mathcal{N}^*(1) = \frac{1}{2}$ and $\Phi[t_1](\beta) = \frac{1}{2} + \frac{1}{\pi}\arctan(\beta)$. This result is stated in Proposition 2.7 of [1], and is proved here via the Mellin transform.

10.4.1. Mellin Transform of Owen's T Function. Another peculiar result from the Mellin transform is

LEMMA 10.2.

$$T(x,\beta) \overset{\mathcal{M}}{\longleftrightarrow} s^{-1}\,\mathcal{N}^*(s+1)\,\left[\Phi[t_{s+1}](\beta\sqrt{s+1}) - \frac{1}{2}\right] \tag{10.10}$$

△

PROOF. Define the upper incomplete integral as

$$\begin{aligned}\Gamma_f(x) := \int_x^\infty \mathcal{N}(x;\beta)\,dx &= 1 - \Phi_{SN}(x;\beta)\\ &= 1 - \Phi_{\mathcal{N}}(x) + 2\,T(x,\beta)\end{aligned}$$

According to Lemma 2.5, its Mellin transform is

$$\begin{aligned}\Gamma_f(x) &\overset{\mathcal{M}}{\longleftrightarrow} s^{-1}\,\mathcal{N}^*(s+1;\beta)\\ &= 2s^{-1}\,\mathcal{N}^*(s+1)\,\Phi[t_{s+1}](\beta\sqrt{s+1})\end{aligned}$$

Combining the two results above, we obtain

$$T(x,\beta) = \frac{\Gamma_f(x) - (1-\Phi_{\mathcal{N}}(x))}{2} \overset{\mathcal{M}}{\longleftrightarrow} s^{-1}\,\mathcal{N}^*(s+1)\,\left[\Phi[t_{s+1}](\beta\sqrt{s+1}) - \frac{1}{2}\right]$$

where $1-\Phi_{\mathcal{N}}(x) \overset{\mathcal{M}}{\longleftrightarrow} s^{-1}\,\mathcal{N}^*(s+1)$.

□

10.5. Moments

LEMMA 10.3. According to Section 2.1.2, by assigning $s = n+1$, the Mellin transform is converted to the moment formula. It is easy to show that the n-th moment of Z is

$$\begin{aligned}\mathbb{E}(Z^n) = \mathbb{E}(X^n|\mathcal{N}(\beta)) &= \mathcal{N}^*(n+1;\beta) + (-1)^n\mathcal{N}^*(n+1;-\beta)\\ &= 2\mathcal{N}^*(n+1) \times \begin{cases}1, & \text{when } n \text{ is even,}\\ 1 - 2\Phi[t_{n+1}](-\beta\sqrt{n+1}), & \text{when } n \text{ is odd.}\end{cases}\end{aligned} \tag{10.11}$$

The even moments are identical to those of $\mathcal{N}(0,1)$. It is the odd moments that make the difference when $\beta \neq 0$.

△

The first four moments of Z' have simple analytic forms. Its first moment is

$$\mu_z = b\,\delta, \quad \text{where } b = \sqrt{2/\pi}. \tag{10.12}$$

The second moment is simply 1. Its variance is

$$\sigma_z^2 = 1 - (b\,\delta)^2. \tag{10.13}$$

The third moment is $b\,\delta(3-\delta^2)$. Its skewness is

$$\gamma_1\{Z\} = \frac{4-\pi}{2}\,\frac{\mu_z^3}{\sigma_z^3}. \tag{10.14}$$

The fourth moment is 3. Its kurtosis is

$$\gamma_2\{Z\} = 2(\pi-3)\,\frac{\mu_z^4}{\sigma_z^4}. \tag{10.15}$$

The maximum skewness of SN is approximately 0.9953 and the maximum kurtosis is 0.8692. They are not very interesting, since the extremal distribution is just a half-normal distribution.

However, these analytical forms are useful when SN is extended to GAS-SN. Both skewness and kurtosis are extended to much wider ranges, or even infinity!

CHAPTER 11

GAS: Generalized Alpha-Stable Distribution (Experimental)

In this chapter, we show how the *degrees of freedom* k is added to the α-stable distribution L_α^θ using the Mellin transform approach. This experiment is an early attempt and one of the cleanest approaches to understanding how k interacts with skewness. It is a valuable lesson on the mathematical structure of the α-stable distribution. Therefore, it is documented in this chapter.

With this note, the readers not interested in this mathematical exploration can skip this chapter.

A new distribution results, which is called the generalized α-stable distribution (GAS), with the notation $L_{\alpha,k}^\theta$. The distribution is structurally elegant and capable of properly generating skewness. However, there are discontinuity issues with the reflection rule.

The discontinuity is a major flaw that prevents the distribution from being useful in real-world application. A method to remedy it is proposed, which is documented in this chapter. The value of this chapter is to understand the origin of the fractional χ distribution and GSaS.

After learning this hard lesson, I turned to the skew-normal approach, which can generate skewness without any problem with the continuity of the PDF. And it is also theoretically elegant. After this chapter, all subsequent chapters are based on the skew-normal approach.

11.1. Definition

First, we recap the Mellin transform (4.4) of the PDF of the α-stable distribution from Section 4.3,

$$L_\alpha^\theta(x) \overset{\mathcal{M}}{\longleftrightarrow} \epsilon \left[\frac{\Gamma(s)}{\Gamma(1-\gamma+\gamma s))}\right] \left[\frac{\Gamma(\epsilon(1-s))}{\Gamma(\gamma(1-s))}\right].$$

It is interpreted in Lemma 4.2 as a multiplication of two components,

$$L_\alpha^\theta(x) \overset{\mathcal{M}}{\longleftrightarrow} \tilde{M}_\gamma^*(s)\, {\overline{\chi}_{\alpha,1}^\theta}^*(2-s).$$

The PDF of the second term $\overline{\chi}_{\alpha,1}$ is defined as

$$\overline{\chi}_{\alpha,1}^\theta(x) \overset{\mathcal{M}}{\longleftrightarrow} {\overline{\chi}_{\alpha,1}^\theta}^*(s) \ \propto \frac{\Gamma(\epsilon(s-1))}{\Gamma(\gamma(s-1))},$$

apart from the normalization constant and scale in the PDF. It is interpreted as the FCM of "one degree of freedom" in Section 7.1.

In (7.1) it is shown that the "degrees of freedom" parameter k is added to the FCM by replacing $s-1$ with $s+k-2$ such that

$$\overline{\chi}_{\alpha,k}^\theta(x) \overset{\mathcal{M}}{\longleftrightarrow} {\overline{\chi}_{\alpha,k}^\theta}^*(s) \ \propto \frac{\Gamma(\epsilon(s+k-1))}{\Gamma(\gamma(s+k-1))}.$$

Next, it is natural to use ${\overline{\chi}_{\alpha,k}^\theta}^*(s)$ in the Mellin space to extend L_α^θ as follows.

Definition 11.1 (The ratio-distribution representation of (unadjusted) GAS). The Mellin transform of the PDF of (unadjusted) GAS is defined as

$$\tilde{L}_{\alpha,k}^\theta(x) \overset{\mathcal{M}}{\longleftrightarrow} \tilde{M}_\gamma^*(s)\, {\overline{\chi}_{\alpha,k}^\theta}^*(2-s) \tag{11.1}$$

Based on the Mellin transform, its PDF can be written in a ratio distribution form,

$$\tilde{L}^{\theta}_{\alpha,k}(x) := \int_0^{\infty} \tilde{M}_{\gamma}(xs)\, \bar{\chi}^{\theta}_{\alpha,k}(s)\, s\, ds \quad (x \geq 0) \tag{11.2}$$

Since the Mellin integral is only valid for $x \geq 0$, it is supplemented with *the reflection rule*:

$$\tilde{L}^{\theta}_{\alpha}(-x) := \tilde{L}^{-\theta}_{\alpha}(x) \tag{11.3}$$

Thus, we have constructed a version of GAS for $x \in \mathbb{R}$, which produces fat tails and skewness -

(1) $\tilde{L}^{\theta}_{\alpha,k}$ subsumes the α-stable distribution L^{θ}_{α}.
(2) $\tilde{L}^{\theta}_{\alpha,k}$ subsumes Student's t distribution t_k.
(3) $\tilde{L}^{\theta}_{\alpha,k}$ subsumes the power-exponential distribution, with the proper definition of negative k in FCM.

What is wrong with it? The problem is that the PDF and its derivatives are discontinuous at $x = \pm 0$ when $k \neq 1$ and $\theta \neq 0$.

The remaining sections of this chapter will explain this problem and provide a remediation. The reader who just wants to explore the skew-normal implementation can safely skip the rest of this chapter. The conclusion is that such discontinuity makes the PDF far from mathematical elegance, which motivates the author to explore other alternatives. The answer is to abandon the M-Wright kernel for skewness ($\tilde{M}_{\gamma}(xs)$ in (11.2)), and integrate with the skew-normal distribution, outlined in the next chapter.

11.2. Limitation

The issue of discontinuity of the PDF $\tilde{L}^{\theta}_{\alpha,k}(x)$ at $x = 0$ is encountered when $k \neq 1$. We lay out a generic framework to understand and address it.

Assume that the unadjusted two-sided density function is $\tilde{f}(x) := \tilde{L}^{\theta}_{\alpha,k}(x)$, which is discontinuous at $x = 0$. It also must satisfy the reflection rule, where, for $x > 0$, $\tilde{f}(x) := \tilde{f}^{+}(x)$ and $\tilde{f}(-x) := \tilde{f}^{-}(-x)$.

$\tilde{f}(x)$ can be expanded at $x = 0$ in terms of x by

$$\tilde{f}^{\pm}(x) := \tilde{L}^{\pm\theta}_{\alpha,k}(x) = \tilde{f}^{\pm}_0 + \tilde{f}^{\pm}_1\, x + ... \tag{11.4}$$

where $\tilde{f}^{\pm}_0$ are the densities at $x = 0$, and $\tilde{f}^{\pm}_1$ are the respective slopes (aka the first derivatives).

The series expansion can be achieved via either (11.2), or (11.1) in conjuction with Ramanujan's master theorem in Section 2.2, such that

$$\tilde{f}^{+}_0 = \frac{\gamma^{1-\gamma}}{\Gamma(1-\gamma)}\, E(X|\bar{\chi}^{\theta}_{\alpha,k}), \tag{11.5}$$

$$\tilde{f}^{+}_1 = \frac{-\gamma^{1-2\gamma}}{\Gamma(1-2\gamma)}\, E(X^2|\bar{\chi}^{\theta}_{\alpha,k}). \tag{11.6}$$

Notice that they are based on the first and second moments of $\bar{\chi}^{\theta}_{\alpha,k}$. $(\tilde{f}^{-}_0, \tilde{f}^{-}_1)$ are obtained by applying the reflection rule from $(\tilde{f}^{+}_0, \tilde{f}^{+}_1)$. That is, θ is replaced with $-\theta$, and γ with $1-\gamma$ in every occurrence of the formula.

Furthermore, it is known that

$$\int_0^{\infty} \tilde{f}^{+}(x)\, dx = \gamma, \qquad \int_0^{\infty} \tilde{f}^{-}(x)\, dx = 1-\gamma. \tag{11.7}$$

These two are the only conditions required for $\tilde{f}^{\pm}(x)$.

The discontinuity occurs because $\tilde{f}^{+}_0 \neq \tilde{f}^{-}_0$ and $\tilde{f}^{+}_1 \neq \tilde{f}^{-}_1$ when $k \neq 1$ and $\theta \neq 0$. In fact, this is true for all orders of derivatives $\tilde{f}^{+}_n \neq \tilde{f}^{-}_n$ in the n-th term, $\tilde{f}^{\pm}_n\, x^n$.

Obviously, when $\theta = 0$, the density function is symmetric by definition: $\tilde{f}^+(x) = \tilde{f}^-(x)$. There is no issue here. So the issue is specific to the injection of skewness from $\theta \neq 0$.

On the other hand, when $k = 1$, the density function is continuous under the reflection rule, regardless the value of θ. This is the original α-stable distribution. It is perfectly fine. So the issue is specific to our attempt of adding degrees of freedom $k \neq 1$.

Either one of θ or k are fine, but when we try to do both, the distribution is broken, so to speak. That is the limitation. The dilemma is that adding θ and k is exactly what we try to achieve.

11.3. Workaround

An adjustment algorithm is proposed such that the PDF and its first derivative are continuous.

DEFINITION 11.2 (The adjusted GAS). The PDF of the adjusted GAS is defined as

$$L^{\pm\theta}_{\alpha,k}(x) := \frac{1}{A^{\pm}\sigma^{\pm}}\,\tilde{f}^{\pm}(x)\left(\frac{x}{\sigma^{\pm}}\right) \quad (x \geq 0) \tag{11.8}$$

It is required that (a) the new density function satisfies the reflection rule of $L^{\theta}_{\alpha,k}(-x) := L^{-\theta}_{\alpha,k}(x)$; (b) $A^{\pm}, \sigma^{\pm}$ are constrained by the continuity conditions that, at $x = 0$, both its density is continuous: $L^{\theta}_{\alpha,k}(0) = L^{-\theta}_{\alpha,k}(0)$; and its slope is continuous: $\frac{d}{dx} L^{\theta}_{\alpha,k}(0) = -\frac{d}{dx} L^{-\theta}_{\alpha,k}(0)$.

With such definition, we proceed to find the solutions of $A^{\pm}, \sigma^{\pm}$. The solutions form a distribution family. There is a canonical solution, simple and elegant, from which all other solutions are derived as a member of the location-scale family.

A member in the location-scale family shares the same "shapes" such as the skewness and kurtosis. Apart from the location and scale, it brings nothing new to the table. Hence, we can focus on analyzing the canonical distribution.

DEFINITION 11.3 (Two essential quantities for the canonical distribution). We define two essential quantities:

$$\Sigma := -\frac{\tilde{f}^+_0}{\tilde{f}^-_0}\frac{\tilde{f}^-_1}{\tilde{f}^+_1} \tag{11.9}$$

$$\Psi := \Sigma\,\frac{\tilde{f}^+_0}{\tilde{f}^-_0} \quad = -\left(\frac{\tilde{f}^+_0}{\tilde{f}^-_0}\right)^2 \frac{\tilde{f}^-_1}{\tilde{f}^+_1} \tag{11.10}$$

Notice that $\tilde{f}^+_0/\tilde{f}^-_0$ is the ratio of the original densities from two sides of $x = 0$. And $\tilde{f}^-_1/\tilde{f}^+_1$ is the ratio of the slopes of the two sides. Since $\tilde{f}^-_1, \tilde{f}^+_1$ always have the opposite signs, Σ is a positive quantity.

Note that Σ is singular when $\gamma = 1/2$. Both $\tilde{f}^-_1, \tilde{f}^+_1$ approach zero at the same speed. Hence, $\Sigma \to 1$ and $\Psi \to 1$.

The most important contribution is the discovery of the canonical distribution.

DEFINITION 11.4 (The canonical GAS). The canonical GAS distribution is defined according to $\sigma^+ = 1$ and $\sigma^- = \Sigma$. Hence, its PDF for $x \geq 0$ is (with the hat symbol)

$$\widehat{L}^{\theta}_{\alpha,k}(x) := \frac{1}{A^+}\,\tilde{f}^+(x) \tag{11.11}$$

$$\widehat{L}^{-\theta}_{\alpha,k}(x) := \frac{1}{A^-\Sigma}\,\tilde{f}^-\left(\frac{x}{\Sigma}\right) \tag{11.12}$$

where $A^+ = \gamma + \Psi(1-\gamma)$ and $A^- = A^+/\Psi$ from Lemma 11.7.

The reflection rule applies: $\widehat{L}^{\theta}_{\alpha,k}(-x) := \widehat{L}^{-\theta}_{\alpha,k}(x)$.

11.3.1. The Location-scale Family. The following lemmas show that all other solutions must obey $\sigma^-/\sigma^+ = \Sigma$. They are just the location-scale family of the canonical distribution.

Briefly, all other solutions are defined by a choice of scale $\sigma^+ > 0$, such that

$$L^{\theta}_{\alpha,k}(x) := \frac{1}{\sigma^+}\,\widehat{L}^{\theta}_{\alpha,k}\left(\frac{x}{\sigma^+}\right) \tag{11.13}$$

For instance, we found that $\sigma^+ = \Sigma^\gamma$ to be a very good alternative. In the remark of Definition 11.9, we show that the n-th moment of $L^{\theta}_{\alpha,k}$ is just that of $\widehat{L}_{\alpha,k}$ multiplied by its scale $(\sigma^+)^n$.

LEMMA 11.5. The requirement that the density and slope of the *adjusted* density function should be smooth at $x = 0$ leads to

$$\frac{1}{A^+\sigma^+}\,\tilde{f}^+_0 = \frac{1}{A^-\sigma^-}\,\tilde{f}^-_0 \tag{11.14}$$

$$\frac{1}{A^+(\sigma^+)^2}\,\tilde{f}^+_1 = -\frac{1}{A^-(\sigma^-)^2}\,\tilde{f}^-_1 \tag{11.15}$$

△

PROOF. To solve $A^\pm$ and $\sigma^\pm$, take (11.8) and carry out the series expansions from (11.4):

$$L^{\pm\theta}_{\alpha,k}(x) = \frac{\tilde{f}^\pm_0}{A^\pm\sigma^\pm} + \frac{\tilde{f}^\pm_1}{A^\pm(\sigma^\pm)^2}\,x + ... \tag{11.16}$$

(11.14) is straightforward from requiring $L^{\theta}_{\alpha,k}(0) = L^{-\theta}_{\alpha,k}(0)$ in (11.16). Likewise, (11.15) is the result of $\frac{d}{dx}L^{\theta}_{\alpha,k}(0) = \frac{d}{dx}L^{-\theta}_{\alpha,k}(0)$ from (11.16). □

LEMMA 11.6. The equations in Lemma 11.5 lead to the following invariant:

$$\frac{\sigma^-}{\sigma^+} = \Sigma \tag{11.17}$$

△

PROOF. Divide the LHS and RHS of (11.14) by those of (11.15) respectively,

$$\sigma^+\frac{\tilde{f}^+_0}{\tilde{f}^+_1} = -\sigma^-\frac{\tilde{f}^-_0}{\tilde{f}^-_1}$$

Rearrange the items and we obtain (11.17). □

LEMMA 11.7. The solution for $A^\pm$ are

$$A^+ = \gamma + \Psi(1-\gamma) \tag{11.18}$$

$$A^+/A^- = \Psi \tag{11.19}$$

△

PROOF. (11.19) is derived by rearranging the items in (11.14) and following the definition of Ψ.

(11.18) is derived from the fact that the total density of the adjusted distribution should be equal to 1, that is, $\int_{-\infty}^{\infty} f(x)dx = 1$. Hence,

$$\int_0^\infty f^+(x)dx + \int_0^\infty f^-(x)dx = \frac{1}{A^+}\int_0^\infty \tilde{f}^+(x)dx + \frac{1}{A^-}\int_0^\infty \tilde{f}^-(x)dx = 1$$

Apply (11.7), we get $\frac{\gamma}{A^+} + \frac{1-\gamma}{A^-} = 1$. Multiply it by A^+ on both sides, we obtain (11.18). □

We've shown that $A^\pm$ are well-defined constants based on (α, k, θ), while $\sigma^\pm$ is a choice of parametrization, constrained by (11.17).

11.4. Moments

The structure of the *moments* reveals critical information about the adjusted distribution. We show the moment formula of the canonical distribution, and how the location-scale family relates to it.

To simplify the notations below, let

- $f^{\pm} = L^{\pm\theta}_{\alpha,k}$ be the adjusted distribution family,
- $\widehat{f}^{\pm} = \widehat{L}^{\pm\theta}_{\alpha,k}$ be the canonical distribution,
- $\tilde{f}^{\pm} = \tilde{L}^{\pm\theta}_{\alpha,k}$ be the original (unadjusted) distribution.

First, the n-th one-sided moments of the adjusted distribution are ($x > 0$)

$$E(X^n|f^{\pm}) = \frac{1}{A^{\pm}\sigma^{\pm}} \int_0^{\infty} x^n \, \tilde{f}^{\pm}(x/\sigma^{\pm}))dx = \frac{(\sigma^{\pm})^n}{A^{\pm}} E(X^n|\tilde{f}^{\pm}) \tag{11.20}$$

where $E(X^n|\tilde{f}^{\pm})$ are the original n-th one-sided moments. They can be obtained from the Mellin transform (11.1).

The n-th total moment, given the notation of m_n, is the sum of $E(X^n|f^+)$ and $(-1)^n E(X^n|f^-)$. We show the following.

LEMMA 11.8. The n-th total moment of the adjusted distribution is based on the original one-sided moments such as

$$m_n := E(X^n|f) = \frac{(\sigma^+)^n}{A^+} \left[E(X^n|\tilde{f}^+) + \Psi(-\Sigma)^n \, E(X^n|\tilde{f}^-)\right] \tag{11.21}$$

△

PROOF. By definition, we have

$$\begin{aligned} m_n := E(X^n|f) &= \int_{-\infty}^{\infty} x^n \, f(x)dx = \int_0^{\infty} x^n \, f^+(x)dx + (-1)^n \int_0^{\infty} x^n \, f^-(x)dx \\ &= E(X^n|f^+) + (-1)^n E(X^n|f^-) \end{aligned}$$

Apply (11.20), we get

$$m_n = \frac{(\sigma^+)^n}{A^+} E(X^n|\tilde{f}^+) + \frac{(-\sigma^-)^n}{A^-} E(X^n|\tilde{f}^-)$$

Factor out $\frac{(\sigma^+)^n}{A^+}$, apply $\sigma^-/\sigma^+ = \Sigma$ from Lemma 11.6, and $A^+/A^- = \Psi$ from 11.7, we obtain (11.21). □

LEMMA 11.9 (The moments of the canonical distribution). The n-th moment of the canonical distribution is

$$\widehat{m}_n := E(X^n|\widehat{f}) = \frac{1}{A^+} \left[E(X^n|\tilde{f}^+) + \Psi(-\Sigma)^n \, E(X^n|\tilde{f}^-)\right] \tag{11.22}$$

△

PROOF. Lemma 11.8 shows that the canonical distribution $\widehat{f}$ is obtained by letting $\sigma^+ = 1$ and $\sigma^- = \Sigma$. Put them to (11.21), we obtain (11.22). □

Lastly, compare (11.21) with (11.22). We reach $m_n = (\sigma^+)^n \, \widehat{m}_n$. That is, all other members in the adjusted distribution family are rescaled canonical distributions.

CHAPTER 12

GAS-SN: Generalized Alpha-Stable Distribution with Skew-Normal

This fractional univariate distribution combines the features from a classic skew-normal distribution that provides skewness and a fractional distribution that provides fatter tails. The resulting distribution is analytically tractable. The PDF and all of its derivatives are continuous everywhere in $\mathbb{R}$.

12.1. Definition

DEFINITION 12.1. Assume $Z_0 \sim SN(0,1,\beta)$ is a skew-normal variable and $V \sim \overline{\chi}_{\alpha,k}$ is an FCM variable.

Then $Z \sim Z_0/V$ is a variable with a GAS-SN distribution. We use the notation $Z \sim L_{\alpha,k}(\beta)$ for this standard distribution.

Assume $\mathcal{N}(x)$ and $\Phi_{\mathcal{N}}(x)$ are the PDF and CDF of $N(0,1)$. The PDF of Z is

$$L_{\alpha,k}(x;\beta) = 2\int_0^\infty \mathcal{N}(xs)\,\Phi_{\mathcal{N}}(\beta xs)\,\overline{\chi}_{\alpha,k}(s)\,s\,ds. \tag{12.1}$$

This is the fractional extension of (10.2).

Its CDF is

$$\begin{aligned}\Phi[L_{\alpha,k}(\beta)](x) &:= \int_0^\infty \Phi_{SN}(xs;\beta)\,\overline{\chi}_{\alpha,k}(s)\,ds. \\ &= \int_0^\infty \left[\Phi_{\mathcal{N}}(xs) - 2\,T(xs,\beta)\right]\overline{\chi}_{\alpha,k}(s)\,ds.\end{aligned} \tag{12.2}$$

where $\Phi_{SN}(xs;\beta)$ is the CDF of $SN(0,1,\beta)$ in (10.3), and $T(h,a)$ is the Owen's T function.

We can clearly see that the CDF has two components: One from the symmetric part, and the other skew. The second component vanishes due to $T(h,0)=0$.

12.1.1. GAS-SN Subsumes GSaS.

LEMMA 12.2. When $\beta = 0$, it becomes a symmetric distribution, previously called GSaS. The notation of $L_{\alpha,k}$ is given in [15].

The PDF of a GSaS is

$$L_{\alpha,k}(x) = \int_0^\infty \mathcal{N}(xs)\,\overline{\chi}_{\alpha,k}(s)\,s\,ds. \tag{12.3}$$

When $\alpha \to 2$ or $k \to \infty$, the symmetric distribution approaches a normal distribution $N(0,\alpha^{2/\alpha})$ (Section 8.2 of [15]).

△

This integral is a normal mixture (9.1) that enjoys several nice properties outlined in Chapter 9.

In particular, the generalized exponential power distribution can be obtained via the characteristic function transform in Lemma 9.2 (Section 9 of [15]). We point out that the skew extension is straightforward, but leave the detailed description to future research.

12.1.2. GAS-SN Subsumes Skew-t Distribution. An important bridge between SN and GAS-SN is the skew-t (ST) distribution. It is documented in Section 4.3 of [1].

ST is fully consistent with GAS-SN by setting $\alpha = 1$. That is, in his notation, $T(\beta, k) = L_{1,k}(\beta)$.

12.2. The Location-Scale Family

Its location scale family is $Y = \xi + \omega Z \sim L_{\alpha,k}(\xi, \omega^2, \beta)$. Its PDF becomes

$$\phi(x) = \frac{1}{\omega} L_{\alpha,k}\left(\frac{x-\xi}{\omega}; \beta\right). \quad (x \in \mathbb{R}) \tag{12.4}$$

In real-world applications, this PDF is used for optimization, e.g. in the maximum likelihood estimation (MLE). See Section 12.9.

12.3. Mellin Transform

The Mellin transform of the PDF follows the rule of the ratio distribution. From (10.8) and (7.2), we have

$$\begin{aligned} L_{\alpha,k}(x;\beta) &\overset{\mathcal{M}}{\longleftrightarrow} L^*_{\alpha,k}(s;\beta) \qquad (12.5)\\ &= \mathcal{N}^*(s;\beta)\, \overline{\chi}^*_{\alpha,k}(2-s) \\ &= \left[2\,\Phi[t_s](\beta\sqrt{s})\right] \times \left[\mathcal{N}^*(s)\, \overline{\chi}^*_{\alpha,k}(2-s)\right] \qquad (12.6) \end{aligned}$$

Notice that the contribution for the skewness is $2\,\Phi[t_s](\beta\sqrt{s})$ in the first bracket, which becomes one if $\beta = 0$.

The second bracket is the Mellin transform of the GSaS PDF. From (2.9) and (7.2), it is

$$\begin{aligned} L_{\alpha,k}(x) &\overset{\mathcal{M}}{\longleftrightarrow} L^*_{\alpha,k}(s) = \mathcal{N}^*(s)\, \overline{\chi}^*_{\alpha,k}(2-s) \qquad (12.7)\\ &= \frac{1}{2\sqrt{\pi}} \left(\frac{2}{\sigma}\right)^{s-1} \Gamma\left(\frac{s}{2}\right) \frac{\Gamma((k-1)/2)}{\Gamma((k-1)/\alpha)} \frac{\Gamma((k-s)/\alpha)}{\Gamma((k-s)/2)}, \end{aligned}$$

where $\sigma := k^{1/2-1/\alpha}$ and $k > 0$ is assumed.

12.4. Moments

Based on $\mathbb{E}(X^n|\mathcal{N}(\beta))$ from (10.11), the n-th moment of Z is

$$\begin{aligned} \mathbb{E}(X^n|L_{\alpha,k}(\beta)) &:= \mathbb{E}(X^n|\mathcal{N}(\beta))\, \mathbb{E}(X^{-n}|\overline{\chi}_{\alpha,k}) \qquad (12.8)\\ &= 2\,\mathcal{N}^*(n+1)\, \mathbb{E}(X^{-n}|\overline{\chi}_{\alpha,k}) \\ &\quad \times \begin{cases} 1, & \text{when } n \text{ is even,} \\ 1 - 2\Phi[t_{n+1}](-\beta\sqrt{n+1}), & \text{when } n \text{ is odd.} \end{cases} \end{aligned}$$

Its first moment is $\mu_z = b\,\delta$, where $b = \sqrt{2/\pi}\, \mathbb{E}(X^{-1}|\overline{\chi}_{\alpha,k})$.

The second moment is $\mathbb{E}(X^{-2}|\overline{\chi}_{\alpha,k})$. Its variance is

$$\sigma_z^2 = \mathbb{E}(X^{-2}|\overline{\chi}_{\alpha,k}) - (b\,\delta)^2. \tag{12.9}$$

To simplify the symbology, let $q_n := \mathbb{E}(X^{-n}|\overline{\chi}_{\alpha,k})$. The third moment is $\delta_3\, q_3$, where $\delta_3 = \sqrt{\frac{2}{\pi}}\delta(3-\delta^2)$. The fourth moment is $3\,q_4$. To carry out the skewness γ_1 and excess kurtosis γ_2,

$$\begin{aligned} \gamma_1 \times \sigma_z^{3/2} &= \delta_3\, q_3 - 3\mu_z q_2 + 2\mu_z^3, \\ \gamma_2 \times \sigma_z^4 &= 3(q_4 - q_2^2) - 4\mu_z(\gamma_1 \times \sigma_z^{3/2}) + 2\mu_z^4. \end{aligned}$$

The maximum skewness and kurtosis can be infinite. Since $\delta = \sin\theta$, where $\beta = \tan\theta$, we have $\delta \in [-1, 1]$. Infinity has to come from q_3 and q_4.

A typical example is the skew-t distribution at $\alpha = 1$. It is well known that kurtosis approaches infinity when k approaches 4 from above, and the skewness approaches infinity when k approaches 3 from above.

12.4.1. Excess Kurtosis of GSaS. It is important to understand the behavior of excess kurtosis γ_2. However, the presence of skewness adds more complexity to γ_2. Consider the symmetric case where $\beta = 0$, and we quote the result from [15] below.

The excess kurtosis of GSaS is plotted in Figure 12.1 in the (k, α) coordinate. Notice that a major division occurs along the line of $k = 5 - \alpha$. In the region where $0 < k \leq 5 - \alpha$, there are complicated patterns caused by the infinities of the gamma function. Only small pockets of valid kurtosis exist.

LEMMA 12.3. In the region where $k > 5 - \alpha$, the excess kurtosis of GSaS is a continuous function with positive values. At large k's, the closed form of the moments can be expanded by Sterling's formula. The excess kurtosis γ_2 becomes part of a linear equation:

$$\left(\epsilon - \frac{1}{2}\right) = \left(\frac{k-3}{4}\right) \log\left(1 + \frac{\gamma_2}{3}\right), \quad \text{where } \epsilon = 1/\alpha \tag{12.10}$$

This equation shows how GSaS works under the **Central Limit Theorem**. GSaS approaches a normal distribution when γ_2 becomes zero. This can happen from two directions: when $\alpha \to 2$ or when $k \to \infty$.

△

The contour plot of excess kurtosis is shown in the (k, ϵ) coordinate in Figure 12.2. It is visually amusing. Notice the singular point at $\epsilon = 1/2, k = 3$.

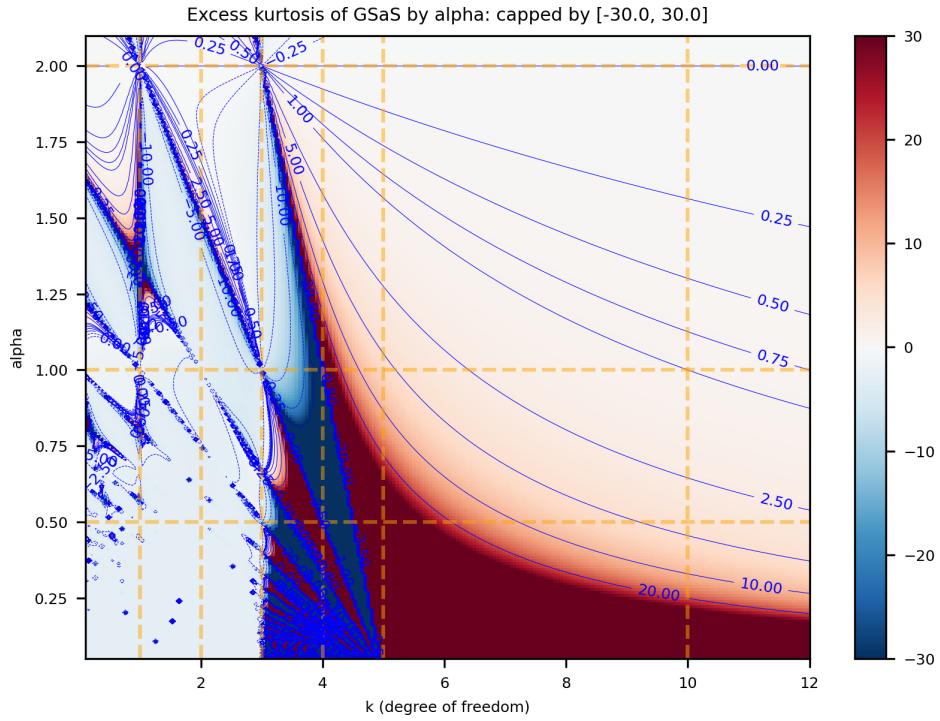

FIGURE 12.1. The contour plot of excess kurtosis in GSaS by (k, α).

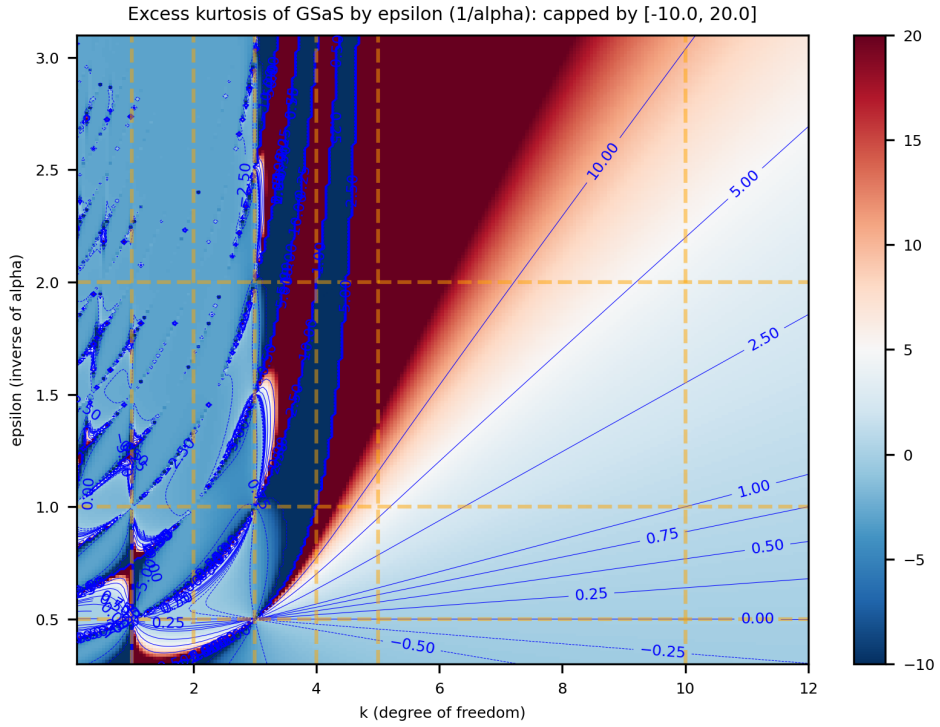

FIGURE 12.2. The contour plot of excess kurtosis in GSaS by (k, ϵ) where $\epsilon = 1/\alpha$. This best describes the linearity in (12.10) for large k's.

12.5. Tail Behavior

The tail behavior of GAS-SN is a "modified GSaS" type. Hence, it is well within what was known. Without losing generality, assume $\beta > 0$, that the decay of the left tail is more pronounced than that of the right tail. But it still follows the same power law of x^{-k} as in a $L_{\alpha,k}$.

It takes a small tweak to GSaS to capture that behavior.

DEFINITION 12.4. The shifted GSaS is defined as

$$L_{\alpha,k}(x||\mu) = \int_0^\infty \mathcal{N}(xs - \mu)\, \overline{\chi}_{\alpha,k}(s)\, s\, ds \tag{12.11}$$

Note that the shift μ is not a location parameter that shifts x. It is a shift inside the argument of $\mathcal{N}(\,)$. When $\mu = 0$, it is restored to the PDF of GSaS, $L_{\alpha,k}(x)$.

We use the following approximation of the erf function in (12.1)[**11**]

$$1 - \text{erf}(x) \approx \frac{1}{B\sqrt{\pi}\, x}(1 - e^{-Ax})\, e^{-x^2} \quad (x \geq 0) \tag{12.12}$$

where $A = 1.98$ and $B = 1.135$. It is much better than the first-order expansion of $e^{-x^2}/(\sqrt{\pi}x)$ for the entire range of $x \in [0, \infty)$.

LEMMA 12.5. The left tail $(x < 0)$ of the PDF in (12.1) can be approximated by

$$\widehat{L}_{\alpha,k}(x;\beta) = \frac{G}{\beta x}\left[e^{\mu^2/2}\, L_{\alpha,k-1}\,(qx||\mu) - L_{\alpha,k-1}\,(qx)\right] \tag{12.13}$$

where

$$\mu = \frac{A\,\delta}{\sqrt{2}}$$
$$q = \sqrt{1+\beta^2}\,\frac{\sigma_{\alpha,k}}{\sigma_{\alpha,k-1}}$$
$$G = \sqrt{\frac{2}{\pi}}\frac{B\,C_{\alpha,k}}{\sigma_{\alpha,k-1}\,C_{\alpha,k-1}}$$

and both $C_{\alpha,k} = \frac{\alpha\Gamma((k-1)/2)}{\Gamma((k-1)/\alpha)}$ and $\sigma_{\alpha,k}$ are according to FCM in (7.4).

The right tail ($x > 0$) is simply

$$L_{\alpha,k}(x) - \widehat{L}_{\alpha,k}(-x;\beta) \tag{12.14}$$

where the second term $\widehat{L}_{\alpha,k}(-x;\beta)$ becomes much smaller than the first term as $x \to \infty$. △

Proof. TODO add more content here.

□

12.6. Maximum Skewness and Half GSaS

When $\beta \to \pm\infty$, a GAS-SN becomes a half-GSaS, which is a one-sided distribution with the notation of $L^{\pm}_{\alpha,k} := L_{\alpha,k}(\beta = \pm\infty)$. Its PDF is

$$L^{+}_{\alpha,k}(x) = \begin{cases} 2L_{\alpha,k}(x) & \text{if } x \geq 0, \\ 0 & \text{otherwise.} \end{cases} \tag{12.15}$$

It follows the reflection rule of $L^{-}_{\alpha,k}(x) = L^{+}_{\alpha,k}(-x)$. Hence, we only need to study the $+\infty$ case.

A half-GSaS possesses the maximum skewness that a GAS-SN family can achieve for a given pair of (α, k). In Section 10.5, it was mentioned that the maximum skewness of the SN family is only 0.9953. GAS-SN allows the skewness to reach infinity potentially.

From (12.7), the n-th moment is

$$\mathbb{E}(X^n|L^{+}_{\alpha,k}) = 2L^{*}_{\alpha,k}(n+1)$$
$$\mathbb{E}(X^n|L^{-}_{\alpha,k}) = 2L^{*}_{\alpha,k}(n+1)\,(-1)^n \tag{12.16}$$

Therefore, it is straightforward to calculate the skewness.

The skewness of half-GSaS $L^{+}_{\alpha,k}$ is shown in Figure 12.3 in the (k,α) coordinate. There is a clear division of infinity by the line from $(2,2)$ to $(4,0)$.

The contour plot of the skewness is shown in the (k,ϵ) coordinate in Figure 12.4. Each contour line approaches a straight line as k increases.

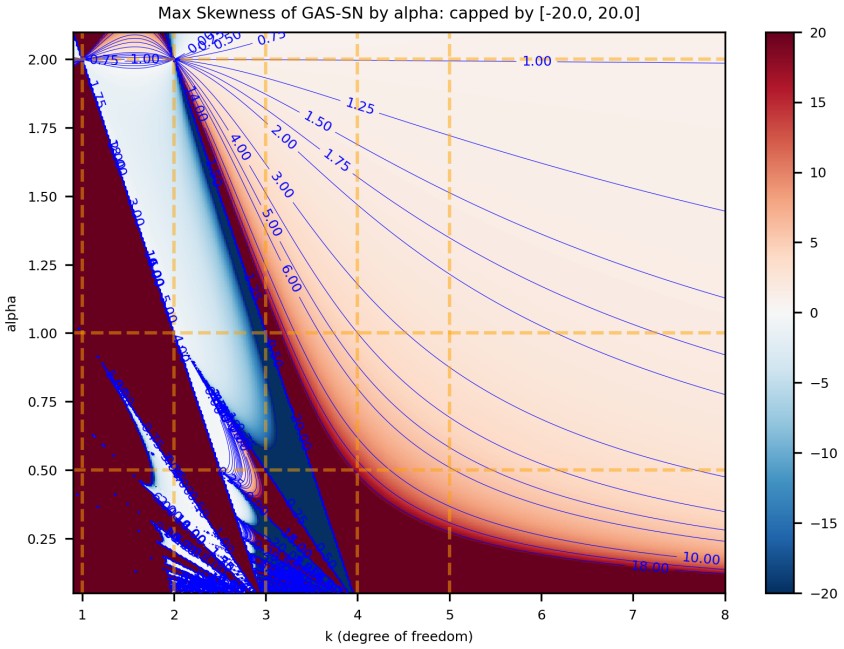

FIGURE 12.3. The contour plot of skewness of the half-GSaS $L^+_{\alpha,k}$ by (k, α). This represents the maximum skewness that the GAS-SN family can achieve.

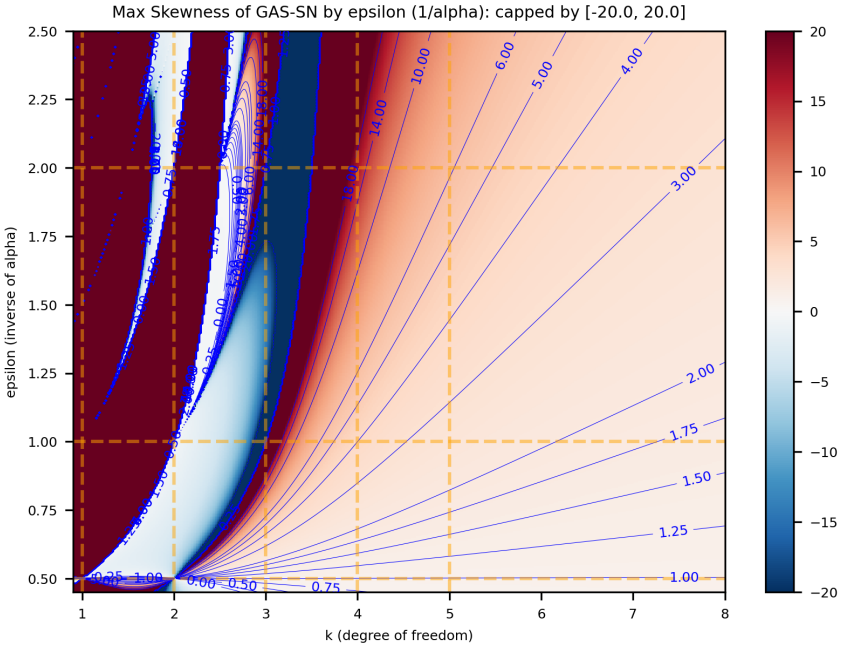

FIGURE 12.4. The contour plot of skewness of the half-GSaS $L^+_{\alpha,k}$ by (k, ϵ) where $\epsilon = 1/\alpha$. Each contour line approaches a straight line as k increases.

12.7. Fractional Skew Exponential Power Distribution

As shown in Definition 3.6 and Section 9 of [15], the negative k space is reserved for the fractional exponential power distribution, whose PDF is $\mathcal{E}_{\alpha,k}(x) := L_{\alpha,-k}(x)$. All it takes is to have $\overline{\chi}_{\alpha,k}(s)$ in (12.1) properly defined for negative k, which is done in (7.8).

It is natural to extend it with the skew-normal family such that its PDF becomes

$$\mathcal{E}_{\alpha,k}(x;\beta) = L_{\alpha,-k}(x;\beta). \tag{12.17}$$

Then we obtain another flexible skew distribution with a different type of tail behavior. Detailed analysis of this distribution is left for future research.

12.8. Quadratic Form

A squared GAS-SN variable Q is distributed as a fractional F distribution with $d = 1$. That is,

$$Q := \left(\frac{Y-\xi}{\omega}\right)^2 = Z^2 \sim F_{\alpha,1,k}, \quad \text{for all } \beta. \tag{12.18}$$

Notice that Q is based on the standard variable Z, which is invariant to the location and scale. See Chapter 8 for more detail.

12.9. Univariate MLE

In this section, we document how we fit the one-dimensional data with univariate GAS-SN. The main algorithm is *maximum likelihood estimation* (MLE), supplemented with several components of regularization.

We applied the MLE fitting on the daily returns of VIX and SPX from 1990 to mid-2025, each about 8900 samples. The MLE program is implemented in **python** and **scipy** on github at https://github.com/slihn/gas-impl/blob/main/gas_impl/mle_gas_sn.py.

In the univariate case, the hyperparameter space is $\Theta = \{\alpha, k, \beta, \omega, \xi\}$, where $\alpha \in (0,2)$, $k \in (2,\infty)$, $\omega > 0$, and $\beta, \xi \in \mathbb{R}$. Assume there are N samples in the data set, $Y = \{y_i, i \in 1,2,...,N\}$, the main component of the objective function is the minus log-likelihood (MLLK):

$$\text{MLLK}(\Theta) = -\frac{1}{N}\sum_{i=1}^{N} \log(\phi(y_i;\Theta)) \tag{12.19}$$

where $\phi(y;\Theta)$ is the PDF of the univariate location scale family (12.4).

Additional components of regularization are added to the objective function $\ell(\Theta)$. Specifically, the L2 distances between the empirical and theoretical statistics are added as follows:

- Skewness: $|\Delta\gamma_1|^2 := |\Delta\text{skewness}(Y)|^2$. Section 12.4.
- Kurtosis: $|\Delta\gamma_2|^2 := |\Delta\text{kurtosis}(Y)|^2$. Section 12.4.
- The mean of the quadratic form: $\Delta\mu_Q^2 := |\Delta\text{mean}(Q)|^2$. Section 15.6.

The MLE seeks the optimal Θ that minimizes the objective function:

$$\hat{\Theta} = \text{argmin } \ell(\Theta) \tag{12.20}$$

$$\text{where } \ell(\Theta) = \text{MLLK}(\Theta) + |\Delta\gamma_1|^2 + |\Delta\gamma_2|^2 + \Delta\mu_Q^2 \tag{12.21}$$

A custom version of the stochastic descent (SD) algorithm is developed. Our experience shows that it is better to standardize the data set to one standard deviation, so that all parameters in Θ are approximately on the same scale.

It is also important to control the learning rate so that it does not take a too large step on α, empirically, no more than 0.01 per step. This ensures that the SD does not wander into the *undefined* regions for $\ell(\Theta)$. This is particularly important for the SPX fit below.

The SD algorithm calculates the gradients for each hyperparameter. And make a small move along the direction that is most likely to minimize $\ell(\Theta)$. The scale of the move is based on the learning rate, which can be dynamically adjusted. Some randomness is added to the small move. This allows the algorithm to explore the nearby region and increases its choices.

12.10. Examples of Univariate MLE Fits

12.10.1. VIX fit. Figure 12.5 shows the result of the MLE fit to the daily VIX returns from 1990 to mid-2025. Data are standardized to one standard deviation. This helps the SD algorithm to move correctly in all dimensions of Θ.

The VIX data are right-skewed. The sample skewness of 2.0 is quite high. The right tail is very stretched due to several high-profile *panic selling* events where the VIX tends to jump a lot in a day. This tail creates a very high kurtosis of $\sim$17.

The top two graphs compare the histogram with the theoretical PDF. The right graph shows the density on logarithmic scale so that we can examine how the tails are fitted (down to the 10^{-3} level). Obviously, the right tail larger than 7 is not properly captured by the theoretical PDF.

The parameters of the theoretical distribution are: α is slightly below 0.8, k is in the neighborhood of 5, and β is near 1. The reader is encouraged to locate this point of (α, k) in Figure 12.1.

The PP-plot in the bottom left graph shows that the overall fit is satisfactory. The 45-degree line is very clear. This plot is less sensitive to the tails.

The QQ-plot of the quadratic form (or called the squared variable) is shown in the bottom right graph. It is a powerful tool for studying how the combined tail (in absolute terms) is doing. The 45-degree line is OK below 20, but as the quantiles get larger, the observed quantiles start to tilt upward. This means the top 0.5 percent of the combined tail is not properly captured by the distribution.

12.10.2. SPX fit. Figure 12.6 shows the result of the MLE fit to the daily SPX returns from 1990 to mid-2025. The data is also standardized to one standard deviation.

The SPX data are left skewed. The sample skewness of less than -0.1 is mild. The tails are stretched due to several high-profile one-day panic selling events. The tails create a very high kurtosis of $\sim$11 (but not a lot of skewness).

The top two graphs compare the histogram with the theoretical PDF. The graph on the right shows the density on a logarithmic scale so that we can examine how the tails are fitted (down to the 10^{-3} level). Obviously, tails larger than 7 are not captured well by the theoretical PDF.

The parameters of the theoretical distribution are: α is near 0.9, k is in the neighborhood of 3.1, and β is near 0. This region is close to t_3, which is quite peculiar, since theoretical skewness and kurtosis barely exist and are very sensitive to α, k, β. It is not easy to find this point visually in Figure 12.1. This strange result remains a topic for future research.

The PP-plot in the bottom left graph shows that the overall fit is satisfactory. The 45-degree line is OK. But there is a small bump between 0 and 0.2. It is well known from the market regime models, for example [**29**], that the crash regime has a negative mean return. This causes the effect of this bump on the left side of the distribution.

In the QQ-plot of the quadratic form, the 45-degree line is OK below 100, but as the quantiles get larger, the observed quantiles start to tilt downward. The far most 10 data points of the combined tail are not properly captured by the distribution.

Notice how far the quantiles have stretched. The theoretical mean is 2.8, while the largest point is near 700 (26^2). It spans almost 3 orders of magnitude.

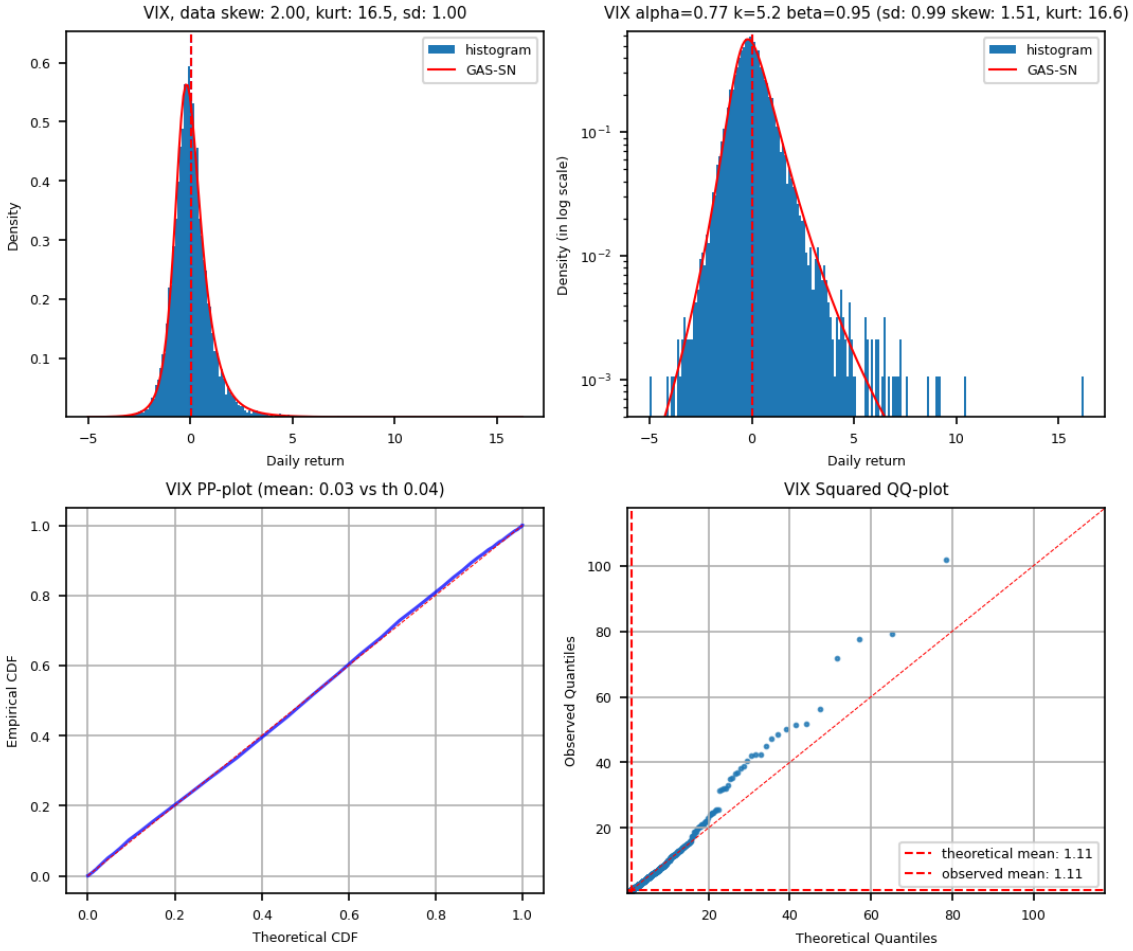

FIGURE 12.5. The MLE fit of VIX daily returns from 1990 to mid-2025. Data is standardized to one standard deviation. Sample skewness is 2.0, sample kurtosis is 16.5. $\hat{\Theta} = \{\alpha = 0.77, k = 5.2, \beta = 0.95\}$. Top left: the PDF vs histogram. Top right: the log-density vs histogram. Bottom left: the PP-plot. Bottom right: the QQ-plot of the quadratic form.

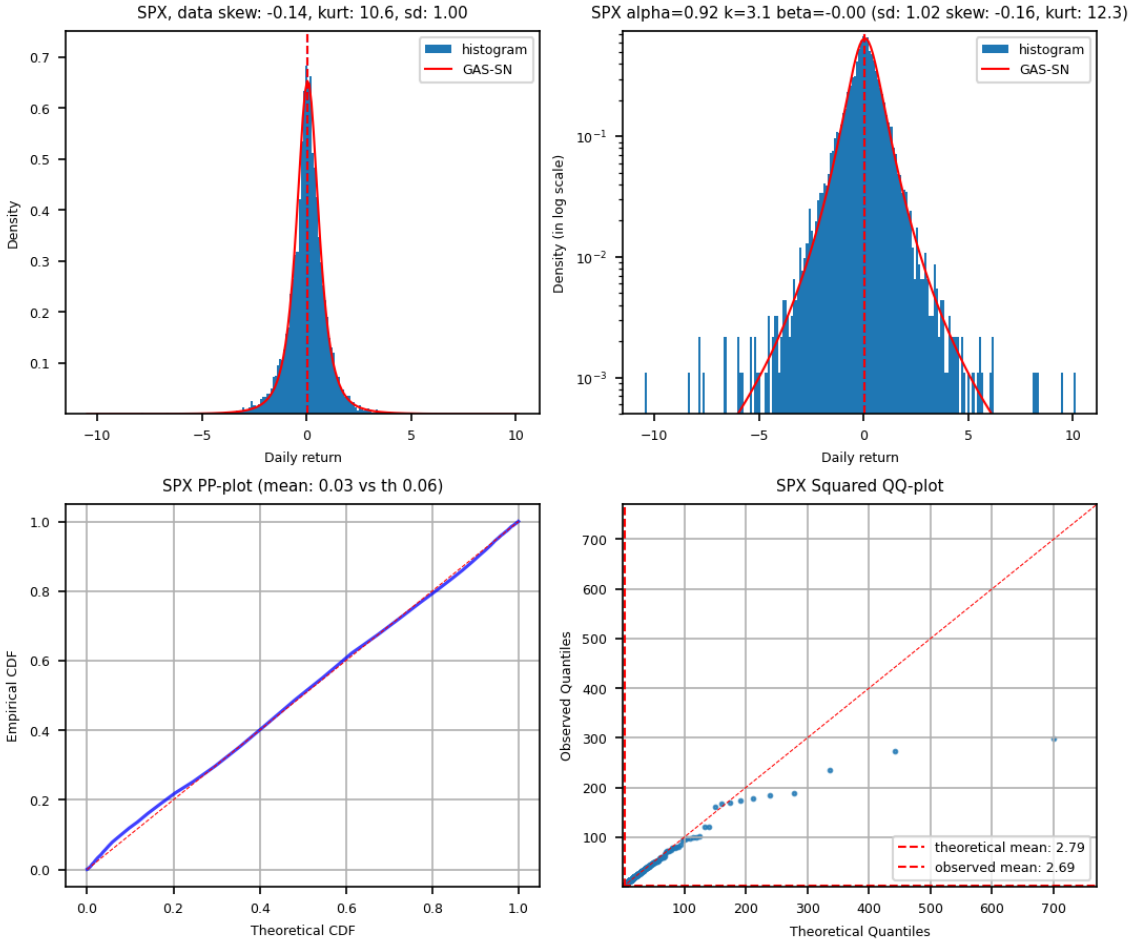

FIGURE 12.6. MLE fit of SPX daily log returns from 1990 to mid-2025. Data is standardized to one standard deviation. Sample skewness is -0.14, sample kurtosis is 10.6. $\hat{\Theta} = \{\alpha = 0.92, k = 3.1, \beta = 0.0\}$. Top left: the PDF vs histogram. Top right: the log-density vs histogram. Bottom left: the PP-plot. Bottom right: the QQ-plot of the quadratic form.

CHAPTER 13

Fractional Feller Square-Root Process

This chapter is copied from Section 11 of [15] for the generation of random variables for FG, FCM, and FCM2. Combining this with an SN variable provides a path to generate the random variable for GAS-SN and beyond.

For example, assuming that a sequence of random numbers $\{S_t > 0\}$ can be generated for FCM, it is straightforward to simulate random numbers $\{X_t\}$ for GAS-SN using the ratio of $X_t = Y_t/S_t$, where Y_t is a standard skew-normal variable $Y_t \sim SN(0, 1, \beta)$ in Chapter 12.

Instead of randomly generating $\{S_t\}$, we propose an innovative method based on *Feller square-root process*[7]. Given a user-specific volatility $\sigma_u > 0$ that describes how fast S_t should change, a scalar function $\mu(x)$, and a scale parameter $\theta_u > 0$ (default to 1), we assume that the random variable S_t should evolve according to the following generalized process:

$$dS_t = \sigma_u^2\, \mu\left(\frac{S_t}{\theta_u}\right) dt + \sigma_u \sqrt{S_t}\, dW_t \tag{13.1}$$

As $t \to \infty$, $\{S_t\}$ will be distributed as the equilibrium distribution for which $\mu(x)$ is designated.

13.0.1. The Fokker-Planck Equation. The $\mu(x)$ solution can be derived from the Fokker-Planck equation. We obtain the following beautiful relation:

LEMMA 13.1. *$\mu(x)$ is one half of the elasticity of the terminal density function $p(x)$ of S_t at $t \to \infty$ plus one half:*

$$\mu(x) = \frac{1}{2}\mathcal{L}\, p(x) + \frac{1}{2} \tag{13.2}$$

where $\mathcal{L}(\cdot) := x\frac{d}{dx}\log(\cdot)$ is the elasticity operator defined in Section 3.6.

△

PROOF. Assume $p(x, t)$ is the density function of (13.1) for S_t. It should satisfy the Fokker-Planck equation ($\theta_u = 1$):

$$\frac{\partial}{\partial t}p(x,t) = -\frac{\partial}{\partial x}\left[\sigma_u^2\, \mu(x)\, p(x,t)\right] + \frac{\partial^2}{\partial x^2}\left[\frac{1}{2}(\sigma_u\sqrt{x})^2\, p(x,t)\right]$$

As $t \to \infty$, $p(x, t)$ approaches the terminal density function $p(x)$. The time dependency is removed. σ_u^2 cancels out from both sides and is irrelevant to the solution. The ODE of $p(x)$ becomes

$$\frac{\partial}{\partial x}\left(\mu(x)\, p(x)\right) = \frac{1}{2}\frac{\partial^2}{\partial x^2}\left(x\, p(x)\right)$$

Apply $\int_x^\infty dx$ to both sides. Assuming that $\mu(x)p(x)$ at $x = \infty$ should be zero, we get

$$\mu(x)p(x) = \frac{1}{2}\frac{d}{dx}\left(x\, p(x)\right) = \frac{1}{2}\left(x\frac{d}{dx}p(x) + p(x)\right)$$

Moving $p(x)$ from LHS to RHS, we obtain (13.2).

□

13.0.2. Generation of Random Variables for FG.

LEMMA 13.2. The $\mu(x)$ solution for FG is obviously

$$\mu(x) = \frac{1}{2}\mathcal{L}\,\mathfrak{N}_\alpha(x;\sigma,d,p) + \frac{1}{2}$$

With Lemma 3.5, $\mu(x)$ is reduced to a function of $\mathcal{L}\,M_\alpha(x)$:

$$\mu(x) = \frac{p}{2}\left[\mathcal{L}\,M_\alpha\right]\left(\left(\frac{x}{\sigma}\right)^p\right) + \frac{d+p}{2}. \tag{13.3}$$

△

As an application, since $\mathcal{L}\,M_{1/2}(x) = -x^2/2$ from Section 3.6, we obtain a simple power-law solution at $\alpha = 1/2$:

$$\mu(x)|_{\mathfrak{N}_{1/2}} = -\frac{p}{4}\left(\frac{x}{\sigma}\right)^{2p} + \frac{d+p}{2} \tag{13.4}$$

Note that (13.4) at $p = 1/2$ subsumes the renown Cox–Ingersoll–Ross (CIR) model[4] since the $\mu(x)$ of the model is a linear $a(b-x)$ type, according to its stochastic process of $dS_t = a(b - S_t)\,dt + \sigma_u\sqrt{S_t}\,dW_t$.[1]

To prepare for the solution of FCM, we prefer to use $Q_\alpha(x)$ defined in (3.30):

$$Q_\alpha(x) := -\frac{W_{-\alpha,-1}(-x)}{W_{-\alpha,0}(-x)}$$

LEMMA 13.3. From (3.32), the $\mu(x)$ solution of a FG in terms of $Q_\alpha(x)$ is

$$\mu(x) = \frac{p}{2\alpha}Q_\alpha\left(\left(\frac{x}{\sigma}\right)^p\right) + \left(\frac{d}{2} - \frac{p}{2\alpha}\right) \tag{13.5}$$

Notice that p/α and d are just constant terms, and σ only affects the scale of x. Neither of them has any effect on the shape of $\mu(x)$.

△

13.1. Generation of Random Variables for FCM

Obviously, what really matters for GAS-SN and GSaS is the solution of FCM, The $\mu(x)$ solution for $\overline{\chi}_{\alpha,k}$ is denoted as $\mu_{\alpha,k}(x)$. Note that from this point on, $\alpha \in (0,2)$.

To further simplify the symbology for FCM, define

$$Q_\alpha^{(\chi)}(z) := Q_{\frac{\alpha}{2}}\left(z^\alpha\right),\ \text{where } \alpha \in (0,2).$$

Assuming $k > 0$, we set $\sigma = \sigma_{\alpha,k}, d = k-1, p/\alpha = 2$ and α replaced by $\alpha/2$ in (13.5). We get

$$\mu_{\alpha,k}(x) = Q_\alpha^{(\chi)}\left(\frac{x}{\sigma_{\alpha,k}}\right) + \left(\frac{k-3}{2}\right) \tag{13.6}$$

For validation, $\mu_{1,k}(x) = k(1-x^2)/2$ can be used to simulate Student's t. And $\mu_{\alpha,1}(x)$ provides a method to simulate an SaS $L_{\alpha,1}(x)$:

$$\mu_{\alpha,1}(x) = Q_\alpha^{(\chi)}\left(\sqrt{2}x\right) - 1$$

Fig. 13.1 shows a simulation of random variables based on the (α,k) parameter obtained from the fit of the S&P 500 daily log returns. The rest of the parameters are in the caption of the figure. First, as outlined above, $\mu_{\alpha,k}(s)$ is calculated analytically as shown in the right graph. Second, it enables

[1] It can also be subsumed by the FG at $\alpha = 0, p = 1$. But $\alpha = 0$ is a singular point and we prefer to avoid using it when possible.

the FG simulation $\{S_t\}$ as shown in the left graph. Third, GSaS $\{X_t\}$ is simulated via $X_t = \mathcal{N}/S_t$, where $\mathcal{N}$ is drawn from a standard normal variable.

The simulation is performed daily. The duration of the sampling is 200,000 years. The red areas are histograms of the simulated data. The blue lines are from the theoretical density functions. They match well.

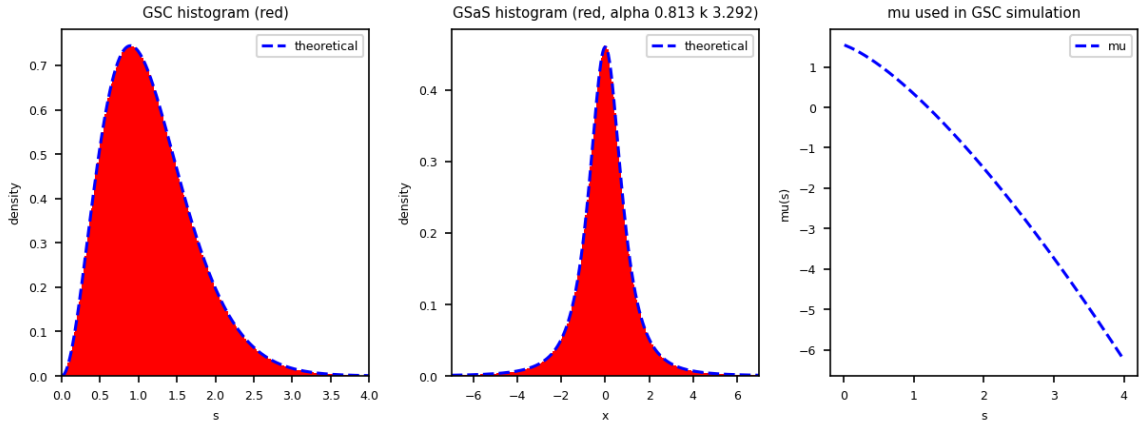

FIGURE 13.1. Simulation of random variables based on the (α, k) parameters obtained from the fit of the S&P 500 daily log returns. The red areas are the histograms from simulated data. The blue lines are from theoretical formulas. The settings of the simulation are $\alpha = 0.813, k = 3.292, dt = 1/365, \sigma_u = 0.85$. Sampling duration is 200,000 years. The simulation takes 11 minutes in python. $\mu_{\alpha,k}(s)$ is discretized to 0.01 and cached to increase performance.

13.2. Generation of Random Variables for FCM2

LEMMA 13.4. The $\mu(x)$ solution for $\overline{\chi}^2_{\alpha,k}$ is

$$\mu^{(2)}_{\alpha,k}(x) = \frac{1}{2}\mu_{\alpha,k}\left(\sqrt{x}\right) \tag{13.7}$$

△

PROOF. From (7.14), we have

$$\overline{\chi}^2_{\alpha,k}(x) := \mathfrak{N}_{\alpha/2}(x; \sigma = \sigma^2_{\alpha,k}, d = (k-1)/2, p = \alpha/2) \qquad (k > 0)$$

Combined with (13.5), we obtain the solution for $\overline{\chi}^2_{\alpha,k}$ as

$$\begin{aligned}\mu^{(2)}_{\alpha,k}(x) &= \frac{1}{2}Q_{\alpha/2}\left(\left(\frac{\sqrt{x}}{\sigma_{\alpha,k}}\right)^{\alpha}\right) + \left(\frac{k-1}{4} - \frac{1}{2}\right) \\ &= \frac{1}{2}Q^{(\chi)}_{\alpha}\left(\frac{\sqrt{x}}{\sigma_{\alpha,k}}\right) + \frac{k-3}{4},\end{aligned}$$

which is just

$$\mu^{(2)}_{\alpha,k}(x) = \frac{1}{2}\mu_{\alpha,k}\left(\sqrt{x}\right).$$

□

This solution can be used to simulate the F distribution in Chapter 8. Let $U_1 \sim \chi^2_d/d = \bar{\chi}^2_{1,d}$ and $U_2 \sim \overline{\chi}^2_{\alpha,k}$, then $F_{\alpha,d,k} \sim U_1/U_2$ is a fractional F distribution.

Part 4

Multivariate Distributions

CHAPTER 14

Multivariate SN Distribution - Review

In this chapter, we start to explore the multivariate distributions. Data sets from the real world are often multidimensional. A flexible multivariate distribution framework with skewness and kurtosis can be very useful. That is what we aim to achieve in the next few chapters.

The foundation is the standard multivariate normal distribution $\mathcal{N}_d(0, \bar{\Omega})$, where d is the dimension of the random variable, and $\bar{\Omega}$ is a $d \times d$ correlation matrix[32].

In Chapter 5 of Azzalini, the skew normal distribution $SN_d(0,\bar{\Omega}, \boldsymbol{\beta})$ adds skewness to it from the skew parameter $\boldsymbol{\beta}$ [1]. In its Chapter 6, the skew-elliptical distribution is discussed. The multivariate skew-t distribution $ST_d(0, \bar{\Omega}, \boldsymbol{\beta}, k)$ is constructed by combining $SN_d(0,\bar{\Omega}, \boldsymbol{\beta})$ with $\chi_k/\sqrt{k}$ in a ratio distribution.

Our work builds on top of this concept of the skew-elliptical distribution. By expanding the denominator of $\chi_k/\sqrt{k}$ to the FCM $\overline{\chi}_{\alpha,k}$, the fractional dimension α is added to the shape parameters. This forms a super-distribution family called *multivariate GAS-SN elliptical distribution* with the notation $L_{\alpha,k}(0, \bar{\Omega}, \boldsymbol{\beta})$ for its standard distribution.

The multivariate skew-elliptical distribution has beautiful properties inherited from the multivariate elliptical distribution framework. However, its deficiency is obvious in real-world applications: The structure is multivariate, but the shape parameters α and k are scalars. All dimensions share the same (α, k). This restricts the kurtoses of 1D marginal distributions to a similar range. It even creates some strange phenomena that are hard to interpret in the SPX-VIX 2D fit (see Section 17.1.1).

To overcome such a restriction, we propose a more flexible framework called *multivariate adaptive distribution*, in which the shape parameters $(\boldsymbol{\alpha}, \boldsymbol{k})$ are d dimensional vectors, just like their skew counterpart $\boldsymbol{\beta}$.

The flexibility in shapes comes with an expensive computational cost. It is analogous to the *curse of dimensionality* problem. It becomes much harder to verify the results beyond the bivariate case for the adaptive distribution.

The study of quadratic form $Z^\intercal \bar{\Omega}^{-1} Z$ from the skew-elliptical distribution results in the fractional extension of the F distribution $F_{\alpha,d,k}$. The QQ-plot based on the quadratic form and the fractional F distribution is a powerful validation of the goodness of the fit.

14.1. Definition

We summarize the results of Chapter 5 of Azzalini[1]. On the one hand, we need to clarify the symbology here that is slightly different from that in his book. On the other hand, our multivariate distributions rely on many results from there, which are collected in this chapter.

DEFINITION 14.1. The PDF of a standard multivariate normal distribution $\mathcal{N}_d(0, \bar{\Omega})$ is defined as

$$\mathcal{N}_d(\boldsymbol{x}; \bar{\Omega}) := \frac{1}{(2\pi)^{d/2} \det(\bar{\Omega})^{1/2}} \exp\left(-\frac{1}{2}\boldsymbol{x}^\intercal \bar{\Omega}^{-1} \boldsymbol{x}\right), \quad \boldsymbol{x} \in \mathbb{R}^d. \tag{14.1}$$

where $\bar{\Omega}$ is a $d \times d$ correlation matrix[32]. That is, $\bar{\Omega}$ is positive definite and all its diagonal elements are equal to 1.

DEFINITION 14.2. A standard multivariate skew-normal variable is denoted as $Z \sim SN_d(0,\bar{\Omega},\boldsymbol{\beta})$, where $\boldsymbol{\beta} \in \mathbb{R}^d$ is the skew parameter (or the slant parameter). Its PDF is

$$\mathcal{N}_d(\boldsymbol{x};\bar{\Omega},\boldsymbol{\beta}) := \mathcal{N}_d(\boldsymbol{x};\,\bar{\Omega})\,\Phi_{\mathcal{N}}(\boldsymbol{\beta}^\intercal\boldsymbol{x}), \tag{14.2}$$

where $\Phi_{\mathcal{N}}(x)$ is the CDF of a standard normal distribution $\mathcal{N}(0,1)$.

Notice that this is a multivariate expansion of SN in Section 10.1. When $d = 1$, (14.2) becomes (10.2).

14.2. The Location-Scale Family

Its location-scale family is $Y = \boldsymbol{\xi} + \boldsymbol{\omega}Z \sim SN_d(\boldsymbol{\xi},\Omega,\boldsymbol{\beta})$, where $\boldsymbol{\xi} \in \mathbb{R}^d$ is the location parameter, $\boldsymbol{\omega} = \text{diag}(\omega_1,...,\omega_d)$ is a $d \times d$ diagonal scale matrix ($\omega_i > 0, \forall i$) and $\Omega = \boldsymbol{\omega}\bar{\Omega}\boldsymbol{\omega}$.

The PDF of Y becomes

$$f_Y(\boldsymbol{x}) = \det(\boldsymbol{\omega})^{-1}\,\mathcal{N}_d(\boldsymbol{z};\bar{\Omega},\boldsymbol{\beta}), \tag{14.3}$$

where $\boldsymbol{z} = \boldsymbol{\omega}^{-1}(\boldsymbol{x}-\boldsymbol{\xi})$.

The location-scale distribution is used for real-world applications. Internally, it has to be calculated via the standard distribution. The main reason is that $\boldsymbol{\beta}$ has to work with $\boldsymbol{z}$ and $\bar{\Omega}$, instead of $\boldsymbol{x}$ and $\boldsymbol{\omega}$.

14.3. Quadratic Form

DEFINITION 14.3. The quadratic form of a multivariate SN distribution (MSN) is defined as

$$Q := \frac{1}{d}(Y-\boldsymbol{\xi})^\intercal\Omega^{-1}(Y-\boldsymbol{\xi}) = \frac{1}{d}Z^\intercal\bar{\Omega}^{-1}Z. \tag{14.4}$$

Q distributes as $\chi^2_d/d = \bar{\chi}^2_{1,d}$ for all $\boldsymbol{\beta}$. The distribution of Q is independent of $\boldsymbol{\beta}$. This is an important property due to the rotational invariance of the elliptical distribution.

Notice that our definition of Q is slightly different from that of Azzalini. We prefer to have the distribution of Q tied to the FCM and the fractional F distribution directly without any constant adjustment. This will make things much simpler in Section 15.6.

To prove $Q \sim \chi^2_d/d$, we quote Corollary 5.9 from [1] below for a skew-normal distribution with 0 location:

LEMMA 14.4. If $Y \sim SN_d(0,\Omega,\boldsymbol{\beta})$ and A is a $d \times d$ symmetric matrix, then

$$Y^\intercal AY = X^\intercal AX$$

where $X \sim \mathcal{N}_d(0,\Omega)$. △

This lemma allows $\boldsymbol{\beta}$ to be removed from the statistics of Q. Hence, $Q \sim X^\intercal\Omega^{-1}X/d \sim \chi^2_d/d$.

14.4. Stochastic Representation

Assuming $X_0 \sim \mathcal{N}_d(0,\bar{\Omega})$ and $X_1 \sim \mathcal{N}(0,1)$, then the first representation of $Z \sim SN_d(0,\bar{\Omega},\boldsymbol{\beta})$ is

$$Z = \begin{cases} X_0 & \text{if } X_1 > \boldsymbol{\beta}^\intercal X_0, \\ -X_0 & \text{otherwise.} \end{cases} \tag{14.5}$$

This form of selective sampling is quite useful in generating random numbers for Z. It is essentially an extension of (10.1).

This scheme can be rephrased in a more interesting representation. First, define the multivariate version of δ as

$$\boldsymbol{\delta} = (1 + \boldsymbol{\beta}^\intercal \bar{\Omega} \boldsymbol{\beta})^{-1/2} \, \bar{\Omega} \boldsymbol{\beta}, \quad (\boldsymbol{\delta} \in \mathbb{R}^d) \tag{14.6}$$

which is used to construct a $(d+1) \times (d+1)$ correlation matrix

$$\Omega^* = \begin{pmatrix} \bar{\Omega} & \boldsymbol{\delta} \\ \boldsymbol{\delta}^\intercal & 1 \end{pmatrix}.$$

Ω^* is used to generate two marginals, $X_0 \in \mathbb{R}^d$ and $X_1 \in \mathbb{R}$, such that

$$\begin{pmatrix} X_0 \\ X_1 \end{pmatrix} \sim \mathcal{N}_{d+1}(0, \Omega^*),$$

which leads to the second representation

$$Z = \begin{cases} X_0 & \text{if } X_1 > 0, \\ -X_0 & \text{otherwise.} \end{cases} \tag{14.7}$$

This form resembles (10.7). It shows that the function of $\boldsymbol{\delta}$ is to add the correlation between X_0 and X_1 through Ω^* in the selective sampling. This makes (14.7) slightly different from (14.5).

14.5. Moments

The first two moments of Z have simple analytic forms. Its first moment is

$$\mu_z = \mathbb{E}(Z) = b \, \boldsymbol{\delta}, \quad \text{where } b = \sqrt{2/\pi}. \tag{14.8}$$

The second moment is simply $\bar{\Omega}$. Its variance is

$$\Sigma_z = \text{var}\{Z\} = \bar{\Omega} - b^2 \, \boldsymbol{\delta}\boldsymbol{\delta}^\intercal. \tag{14.9}$$

It is easy to obtain $\mathbb{E}\{Y\, Y^\intercal\} = \Omega$ for the location-scale variable Y.

Define the important invariant quantity for the skewness.

$$\beta_* = (\boldsymbol{\beta}^\intercal \bar{\Omega} \boldsymbol{\beta})^{1/2} \geq 0, \tag{14.10}$$

which is a nonnegative scalar quantity. It encapsulates the departure from normality for the distribution.

The quadratic form $\mu_z^\intercal \Sigma_z^{-1} \mu_z$ can be simplified to

$$\mu_z^\intercal \Sigma_z^{-1} \mu_z = \frac{b^2 \beta_*^2}{1 + (1 - b^2)\beta_*^2}. \tag{14.11}$$

A related quantity is

$$\delta_* = (\boldsymbol{\delta}^\intercal \bar{\Omega}^{-1} \boldsymbol{\delta})^{1/2} \tag{14.12}$$

where $\delta_* \in [\, 0, 1)$ has the scale of a positive correlation coefficient.

The two are connected by

$$\delta_*^2 = \frac{\beta_*^2}{1 + \beta_*^2}, \quad \beta_*^2 = \frac{\delta_*^2}{1 - \delta_*^2}.$$

Or in a trigonometric form, there exists an angle $\theta \in [\, 0, \frac{\pi}{2})$ such that $\tan\theta = \beta_*$ and $\sin\theta = \delta_*$. In such an expression, $\theta > 0$ captures the "degree" of departure from normality.

14.6. Canonical Form

The concept of a canonical form in SN is very important and fascinating. Due to the rotational symmetry, an MSN can be rotated and rescaled to an "identity" MSN with a scalar skew parameter.

By Proposition 5.12 of [1], there exists an affine transformation $Z^* = A_*(Y - \boldsymbol{\xi})$ such that $Z^* \sim SN_d(0, \boldsymbol{I}_d, \boldsymbol{\beta}_{Z^*})$, where $\boldsymbol{I}_d$ is a $d \times d$ identity matrix, and $\boldsymbol{\beta}_{Z^*} = (\beta_*, 0, ..., 0)^\intercal$. β_* is defined by (14.10), which is an invariant under transformation.

The variable Z^* is called *the canonical variable*. It is d-dimensional. But only one dimension is skew-normal, which is designated as the first dimension. All other dimensions are standard normal distributions. That is, the PDF of Z^* is

$$\begin{aligned}\mathcal{N}_*(\boldsymbol{x}; \beta_*) &= 2\Phi_{\mathcal{N}}(\beta_* x_1) \prod_{i=1}^{d} \mathcal{N}(x_i) \\ &= \mathcal{N}(x_1; \beta_*) \prod_{i=2}^{d} \mathcal{N}(x_i).\end{aligned}$$

This structure helps tremendously for the subsequent development of the elliptical distribution and adaptive distribution.

Proposition 5.13 in [1] describes how to find such A_*. Due to rotational symmetry, there are many choices of A_*. This is not a problem as long as we always look at the system in quadratic form.

LEMMA 14.5 (Affine Transformation). Let $C = \Omega^{1/2}$ be the unique positive definite symmetric square root of Ω. Define $M = C^{-1}\Sigma C^{-1}$, where $\Sigma = \text{var}\{Y\}$. Let $Q\Lambda Q^\intercal$ denote a spectral decomposition of M, where we assume that the diagonal elements in the eigenvalue matrix Λ are arranged in increasing order.

Let $H = C^{-1}Q$. Then H is the matrix operator to convert Y to Z^*,

$$Z^* = H^\intercal(Y - \boldsymbol{\xi}).$$

Since $\boldsymbol{\delta}_{Z^*} = H^\intercal \boldsymbol{\omega} \boldsymbol{\delta}$ and $\boldsymbol{\beta}_{Z^*} = \boldsymbol{\delta}_{Z^*}/(1 - \delta_*^2)$, the choice of H must make the first element of $\boldsymbol{\delta}_{Z^*}$ a nonnegative number, that is, $\delta_* \geq 0$. All other elements, except the first ones in $\boldsymbol{\delta}_{Z^*}$ and $\boldsymbol{\beta}_{Z^*}$, must be zero. △

REMARK 14.6. The significance of this lemma is that the skew-elliptical distributions derived from the SN framework can only have a single source of skewness. It might be mixed up and not easy to observe in real-world data. But there is only one source from the theoretical perspective. Everything else comes from the multivariate normal distribution.

If we want a more "sophisticated" distribution that provides multiple sources of skewness, we have to go beyond the skew-elliptical distributions.

14.7. 1D Marginal Distribution

We are particularly interested in the 1D marginal distribution, since this is what is actually observed in a data set. When we optimize a data fit, we can add the log-likelihood of the 1D marginal distributions to the objective function, so that the fitting of each dimension is properly addressed.

In fact, for the adaptive distribution, the full 2D likelihood is so compute-intensive that it is too slow to perform MLE on a desktop. The alternative is to compute the sum of the log-likelihoods of each 1D marginal distribution, in addition to the regularization on other statistical quantities, such as the correlation coefficient between each data pair.

We quote the results from Section 5..1.4 of [1] and adapt them to the 1D case.

LEMMA 14.7. (The marginal β) Assume that the marginal is on the first dimension. The correlation matrix is decomposed as

$$\bar{\Omega} = \begin{pmatrix} \bar{\Omega}_{11} & \bar{\Omega}_{12} \\ \bar{\Omega}_{21} & \bar{\Omega}_{22} \end{pmatrix}.$$

The formula can be simplified due to $\bar{\Omega}_{11} = 1$ in the 1D case.

The marginal distribution is $Y_1 \sim SN(\xi_1, \Omega_{11}, \beta_{1(2)})$. Its $\beta_{1(2)}$ is derived as

$$\beta_{1(2)} = \left(1 + \beta_2^{\intercal} \bar{\Omega}_{22.1} \beta_2\right)^{-1/2} \left(\beta_1 + \bar{\Omega}_{12} \beta_2\right) \quad \text{where} \quad \bar{\Omega}_{22.1} = \bar{\Omega}_{22} - \bar{\Omega}_{21} \bar{\Omega}_{12}. \tag{14.13}$$

△

LEMMA 14.8. (The marginals of a bivariate distribution) The bivariate case is quite simple:

$$\bar{\Omega} = \begin{pmatrix} 1 & \rho \\ \rho & 1 \end{pmatrix}. \tag{14.14}$$

Assume that we want to get the marginal β of the i-th dimension, $\beta_{i(j)}$, where j is the other dimension. Then

$$\beta_{i(j)} = \frac{\beta_i + \rho \beta_j}{\sqrt{1 + \beta_j^2 \, |\bar{\Omega}|}} \tag{14.15}$$

where $|\bar{\Omega}| = 1 - \rho^2$. Since Ω_{ii} is ω_i^2, the i-th marginal distribution is $Y_i \sim SN(\xi_i, \omega_i^2, \beta_{i(j)})$. The ξ_i and ω_i are the location and scale parameters in the i-th dimension that can be calculated directly from the data. △

We observe that ρ in the numerator describes how much β_j is mixed with β_i, while $|\bar{\Omega}|$ in the denominator describes how much β_j reduces the scale.

When $\rho = 0$, there is no mixing from the other dimension, only a reduction in total scale. That is, $\beta_{i(j)}|_{\rho=0} = \beta_i / \sqrt{1 + \beta_j^2}$.

CHAPTER 15

Multivariate GAS-SN Elliptical Distribution

15.1. Definition

This chapter follows the structure laid out in Chapter 6 of Azzalini (2013)[1]. We implemented the skew-elliptical distribution by our $\overline{\chi}_{\alpha,k}$, which fully extends his multivariate skew-t distribution.

DEFINITION 15.1. Assume $Z_0 \sim SN_d(0,\bar{\Omega},\boldsymbol{\beta})$ is a $d \times d$ standard multivariate skew-normal (SN) distribution, and $V \sim \overline{\chi}_{\alpha,k}$ is a standard FCM. $\bar{\Omega}$ is a correlation matrix.

Then $Z \sim Z_0/V$ is a $d \times d$ standard multivariate GAS-SN elliptical distribution. It is given the notation of $Z \sim L_{\alpha,k}(0,\bar{\Omega},\boldsymbol{\beta})$.

Equivalently, using the location-scale notation, $Z \sim SN_d(0,\Sigma,\boldsymbol{\beta})$ where $\Sigma = \bar{\Omega}/V^2$.

Assume $\mathcal{N}_d(\boldsymbol{x};\bar{\Omega},\boldsymbol{\beta})$ is the PDF of a standard multivariate normal distribution $\mathcal{N}_d(0,\bar{\Omega})$ [32]. $\Phi_{\mathcal{N}}(x)$ is the CDF of a standard normal distribution.

We expand on the construction of multivariate SN distribution in (14.1) and (14.2). And the PDF of $Z \sim L_{\alpha,k}(0,\bar{\Omega},\boldsymbol{\beta})$ is

$$\begin{aligned} L_{\alpha,k}(\boldsymbol{x};\bar{\Omega},\boldsymbol{\beta}) &= \int_0^\infty ds\, \overline{\chi}_{\alpha,k}(s)\, s^d\, \mathcal{N}_d(\boldsymbol{x}s;\bar{\Omega},\boldsymbol{\beta}) \\ &= 2\int_0^\infty ds\, \overline{\chi}_{\alpha,k}(s)\, s^d\, \mathcal{N}_d(\boldsymbol{x}s;\,\bar{\Omega})\, \Phi_{\mathcal{N}}(\boldsymbol{\beta}^\intercal \boldsymbol{x}\, s). \end{aligned} \tag{15.1}$$

The s^d term comes from $\det(s\boldsymbol{I}_d)$ where $\boldsymbol{I}_d$ is the $d \times d$ identity matrix. It is easy to see how it is reduced to a univariate GAS-SN distribution when $d = 1$.

15.1.1. Multivariate Skew-t Distribution.

An important bridge between multivariate SN and GAS-SN is the multivariate skew-t distribution. It is documented in Section 6.2 of [1].

It is fully consistent with multivariate GAS-SN by setting $\alpha = 1$. That is, in his notation of skew-t: $ST_d(\Omega,\boldsymbol{\beta},k) \sim L_{1,k}(\Omega,\boldsymbol{\beta})$.

15.2. Location-Scale Family

The location-scale family follows the standard procedure: $Y = \boldsymbol{\xi} + \boldsymbol{\omega}Z$, which is denoted as $Y \sim L_{\alpha,k}(\boldsymbol{\xi},\Omega,\boldsymbol{\beta})$, where $\Omega := \boldsymbol{\omega}^\intercal\bar{\Omega}\boldsymbol{\omega}$ is the covariance matrix, and $\boldsymbol{\omega}$ is a $d \times d$ diagonal scale matrix.

The PDF of Y is

$$L_{\alpha,k}(\boldsymbol{x};\,\boldsymbol{\xi},\Omega,\boldsymbol{\beta}) := \det(\boldsymbol{\omega})^{-1} L_{\alpha,k}(\boldsymbol{z};\bar{\Omega},\boldsymbol{\beta}) \tag{15.2}$$

where $\boldsymbol{z} := \boldsymbol{\omega}^{-1}(\boldsymbol{x}-\boldsymbol{\xi})$. Notice that it has to be computed via the standard PDF.

15.3. Moments

The first moment of Z is $\mu_z := b\,\boldsymbol{\delta}$, where $b := \sqrt{2/\pi}\,\mathbb{E}(X^{-1}|\overline{\chi}_{\alpha,k})$.

The second moment of Z is $m_2\,\bar{\Omega}$, where $m_2 = \mathbb{E}(X^{-2}|\overline{\chi}_{\alpha,k})$. Hence, the covariance is

$$\mathrm{var}\{Z\} := \Sigma_z := m_2\,\bar{\Omega} - b^2\,\boldsymbol{\delta}\boldsymbol{\delta}^\intercal$$

The moments of Y follow the rule of the location-scale family. The first moment of Y is $\boldsymbol{\xi} + \boldsymbol{\omega}\,\mu_z$. The covariance of Y is $\boldsymbol{\omega}\,\Sigma_z\,\boldsymbol{\omega}$.

15.4. Canonical Form

The concept of canonical form in GAS-SN is extended from the multivariate SN in Section 14.6. There exists an affine transformation $Z^* = A_*(Y - \boldsymbol{\xi})$ such that $Z^* \sim L_{\alpha,k}(0, \boldsymbol{I}_d, \boldsymbol{\beta}_{Z*})$, where $\boldsymbol{\beta}_{Z*} = (\beta_*, 0, ..., 0)^\intercal$ and β_* is defined by (14.10). And the algorithm of finding A_* is exactly the same as in Section 14.6.

The variable Z^*, which is called *canonical variable*, comprises d independent components. Only one of them contains the skew component. That is, the PDF of Z^* is

$$L_{\alpha,k_*}(\boldsymbol{x}; \beta_*) = 2\int_0^\infty ds\,\overline{\chi}_{\alpha,k}(s)\,s^d \prod_{i=1}^{d} \mathcal{N}(x_i s)\Phi_{\mathcal{N}}(\beta_* x_1\, s). \tag{15.3}$$

It can be further simplified to an elegant univariate-style integral. When $|\boldsymbol{x}| \neq 0$, let $\beta_*(\boldsymbol{x}) := \beta_* x_1/|\boldsymbol{x}| \in \mathbb{R}$, and

$$L_{\alpha,k_*}(\boldsymbol{x}; \beta_*) = (2\pi)^{-(d-1)/2}\int_0^\infty ds\,\overline{\chi}_{\alpha,k}(s)\,s^d\,\mathcal{N}(|\boldsymbol{x}|s; \beta_*(\boldsymbol{x})). \tag{15.4}$$

When $|\boldsymbol{x}| = 0$, It is simply

$$L_{\alpha,k_*}(0; \beta_*) = (2\pi)^{-d/2}\,\mathbb{E}(X^d|\overline{\chi}_{\alpha,k}), \tag{15.5}$$

independent of β_*.

15.5. Marginal 1D Distribution

The construction of the 1D marginal distribution from Y extends directly from Section 14.7, where $\beta_{1(2)}$ is calculated.

Then the marginal distribution is an univariate GAS-SN: $Y_1 \sim L_{\alpha,k}(\xi_1, \Omega_{11}, \beta_{1(2)})$.

15.6. Quadratic Form

The quadratic form is

$$Q := \frac{1}{d}(Y - \boldsymbol{\xi})^\intercal \Omega^{-1}(Y - \boldsymbol{\xi}) = \frac{1}{d} Z^\intercal \bar{\Omega}^{-1} Z. \tag{15.6}$$

This leads to the fractional extension of the classic F distribution.

Q distributes like a fractional F distribution, $Q \sim F_{\alpha,d,k}$ for all β. The QQ-plot between the empirical data and theoretical values is used to evaluate the goodness of a fit. A perfect fit should produce a 45-degree line.

To prove, from Section 15.1, we have $Z \sim Z_0/V$, $Z_0 \sim SN_d(0, \bar{\Omega}, \boldsymbol{\beta})$, and $V \sim \overline{\chi}_{\alpha,k}$. Put them together,

$$Q = \frac{1}{d} Z^\intercal \bar{\Omega}^{-1} Z = \frac{Z_0^\intercal \bar{\Omega}^{-1} Z_0}{d\,V^2} \sim \left(\frac{X^2}{d}\right)/V^2$$

where $X \sim \mathcal{N}_d(0, \bar{\Omega})$, according to Lemma 14.4.

Since $X^2 \sim \chi^2_d$ and $V^2 \sim \overline{\chi}^2_{\alpha,k}$, this leads to $Q \sim F_{\alpha,d,k}$, according to Section 8.1.

Azzalini (2013) provided a point of validation from his multivariate skew-t distribution. From Section 6.2 of [1], Q of a skew-t variable distributes like the classic $F(d, k)$. This is a special case of our fractional F distribution at $\alpha = 1$. That is, $Q \sim F_{1,d,k}$.

15.7. Multivariate MLE

TODO write better

A stochastic gradient decent (SGD) method on the maximum likelihood estimation (MLE) can be implemented efficiently. First, we calculate the sum of the minus-log of the PDF evaluated at every data point. This sum is called MLLK. Then we calculate the gradients for each hyperparameter. And make a small move along the direction that is most likely to minimize the MLLK. The scale of the move is based on a learning rate, which can be adjusted dynamically. Some randomness can be added to the small move. This allows the algorithm to explore the nearby regions, and maybe get "unstuck" over unexpected edges.

Use the bivariate optimization as an example. The hyperparameter space is

$$\Theta = \{\rho, \alpha, k, \beta_1, \beta_2, w_1, w_2, \xi_1, \xi_2\}$$

where $\alpha \in (0, 2)$, $k \in (2, \infty)$, $w_1 > 0, w_2 > 0$, and $\beta_1, \beta_2, \xi_1, \xi_2 \in \mathbb{R}$. Since $\rho \in (-1, 1)$, it is preferred to use a transformed parameter $\rho_\theta = \arctan(\rho/\pi) \in \mathbb{R}$.

It is also found that each dimension in the data set should be normalized to one standard deviation. This allows all the gradients to have similar scales. This helps the SGD algorithm.

Let Y represent the data set of size N, and $L(Y_i; \Theta)$ is the PDF, then

$$\text{MLLK}(\Theta; Y) := -\sum_{i=1}^{N} \log\, L(Y_i; \Theta)$$

$$\text{Gradient}(\Theta) := \left\{ \frac{\partial\, \text{MLLK}(\Theta; Y)}{\partial \Theta_j}, \forall\, \Theta_j \in \Theta \right\}$$

When N is large, it may not be computationally feasible to evaluate every $L(Y_i; \Theta)$. One may use histogram to compress the data into smaller numbers of bins.

Regularization can be added to the MLLK. For instance, we find it makes a lot of sense to add the L2 distances of the skewness and kurtosis on the marginal 1D distributions.

CHAPTER 16

Multivariate GAS-SN Adaptive Distribution (Experimental)

16.1. Definition

The goal of an adaptive distribution is to allow each dimension to have its own shape parameter in α, k. This is the departure from the the elliptical distribution.

Therefore, $\boldsymbol{\alpha} = \{\alpha_i\}$ is a d-dimensional vector, so is $\boldsymbol{k} = \{k_i\}$. We now have a list of standard FCM to work with: $\{\overline{\chi}_{\alpha_i,k_i}, i \in 1, 2..., d\}$.

DEFINITION 16.1. Assume Z_0 is a d-dimensional random variable from a standard $d \times d$ multivariate skew-normal (SN) distribution, $SN_d(0,\bar{\Omega},\boldsymbol{\beta})$, where $\bar{\Omega}$ is a correlation matrix.

Let Z be a d-dimensional random variable. Each element is a ratio distribution such as $Z_i \sim (Z_0)_i/\overline{\chi}_{\alpha_i,k_i}$. Then $Z \sim \overrightarrow{L}_{\boldsymbol{\alpha},\boldsymbol{k}}(0,\bar{\Omega},\boldsymbol{\beta})$ is a standard multivariate GAS-SN adaptive distribution. The arrow-over sign is to emphasize the vector nature of $(\boldsymbol{\alpha},\boldsymbol{k})$.

Assume $\mathcal{N}(x;\bar{\Omega})$ is the PDF of a standard multivariate normal distribution $N(0,\bar{\Omega})$ [32]. $\Phi_{\mathcal{N}}(x)$ is the CDF of a standard normal distribution.

The PDF of $Z \sim \overrightarrow{L}_{\boldsymbol{\alpha},\boldsymbol{k}}(0,\bar{\Omega},\boldsymbol{\beta})$ is

$$\overrightarrow{L}_{\boldsymbol{\alpha},\boldsymbol{k}}(\boldsymbol{x};\bar{\Omega},\boldsymbol{\beta}) = 2\int\cdots\int_0^\infty \mathcal{N}\left(\boldsymbol{s}\,\boldsymbol{x};\bar{\Omega}\right)\,\Phi_{\mathcal{N}}\Big(\boldsymbol{\beta}^{\intercal}(\boldsymbol{s}\,\boldsymbol{x})\Big)\prod_{i=1}^{d} s_i ds_i\,\overline{\chi}_{\alpha_i,k_i}(s_i). \tag{16.1}$$

where $\boldsymbol{s} := \text{diag}(s_1, ..., s_d)$ is the $d \times d$ diagonal matrix from the vector $\{s_i\}$. It is easy to see how it is reduced to a univariate GAS-SN distribution when $d = 1$.

Compared to the elliptical PDF (15.1), the major difference is that (16.1) is a d-dimensional integral. This is much more computationally demanding.

16.2. Location-Scale Family

The location-scale family follows the standard procedure: $Y = \boldsymbol{\xi} + \boldsymbol{\omega}Z$, which is denoted as $Y \sim \overrightarrow{L}_{\boldsymbol{\alpha},\boldsymbol{k}}(\boldsymbol{\xi},\Omega,\boldsymbol{\beta})$. The covariance matrix is $\Omega = \boldsymbol{\omega}^{\intercal}\bar{\Omega}\boldsymbol{\omega}$, and $\boldsymbol{\omega}$ is the $d \times d$ diagonal scale matrix.

The PDF of Y is

$$\overrightarrow{L}_{\boldsymbol{\alpha},\boldsymbol{k}}(\boldsymbol{x};\,\boldsymbol{\xi},\Omega,\boldsymbol{\beta}) := \det(\boldsymbol{\omega})^{-1}\,\overrightarrow{L}_{\boldsymbol{\alpha},\boldsymbol{k}}(\boldsymbol{z};\bar{\Omega},\boldsymbol{\beta}). \tag{16.2}$$

where $\boldsymbol{z} := \boldsymbol{\omega}^{-1}(\boldsymbol{x}-\boldsymbol{\xi})$. Notice that it has to be computed via the standard PDF because the mixtures $\{s_i\}$ must work with the standardized variable Z, not the location-scale variable Y.

16.3. Moments

The first moment of Z is $\mu_z := \boldsymbol{b} \odot \boldsymbol{\delta}$, where $b_i := \sqrt{2/\pi}\,\mathbb{E}(X^{-1}|\overline{\chi}_{\alpha_i,k_i})$ and $\odot$ is the Hadamard product.

The (i,j) element of the second moment of Z is

$$\boldsymbol{m_2}(i,j) := \begin{cases} \mathbb{E}(X^{-2}|\overline{\chi}_{\alpha_i,k_i}) & \text{if } i = j, \\ \bar{\Omega}_{i,j}\mathbb{E}(X^{-1}|\overline{\chi}_{\alpha_i,k_i})\mathbb{E}(X^{-1}|\overline{\chi}_{\alpha_j,k_j}) & \text{if } i \neq j. \end{cases}$$

where $\bar{\Omega}_{i,i} = 1$ is ignored in the first line. Hence, the covariance is

$$\operatorname{var}\{Z\} := \Sigma_z := \boldsymbol{m_2} - \mu_z\,\mu_z^\intercal$$

The moments of Y follow the rule of the location-scale family. The first moment of Y is $\boldsymbol{\xi} + \boldsymbol{\omega}\,\mu_z$. The covariance of Y is $\boldsymbol{\omega}\operatorname{var}\{Z\}\,\boldsymbol{\omega}$.

16.4. Canonical Form

The adaptive distribution *doesn't* enjoy the rotational symmetry that an elliptical distribution has. Its canonical form is *not* particularly useful, since it has no connection to other distributions in the family through an affine transformation.

Assume the variable Z^* is a *canonical variable*. Then $Z^* \sim \overrightarrow{L}_{\boldsymbol{\alpha},\boldsymbol{k}}(0, \boldsymbol{I}_d, \boldsymbol{\beta}_{Z*})$, where $\boldsymbol{\beta}_{Z*} = (\beta_*, 0, ..., 0)^\intercal$ and β_* is defined by (14.10).

The PDF of Z^* is

$$\overrightarrow{L}_{\boldsymbol{\alpha},\boldsymbol{k}_*}(\boldsymbol{x}; \beta_*) = L_{\alpha_1,k_1}(x_1; \beta_*) \prod_{j=2}^{d} L_{\alpha_j,k_j}(x_j). \tag{16.3}$$

We can clearly see that only the first component is GAS-SN, all other components are GSaS, each with its own (α, k) shape.

Only the first component of its μ_z is non-zero, which is $\sqrt{2/\pi}\,\delta_*\,\mathbb{E}(X^{-1}|\overline{\chi}_{\alpha_1,k_1})$. Its $\boldsymbol{m_2}$ is a diagonal matrix where $\boldsymbol{m_2}(i,i) = \mathbb{E}(X^{-2}|\overline{\chi}_{\alpha_i,k_i})$.

16.5. Marginal 1D Distribution

The construction of the 1D marginal distribution from Y extends directly from Section 14.7, where $\beta_{1(2)}$ is calculated.

Then the marginal distribution is an univariate GAS-SN: $Y_1 \sim L_{\alpha_1,k_1}(\xi_1, \Omega_{11}, \beta_{1(2)})$.

16.6. Quadratic Form

TODO The corresponding F distribution is very hard. I have not figured this out yet.

16.7. 2D Adaptive MLE

TODO this needs more refinement since a normal 2D MLE doesn't work here.

TODO I am still working on the numerical method.

A stochastic gradient decent (SGD) method on the maximum likelihood estimation (MLE) can be implemented, but some adjustments are needed. Use the bivariate optimization as an example. The hyperparameter space is

$$\Theta = \{\rho, \alpha_1, \alpha_2, k_1, k_2, \beta_1, \beta_2, w_1, w_2, \xi_1, \xi_2\}$$

where $\alpha_1, \alpha_2 \in (0, 2)$, $k_1, k_2 \in (2, \infty)$, $w_1 > 0, w_2 > 0$, and $\beta_1, \beta_2, \xi_1, \xi_2 \in \mathbb{R}$. Since $\rho \in (-1, 1)$, it is preferred to use a transformed parameter $\rho_\theta = \arctan(\rho/\pi) \in \mathbb{R}$.

The computation of the adaptive PDF is very slow on a desktop, even for two dimensions. The MLLK is modified to perform on the two marginal 1D distributions. We supplement it with a regularization on the L2 distance of the correlation coefficient.

It is also found that each dimension in the data set should be normalized to one standard deviation. This allows all the gradients to have similar scales. This helps the SGD algorithm.

Let Y represent the data set of size N, and $L_m(Y_i;\Theta)$ is the marginal 1D PDF at dimension m $(m = 1...d)$, then

$$\text{MLLK}(\Theta;Y) := -\sum_{i=1}^{N}\sum_{m=1}^{d} \log\, L_m(Y_i;\Theta)$$

$$\text{Gradient}(\Theta) := \left\{ \frac{\partial\, \text{MLLK}(\Theta;Y)}{\partial \Theta_j}, \forall\, \Theta_j \in \Theta \right\}$$

Once the MLLK and gradients are calculated. The program makes a small move along the direction that is most likely to minimize the MLLK. The scale of the move is based on a learning rate, which can be adjusted dynamically. Some randomness can be added to the small move. This allows the algorithm to explore the nearby regions, and maybe get "unstuck" over unexpected edges.

When N is large, it may not be computationally feasible to evaluate every $L(Y_i;\Theta)$. One may use histogram to compress the data into smaller numbers of bins.

More regularization can be added to the MLLK. For instance, we find it makes a lot of sense to add the L2 distances of the skewness and kurtosis on the marginal 1D distributions.

We also regulate the mean of the quadratic form. But the exact distribution of the quadratic form is still under research.

CHAPTER 17

Fitting SPX-VIX Daily Returns with Bivariate Distributions

Two MLE fits are performed for the VIX/SPX daily log returns from 1990 to 2025. The first fit uses the bivariate elliptical GAS-SN distribution. The second fit uses the bivariate adaptive GAS-SN distribution.

The major difference is that the adaptive distribution allows each dimension to have its own (α, k) shape. However, it is much more compute-intensive, it requires alternative methods to work around. And it breaks the rotational symmetry that the elliptical distribution has. This requires a different approach to evaluate the quadratic form.

17.1. Elliptical Fit

The bivariate elliptical MLE program is similar to the univariate MLE program. But the hyper-parameter space is much larger:

$$\Theta = \{\rho, \alpha, k, \beta_1, \beta_2, w_1, w_2, \xi_1, \xi_2\}$$

where $\alpha \in (0, 2)$, $k \in (2, \infty)$, $\omega_1 > 0, \omega_2 > 0$, and $\beta_1, \beta_2, \xi_1, \xi_2 \in \mathbb{R}$. ρ is the correlation coefficient. Since $\rho \in (-1, 1)$, it is preferred to use a transformed parameter $\rho_\theta = \arctan(\rho/\pi) \in \mathbb{R}$. In the program, ρ is converted to $\bar{\Omega}$ according to (14.14).

The bivariate MLE program is implemented in **python** and **scipy** on github at https://github.com/slihn/gas-impl/blob/main/gas_impl/mle_gas_sn_2d.py.

We run the MLE fitting on the daily returns of VIX and SPX from 1990 to mid-2025, about 8900 two-column samples. Each column in the data set is normalized to one standard deviation. This allows all gradients to have similar scales and helps the MLE to operate smoothly.

Assume there are N samples in the data set, $Y = \{\boldsymbol{y}_i, i \in 1, 2, ..., N\}$, the minus log-likelihood (MLLK) is

$$\text{MLLK}(\Theta) = -\frac{1}{N}\sum_{i=1}^{N} \log(L_{\alpha,k}(\boldsymbol{y}_i; \boldsymbol{\xi}, \Omega, \boldsymbol{\beta})) \tag{17.1}$$

where $L_{\alpha,k}(\boldsymbol{x}; \boldsymbol{\xi}, \Omega, \boldsymbol{\beta})$ is the multivariate PDF of the location scale family (15.2).

When N is large, it may not be computationally feasible to compute the PDF on every $\boldsymbol{y}_i$. A histogram may be used to compress the data into a grid of bins.

Two components of regularization are added to the objective function $\ell(\Theta)$. The L2 distances between the empirical and theoretical statistics are added as follows:

- Correlation: $|\Delta\rho(Y)|^2$.
- The mean of the quadratic form: $\Delta\mu_Q^2 := |\Delta\text{mean}(Q)|^2$. Section 15.6.

MLE seeks the optimal Θ that minimizes the objective function:

$$\hat{\Theta} = \text{argmin } \ell(\Theta) \tag{17.2}$$

$$\text{where } \ell(\Theta) = \text{MLLK}(\Theta) + |\Delta\rho(Y)|^2 + \Delta\mu_Q^2 \tag{17.3}$$

17.1.1. The VIX-SPX Bivariate Elliptical Fit. Figure 17.1 shows the results of the bivariate elliptical MLE fit on the VIX/SPX daily log returns. The top two graphs show the 2D scatter plot (left) and the contour plot (right) of the samples. Two overlapping lines are drawn to indicate the angles of the correlation, theoretical vs. empirical. The main accomplishment of this fit is that the correlation coefficient matches nicely at about -0.7.

The contour plot is compared to the theoretical elliptical contour plot in the middle left graph. We note that the sample contours look rectangular instead of elliptical. This is an important research topic left for the future.

The remaining three graphs are for the quadratic form Q in (15.6). The PP-plot in the middle right graph and the QQ-plot in log scale in the bottom right graph show very good match with a clear 45-degree line.

However, the QQ-plot in the bottom left graph is less ideal. The tail is tilted upward after 20. This indicates a poor fit on the outside of the contours. This is probably due to the fact that an elliptical distribution could not capture the rectangular nature of the contours.

17.1.2. The Issue in Marginal Distributions. One major issue with the fit is related to the 1-dimensional marginals. The bivariate MLE finds the best fit at $\alpha = 0.75, k = 4.5$. This is a strange place when we examine it in Figure 12.1. When the bivariate distribution is projected to the 1-dimensional marginal distributions according to Section 15.5, the univariate GAS-SN distributions are near the border of infinite kurtosis.

(The reader is reminded that the degrees of freedom need to be higher than 4 to have valid kurtosis in the Student's t distribution. $k = 4.5$ is in the neighborhood of that threshold.)

Despite the fact that the kurtoses are very off, the graphs in Figures 17.2 and 17.3 generally look good except for one area: We notice a problem in the top right graphs. On the one hand, the theoretical peak in the VIX marginal PDF is higher than the observed peak. On the other hand, the theoretical peak in the SPX marginal PDF is lower than the observed peak.

The guess is that this problem in peak densities has something to do with the different shape parameters (α, k) required for VIX and SPX. However, this is impossible with the current structure of the elliptical distribution. It is an open question how to inject different α's and k's for each dimension.

In summary, it is obviously too naive to think that a single bivariate distribution can describe 35 years of history in the SPX and VIX data. More research remains to be done. A major step forward is to apply this distribution in regime-switching models, such as the Hidden Markov Model (HMM), statistical jump model[**29**], and mixture-VAE model[**23**].

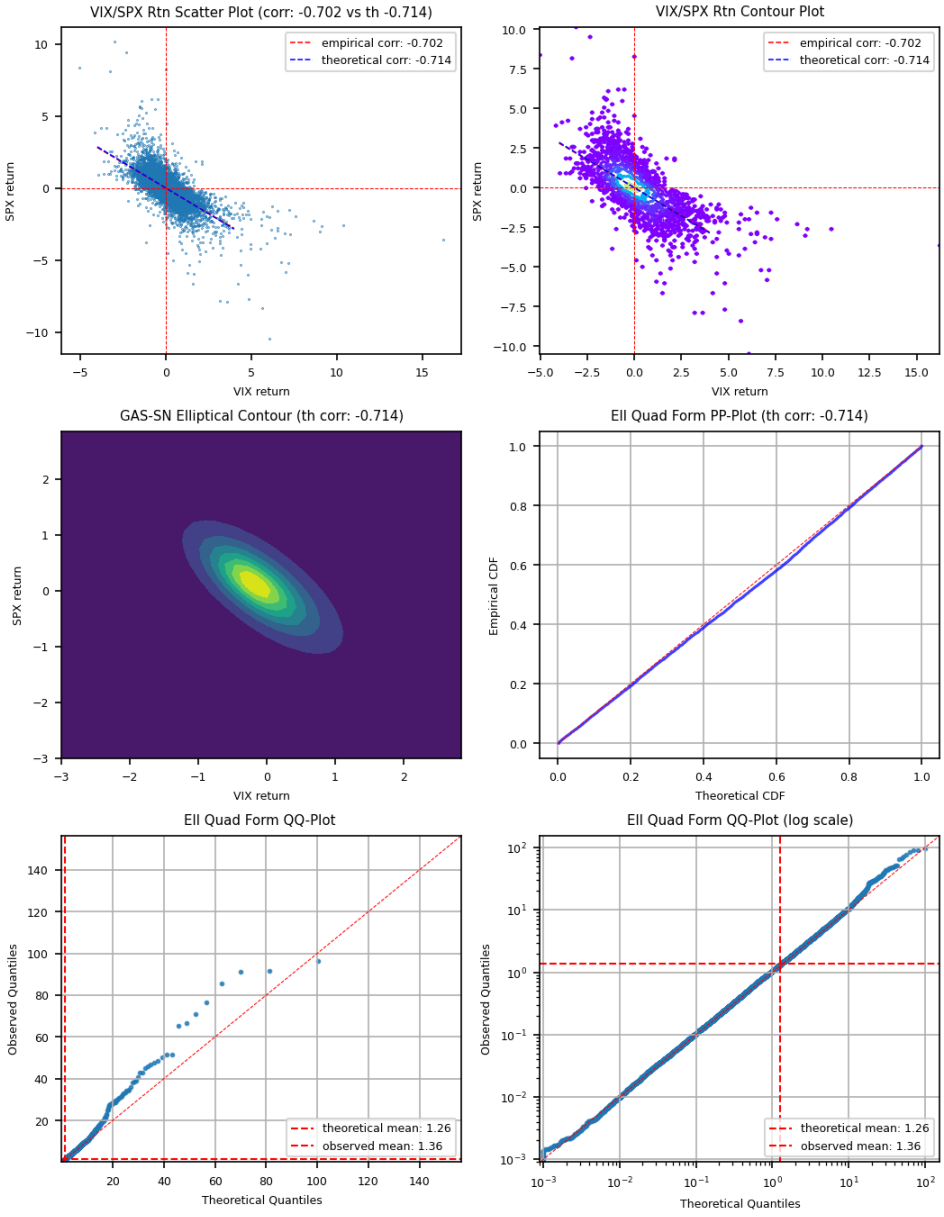

FIGURE 17.1. Elliptical MLE fit of VIX/SPX daily log returns from 1990 to 2025 with the bivariate elliptical GAS-SN distribution. Data is standardized to one standard deviation on each axis. The optimal parameters are: $\hat{\Theta} = \{\rho_\theta = -2.12, \alpha = 0.75, k = 4.5, \beta_0 = 0.78, \beta_1 = 0.27, \omega_0 = 0.92, \omega_1 = 0.88, \xi_0 = -0.35, \xi_1 = 0.19\}$.

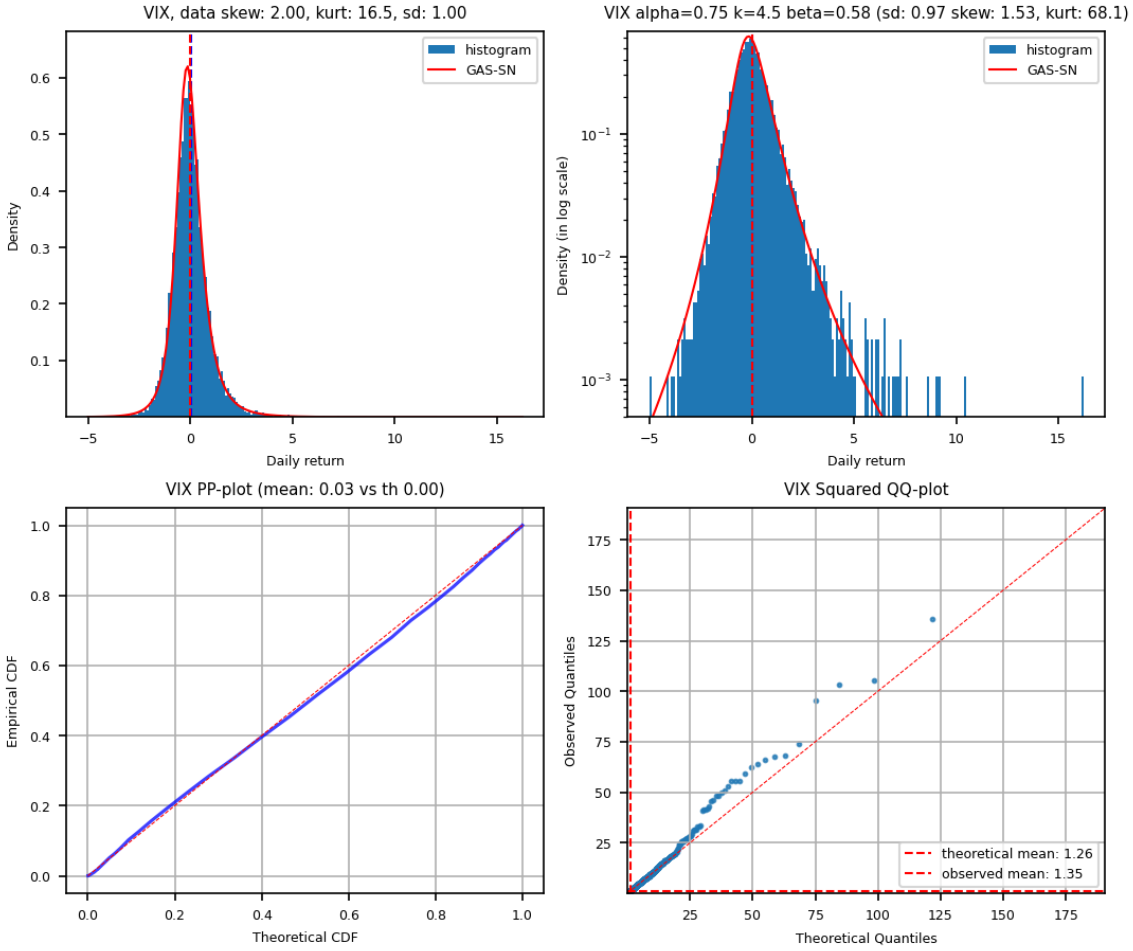

FIGURE 17.2. VIX Marginal from Elliptical MLE fit of VIX/SPX daily log returns from 1990 to 2025 with the bivariate elliptical GAS-SN distribution. Data is standardized to one standard deviation on each axis.

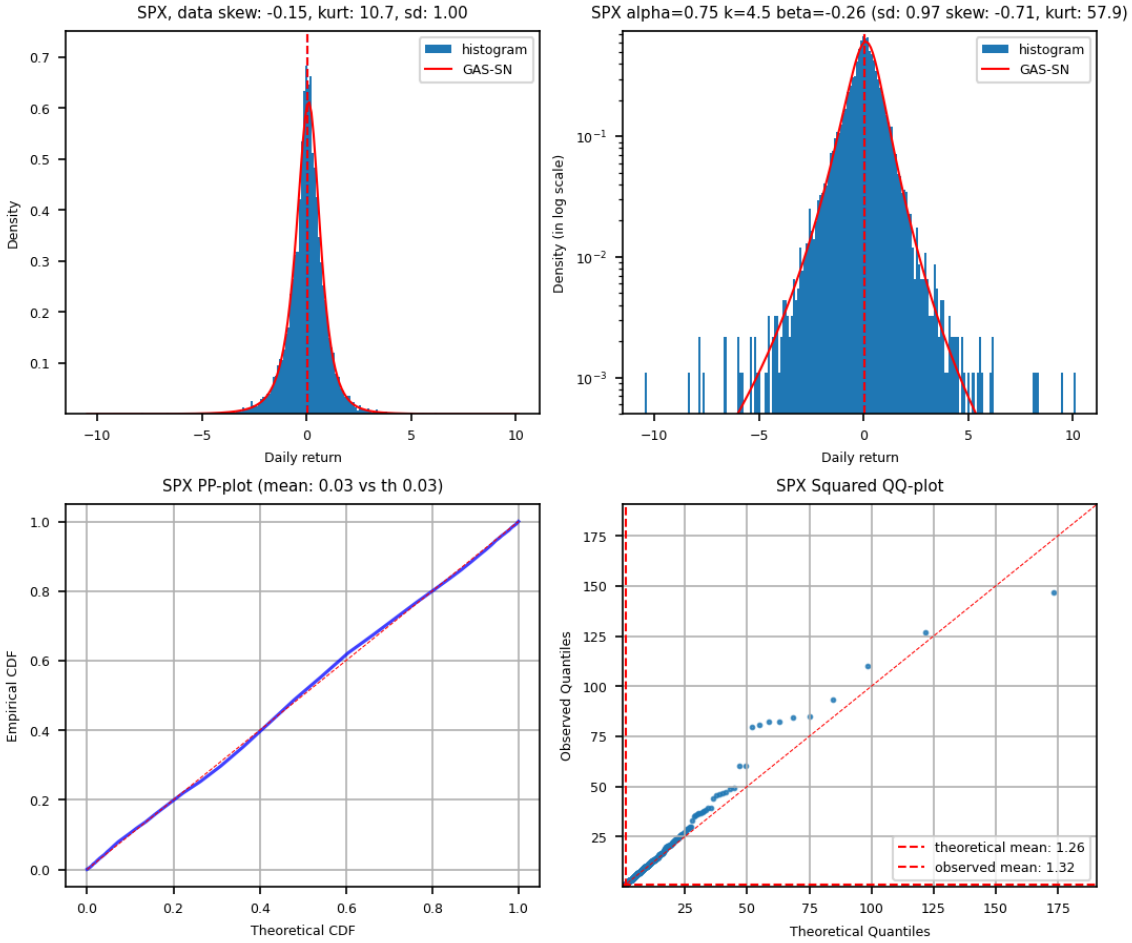

FIGURE 17.3. SPX Marginal from Elliptical MLE fit of VIX/SPX daily log returns from 1990 to 2025 with the bivariate elliptical GAS-SN distribution. Data is standardized to one standard deviation on each axis.

17.2. Adaptive Fit

The adaptive fit is done by MLE on the two marginal distributions with regularization, e.g. the L2 distance between the empirical and theoretical correlations. This is a hack since a direct bivariate MLE is computationally infeasible on my workstation.

The adaptive fit produces the contour plot with somewhat rectangular shapes. That is quite impressive.

The theoretical correlation gets to -0.5, but unable to be closer to the empirical correlation of -0.7.

One would think the adaptive distribution allows each dimension to express its own shape. It should be much easier to produce a good fit. But the interaction between the correlation parameter and the skew parameters is quite complicated.

It is difficult to get the skewness and kurtosis to match in the SPX marginal. It is very complex to navigate the region near $\alpha \approx 1, k \approx 3$. In the Student's t distribution, the skewness and kurtosis are not defined.

The quadratic form needs a multiplier (scale adjustment) to produce a good fit. The origin of this multiplier requires further study.

In the squared QQ plots of the marginals, the fits don't capture the tails as good as the elliptical fits. This is somewhat disappointing.

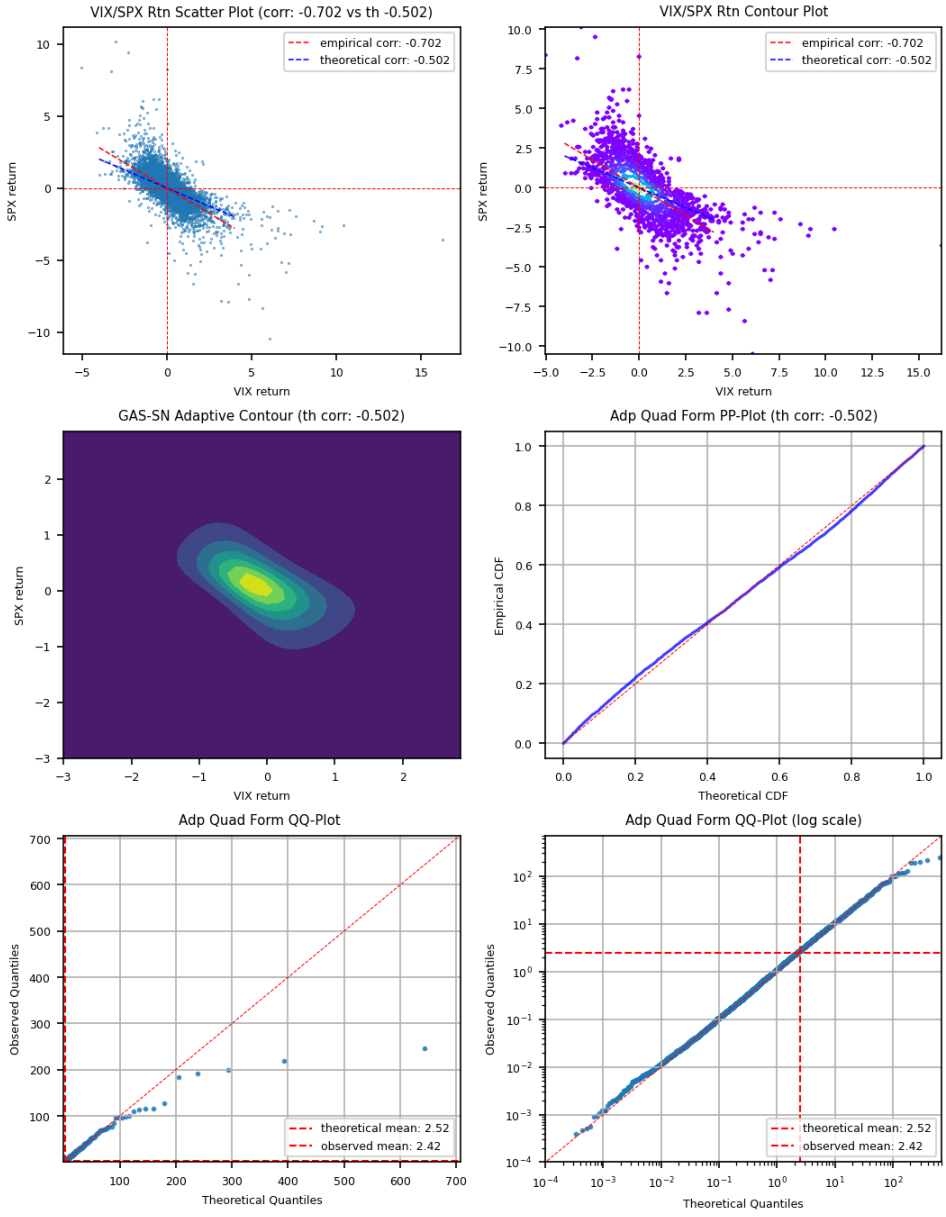

FIGURE 17.4. MLE fit of VIX/SPX daily log returns from 1990 to 2025 with the bivariate adaptive distribution. Data is standardized to one standard deviation on each axis.

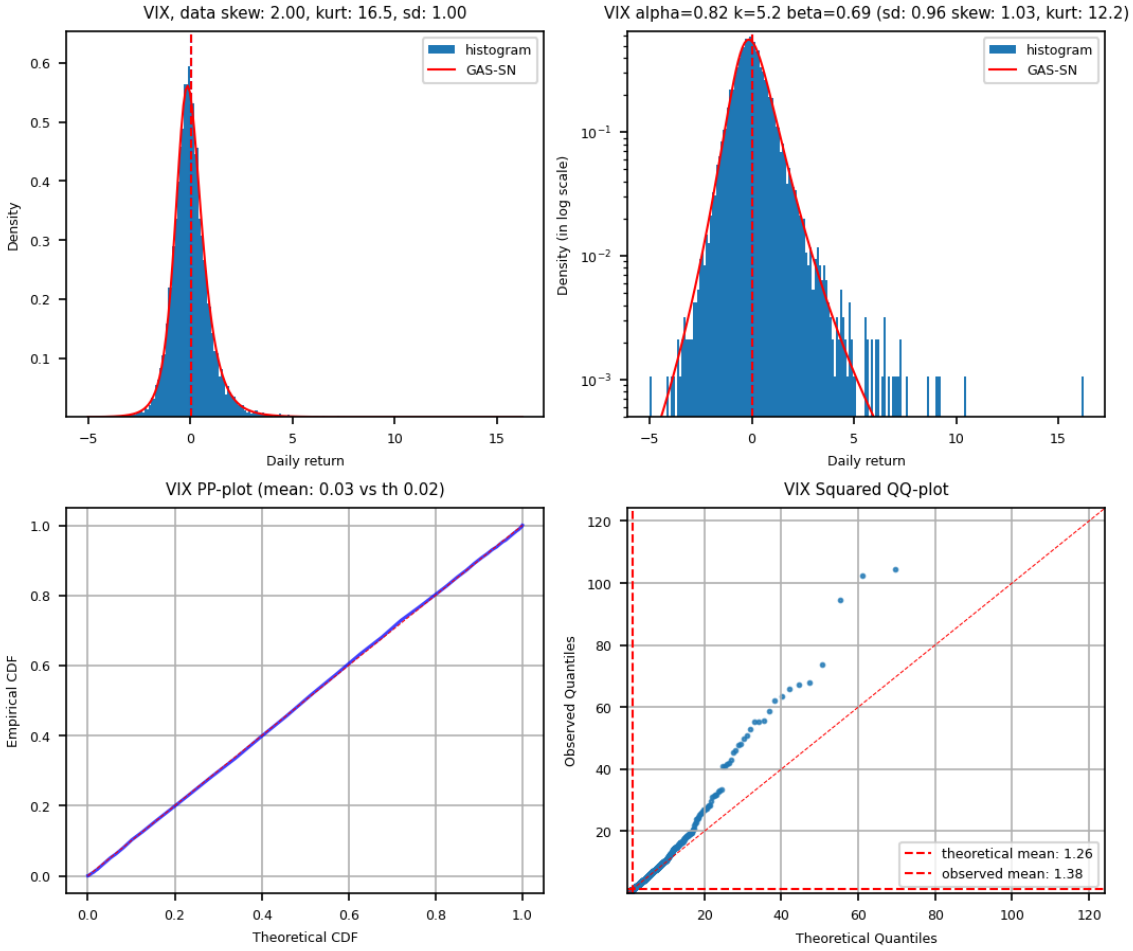

FIGURE 17.5. VIX Marginal from MLE fit of VIX/SPX daily log returns from 1990 to 2025 with the bivariate adaptive GAS-SN distribution. Data is standardized to one standard deviation on each axis.

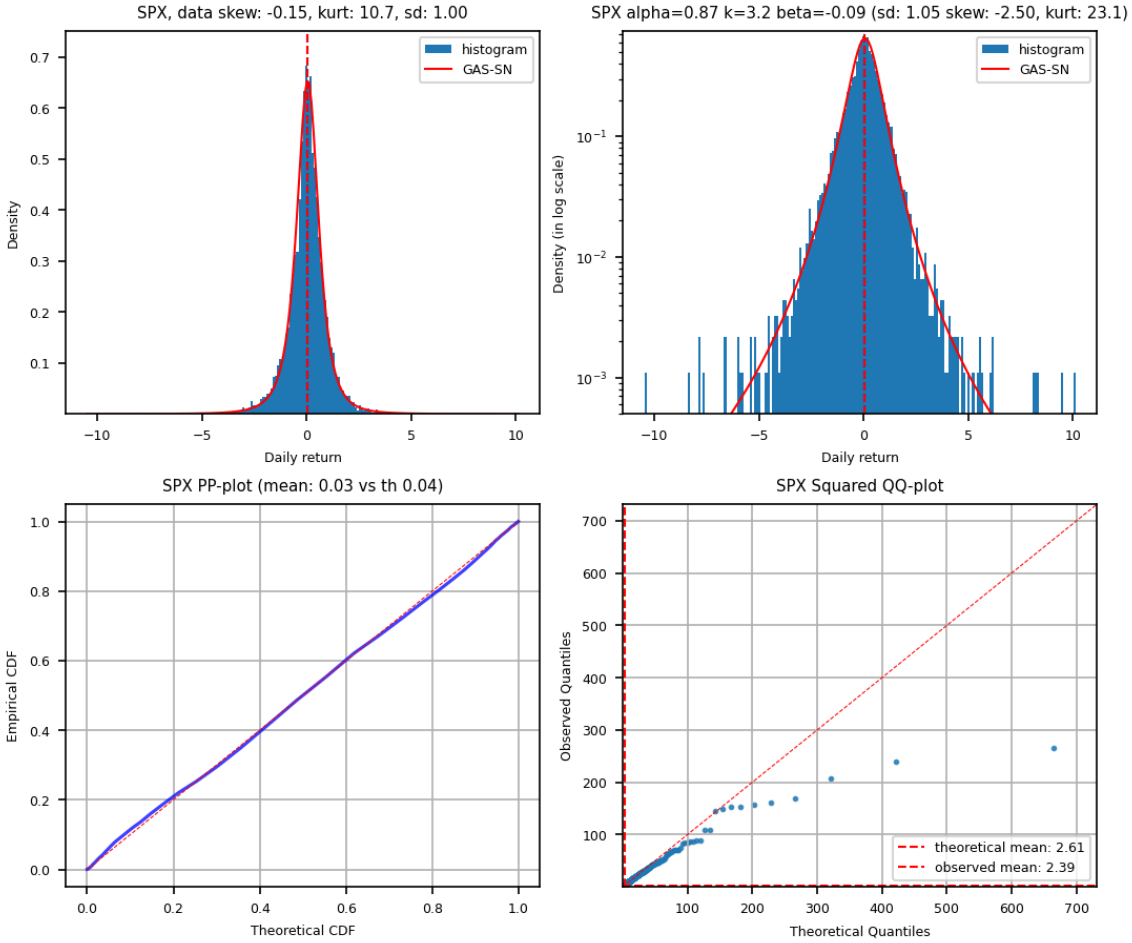

FIGURE 17.6. SPX Marginal from MLE fit of VIX/SPX daily log returns from 1990 to 2025 with the bivariate adaptive GAS-SN distribution. Data is standardized to one standard deviation on each axis.

APPENDIX A

List of Useful Formula

A.1. Gamma Function

Gamma function is used extensively in this paper. First, note that $\Gamma(\frac{1}{2}) = \sqrt{\pi}$. Its **reflection formula** is

$$\Gamma(z)\Gamma(1-z) = \frac{\pi}{\sin(\pi z)} \tag{A.1}$$

And the **Legendre duplication formula** is

$$\Gamma(z)\Gamma(z+1/2) = 2^{1-2z}\sqrt{\pi}\,\Gamma(2z) \tag{A.2}$$

Gamma function Asymptotic: At $x \to 0$, gamma function becomes

$$\begin{aligned} \lim_{x\to 0} \Gamma(x) &\sim \frac{1}{x} \\ \lim_{x\to 0} \frac{\Gamma(ax)}{\Gamma(bx)} &= \frac{b}{a} \qquad (ab \neq 0) \end{aligned} \tag{A.3}$$

For a very large x, assume a, b are finite,

$$\lim_{x\to\infty} \frac{\Gamma(x+a)}{\Gamma(x+b)} \sim x^{a-b} \tag{A.4}$$

Sterling's formula is used to expand the kurtosis formula for a large k, which is:

$$\lim_{x\to\infty} \Gamma(x+1) \sim \sqrt{2\pi x}\Big(\frac{x}{e}\Big)^x, \tag{A.5}$$

$$\text{or } \lim_{x\to\infty} \Gamma(x) \sim \sqrt{2\pi}\, x^{x-1/2} e^{-x}. \tag{A.6}$$

A.2. Transformation

Laplace transform of cosine is[1]

$$\int_0^\infty dt\, \cos(xt) e^{-t/\nu} = \frac{\nu^{-1}}{x^2 + \nu^{-2}} = \frac{\nu}{(\nu x)^2 + 1} \tag{A.7}$$

Gaussian transform of cosine is[2]

$$\begin{aligned} \int_0^\infty dt\, \cos(xt)\, e^{-t^2/2} &= \sqrt{\frac{\pi}{2}}\, e^{-x^2/2} \\ \text{Hence } \int_0^\infty dt\, \cos(xt)\, e^{-t^2/2s^2} &= \sqrt{\frac{\pi}{2}} s\, e^{-(sx)^2/2} \end{aligned} \tag{A.8}$$

[1] See https://proofwiki.org/wiki/Laplace_Transform_of_Cosine

[2] See https://www.wolframalpha.com/input?i=integrate+cos%28a+x%29+e%5E%28-x%5E2%2F2%29+dx+from+0+to+infty

A.3. Half-Normal Distribution

The moments of the half-normal distribution (HN)[3] are used several times. Its PDF is defined as

$$p_{HN}(x;\sigma) := \sqrt{\frac{2}{\pi}}\frac{1}{\sigma}\, e^{-x^2/(2\sigma^2)}\,,\ x>0 \tag{A.9}$$

which is a special case of GG with $d=1, p=2, a=\sqrt{2}\sigma$. Its moments are

$$E_{HN}(T^n) = \sigma^n \frac{2^{n/2}}{\sqrt{\pi}}\,\Gamma\left(\frac{n+1}{2}\right) \tag{A.10}$$

which are the same as those of a normal distribution.

[3] See https://en.wikipedia.org/wiki/Half-normal_distribution

Bibliography

[1] Adelchi Azzalini. *The Skew-Normal and Related Families*. Institute of Mathematical Statistics Monographs. Cambridge University Press, 2013.

[2] H. Bateman and A. Erdélyi. *Higher Transcendental Functions*, volume 3 of *California Institute of Technology Bateman Manuscript Project*. McGraw-Hill Book Company., 1955.

[3] Berndt Bruce C. *Ramanujan's Notebooks, Part I*. Springer New York, NY, 1985.

[4] John C. Cox, Jonathan E. Ingersoll, and Stephen A. Ross. A theory of the term structure of interest rates. *Econometrica*, 53(2):385–407, 1985.

[5] J.C. Crisanto-Neto, M.G.E. da Luz, E.P. Raposo, and G.M. Viswanathan. An efficient series approximation for the lévy α-stable symmetric distribution. *Physics Letters A*, 382(35):2408–2413, 2018.

[6] *NIST Digital Library of Mathematical Functions*. https://dlmf.nist.gov/, Release 1.2.0 of 2024-03-15. F. W. J. Olver, A. B. Olde Daalhuis, D. W. Lozier, B. I. Schneider, R. F. Boisvert, C. W. Clark, B. R. Miller, B. V. Saunders, H. S. Cohl, and M. A. McClain, eds.

[7] William Feller. Two singular diffusion problems. *Annals of Mathematics*, 54(1):173–182, 1951.

[8] William Feller. On a generalization of marcel riesz' potentials and the semi-groups generated by them. *Meddelanden Lunds Universitets Matematiska Seminarium*, pages 73–81, 1952.

[9] William Feller. *An Introduction to Probability Theory and its Applications (2nd Edition)*, volume 2. John Wiley & Sons, Inc., 1971.

[10] Wikimedia Foundation. Inverse distribution, 2023. Retrieved December 1, 2023, from https://en.wikipedia.org/wiki/Inverse_distribution.

[11] George Karagiannidis and Athanasios Lioumpas. An improved approximation for the gaussian q-function. *IEEE Communications Letters*, 11:644–646, 08 2007.

[12] Paul Lévy. *Calcul des Probabilités*. Gauthier-Villars, 1925.

[13] Xiaoyue Li and John M. Mulvey. Optimal portfolio execution in a regime-switching market with non-linear impact costs: Combining dynamic program and neural network. *arXiv preprint*, 6 2023. Available at arXiv: https://arxiv.org/abs/2306.08809.

[14] Stephen H.T. Lihn. Stable count distribution for the volatility indices and space-time generalized stable characteristic function. *SSRN Working Paper*, 7 2020. Available at SSRN: https://ssrn.com/abstract=3659383.

[15] Stephen H.T. Lihn. Generalization of the alpha-stable distribution with the degree of freedom. *arXiv preprint*, 5 2024. Available at arXiv: https://arxiv.org/abs/2405.04693.

[16] F. Mainardi. *Fractional Calculus and Waves in Linear Viscoelasticity: An Introduction to Mathematical Models*. Imperial College Press, 2010. See Appendix F at https://appliedmath.brown.edu/sites/default/files/fractional/36%20TheWrightFunctions.pdf.

[17] Francesco Mainardi and Armando Consiglio. The wright functions of the second kind in mathematical physics. *Mathematics*, 8(6), 2020.

[18] Francesco Mainardi, Yuri Luchko, and Gianni Pagnini. The fundamental solution of the space-time fractional diffusion equation. *Frac. Calc. Appl. Anal.*, 4, 03 2007. See https://arxiv.org/abs/cond-mat/0702419.

[19] Francesco Mainardi and Gianni Pagnini. Mellin-barnes integrals for stable distributions and their convolutions. *Fractional Calculus and Applied Analysis*, 11:443–456, 2008.

[20] Arak Mathai and Hans Haubold. *Fractional and Multivariable Calculus: Model Building and Optimization Problems*. Springer Cham, 12 2017.

[21] Hjalmar Mellin. Zur theorie zweier allgemeinen klassen bestimmter integrale. *Acta Societatis Scientiarum Fennicæ*, page 1–75, 1897.

[22] The mpmath development team. *mpmath: a Python library for arbitrary-precision floating-point arithmetic (version 1.3.0)*, 2023. http://mpmath.org/.

[23] Yuqi Nie, John M. Mulvey, H. Vincent Poor, Chenyu Yu, and Hao Huang. Deep generative models meet statistical methods: A generalized framework for financial regime identification. *SSRN*, 2024. Available at SSRN: https://ssrn.com/abstract=5332057.

[24] John Nolan. *Univariate Stable Distributions, Models for Heavy Tailed Data*. Springer Cham, 01 2020.

[25] Donald B. Owen. Tables for Computing Bivariate Normal Probabilities. *The Annals of Mathematical Statistics*, 27(4):1075 – 1090, 1956.

[26] Richard B. Paris, Armando Consiglio, and Mainardi Francesco. On the asymptotics of wright functions of the second kind. *Fract. Calc. Appl. Anal.*, 24(1):54–72, 01 2021.

[27] Dimiter Prodanov. Computation of the wright function from its integral representation. In *Advances in Nonlinear Dynamics*, volume 1, pages 421–431. Springer Nature Switzerland, 05 2024.

[28] W. R. Schneider. Stable distributions: Fox function representation and generalization. In S. Albeverio, G. Casati, and D. Merlini, editors, *Stochastic Processes in Classical and Quantum Systems*, pages 497–511, Berlin, Heidelberg, 1986. Springer Berlin Heidelberg.

[29] Y. Shu, C. Yu, and J.M. Mulvey. Downside risk reduction using regime-switching signals: a statistical jump model approach. *Journal of Asset Management*, 25:493–507, 2024.

[30] E. W. Stacy. A generalization of the gamma distribution. *The Annals of Mathematical Statistics*, 33(3):1187 – 1192, 1962. See also https://en.wikipedia.org/wiki/Generalized_gamma_distribution.

[31] Student. The probable error of a mean. *Biometrika*, 6:1–25, 1908. See also https://en.wikipedia.org/wiki/Student%27s_t-distribution.

[32] Y.L. Tong. *The Multivariate Normal Distribution*. Research in Criminology. Springer New York, 1990.

[33] Pauli Virtanen, Ralf Gommers, Travis E. Oliphant, Matt Haberland, Tyler Reddy, David Cournapeau, Evgeni Burovski, Pearu Peterson, Warren Weckesser, Jonathan Bright, Stéfan J. van der Walt, Matthew Brett, Joshua Wilson, K. Jarrod Millman, Nikolay Mayorov, Andrew R. J. Nelson, Eric Jones, Robert Kern, Eric Larson, C J Carey, İlhan Polat, Yu Feng, Eric W. Moore, Jake VanderPlas, Denis Laxalde, Josef Perktold, Robert Cimrman, Ian Henriksen, E. A. Quintero, Charles R. Harris, Anne M. Archibald, Antônio H. Ribeiro, Fabian Pedregosa, Paul van Mulbregt, and SciPy 1.0 Contributors. SciPy 1.0: Fundamental Algorithms for Scientific Computing in Python. *Nature Methods*, 17:261–272, 2020.

[34] E. M. Wright. On the coefficients of power series having exponential singularities. *Journal London Math. Soc.*, s1-8, Issue 1 (1933):71–79, 1933.

[35] E. M. Wright. The asymptotic expansion of the generalized bessel function. *Proc. London Math. Soc.*, s2-38, Issue 1 (1935):257–270, 1935.